Title
Interplay of Serotonin and Kappa Opioid Systems in Stress, Anxiety, and Depressive Disorders

Author
Christiansen, Sara Erwin

Publication Date
2022

Peer reviewed|Thesis/dissertation

UNIVERSITY OF CALIFORNIA

Los Angeles

Interplay of Serotonin and Kappa Opioid Systems in Stress, Anxiety, and Depressive Disorders

A dissertation submitted in partial satisfaction of the

requirements for the degree Doctor of Philosophy

in Molecular Toxicology

by

Sara Erwin Christiansen

2022

ABSTRACT OF THE DISSERTATION

Interplay of Serotonin and Kappa Opioid Systems in Stress, Anxiety, and Depressive Disorders

by

Sara Erwin Christiansen

Doctor of Philosophy in Molecular Toxicology

University of California, Los Angeles, 2022

Professor Anne M. Andrews, Co-Chair

Professor Christopher J. Evans, Co-Chair

The serotonin system, among other neurotransmitter systems, plays an important role in mood and anxiety disorders. The etiology of mood and anxiety disorders is still largely unknown. The biggest risk factor for the development of mood and anxiety disorders is stress, which has been found to affect neurotransmitter function and behaviors. My dissertation work set out to investigate (1) the effects of *in utero* stress exposure on neurochemistry and behavior during adulthood and whether concomitant maternal citalopram treatment rescued adverse stress effects, (2) the modulation of serotonin and dopamine by kappa opioid receptors in dysphoria, and (3) the selectivity of optogenetically stimulating dopamine neurons and the interplay between monoamine systems.

The project of my graduate work focused on effects of *in utero* stress exposure and whether treatment with the SSRI, citalopram, could mitigate the adverse effects of prenatal stress. To model anxiety and depressive disorders during pregnancy, I used a mouse model in which pregnant dams underwent a chronic stress paradigm during their pregnancy. A

group of dams received concomitant treatment with citalopram, an SSRI. I then examined developmental neurochemistry, and adult neurochemistry and behaviors. Pups from the stressed group had elevated neurochemical and amino acid tissue levels. Moreover, I found that pups born to stressed dams had increases in anxiety- and depressive- like behavior. The stress induced behavioral effects were rescued in pups that received concomitant *in utero* citalopram exposure. Serotonin concentrations were increased in stress pups after SERT blockade in the vHPC and after a systemic injection of a kappa opioid receptor agonist. My findings suggest beneficial outcomes for treating stress during pregnancy on overall offspring health.

The secondary project my graduate work focused on investigating the interplay of serotonin and kappa opioid receptor systems in aversion. Human and animal studies have shown that kappa opioid receptor agonists produce dysphoric mood states. Research has also shown that while KOR agonists have anxiogenic effects, antagonists are anxiolytic. Nonetheless, the mechanisms by which KOR antagonists reduce anxiety-related or dysphoric behavior remain unclear. Using *In situ* hybridization, I found *Oprk1, Sert, vGlut3* and *vGat* mRNA are co-expressed in the dorsal raphe nucleus, indicating a possible direct or indirect mechanism for KOR-modulation of serotonin transmission. Additionally, I showed local KOR activation with an agonist increases extracellular serotonin levels in both the ventral striatum and ventral hippocampus. This pilot work sets the stage for future studies to concurrently examine neurotransmitter levels during behavioral tests such as conditioned place aversion to better understand the interplay of the serotonin, dopamine, and kappa opioid receptor systems in dysphoria.

The dissertation of Sara Erwin Christiansen is approved.

Catherine Marie Cahill

Jeff Bronstein

David E. Krantz

Christopher J. Evans, Committee Co-Chair

Anne M. Andrews, Committee Co-Chair

University of California, Los Angeles

2022

For my family

Table of Contents

Acknowledgements

I would like to say thank you to all the amazing people that have supported me, mentored me, and helped me through this incredible five-year journey here at UCLA. Without all of you, I would not be where I am today.

First, I would like to thank my advisor and mentor Prof. Anne Andrews. Thank you for helping me grow as a woman in science. It was your encouragement and support that allowed me to push harder, think deeper, and really take my scientific, and life, skills to the next level. For that I am ever grateful. I would also like to thank my entire committee for all of our insightful discussions and providing me with your expertise and support. I would also like to thank the UCLA Center for Study of Opioid Receptors and Drugs of Abuse (CSORDA) and the UCLA Clinical and Translational Science Institute for their support and funding.

Next, I would like to thank my lab mates in the Andrews group specifically Merel, Katie, Olena, Noelle, and Cameron. We have built such a collaborative, open, and fun group. I will greatly miss you all in my next endeavor and can only hope to find a team as fantastic as the one we had here. I would also like to thank all the undergraduate students who helped me to grow as a mentor.

Last, but certainly not least, I want to thank my family for all of their support. To my mom and dad – thank you for always pushing me to overcome challenges and to strive for success. Your love, support, and encouragement throughout my whole life is what propelled me to this moment. To my husband – thank you for your endless love and support. To Jak – you are always a breath of fresh air and a positive distraction when I needed it the most. Finally, to all my friends near and far who have stood by my side and cheered me on during my PhD journey, thank you.

Vita

I received my Bachelor of Science in Forensic and Toxicological Chemistry with a minor in Biology at the West Chester University of Pennsylvania (WCUPA) in 2017. At WCUPA, I was the President of the Women in Science club which promoted and supported the advancement of women perusing STEM careers. I was also actively involved in the Gamma Sigma Epsilon national chemistry honors society.

I began my graduate studies in the fall of 2017 at the University of California, Los Angeles (UCLA) pursuing my doctoral degree in the Molecular Toxicology IDP. After completing two laboratory rotations, I joined the lab of Dr. Anne Andrews in March of 2018. In Dr. Andrews' group, my research has focused on investigating the role of serotonin transmission in mood and anxiety disorders, kappa opioid receptor modulation of serotonin in dysphoria, and assessing *in utero* stress exposure on offspring health.

CHAPTER 1

A review of the mechanisms of the serotonin and kappa opioid systems in stress

Introduction

Stress is ubiquitous, whether day-to-day or highly traumatic. Stress increases susceptibility to major depressive disorder (MDD), anxiety disorders, psychosis, cardiovascular disease, metabolic syndrome (diabetes), cancer, and poor developmental outcomes in children.[1-5] Stress increases the risk of developing a substance use disorder (SUD), as well as relapse in those recovering from SUDs.[1,6,7] The most commonly prescribed treatments for stress-related psychiatric disorders are selective serotonin reuptake inhibitors (SSRIs).[8,9]

The SSRIs inhibit the reuptake of serotonin by serotonin transporters and are more efficacious than placebo.[10-12] Treatment of mood and anxiety disorders with SSRIs, however, takes weeks to produce therapeutic effects, if at all.[10] Around 50% of patients fail to show significant improvement in symptoms after initial treatment attempts.[13,14] Unfortunately, treatment with various medication combinations and doses and/or behavior therapy has not been shown to significantly improve treatment outcomes.[14] The large number of patients who do not find relief with SSRIs and other common antidepressant medications bolsters the need for research into novel biological pathways as possible therapeutic targets.

The kappa opioid system has received interest as a new target for neuropsychiatric disorder drug therapeutics, including for anxiety, depression, and other disorders.[15-17] Kappa opioid receptor (KOR) agonists produce dysphoria, which is one of the main symptoms of neuropsychiatric disorders. Dysphoria is a state of profound unease, unwellness, or dissatisfaction with life, which presents as sadness, numbness, irritability, and mood swings.[8,18] Studies have shown that activation of KORs induces dysphoric mood states in humans and aversion in rodents.[19-21]

Both the serotonin and kappa opioid systems have been implicated in the mechanisms of stress and stress-related psychiatric disorders. While there are many studies pointing to the possible roles of these systems in stress-related disorders, the etiology of stress-related mood disorders is still largely unknown. In this chapter, I review research focused on the roles of the serotonin and kappa opioid systems in the mechanism of stress-induced behavioral disorders. A better understanding of the interplay of the serotonin and kappa opioid systems prior to, during, and after stressful events will improve understanding of the biological basis of stress-related disorders and help to uncover new therapeutic targets.

Stress effects on neurochemical systems & treatment targets

Serotonin system

Serotonin is a monoamine neurotransmitter involved in diverse physiological and psychological functions.[22-24] Serotonin is synthesized from the essential amino acid L-tryptophan.[25] Serotonin is found widely throughout the brain where it interacts with 15 different receptor subtypes.[26-28] The serotonin system has been studied in early life and adult stress susceptibility and neuropsychiatric disorders. Studies suggest a bidirectional interaction between the serotonin system and stress, *i.e.,* stress affects the serotonin system and serotonin system function determines stress susceptibility.[29-35] Thus, there is a relationship between serotonin and stress for vulnerability to developing stress-related disorders, specifically MDD. In this section, I discuss how the effects of early life stress impact the serotonin system, the use of SSRIs for the treatment of stress effects, and possible mechanisms by which stress modulates the serotonin system.

Early life stress & serotonin

Early life stress is a risk factor for developing psychiatric disorders in adulthood.[1] Stress *in utero* can be thought of as a teratogen, which is an agent that disrupts normal fetal development. Disruption of critical developmental processes and/or their timing by stress alters physiological and behavioral outcomes in adulthood and increases risks for developing neuropsychiatric disorders.[36-43] Animal studies also show a relationship between early-life stress and serotonin alterations.[41] For example, in rodents, prenatal maternal stress was found to increase fetal serotonin,[43] increase the rate of serotonin synthesis in the hippocampus,[38] increase tryptophan hydroxylase (TPH) expression and serotonin synthesis in the dorsal raphe nucleus (DRN),[40] and increase $5HT_{1A}$ expression in the hippocampus.[42]

In humans, maternal depression during the second trimester of pregnancy was associated with reduced methylation of the serotonin transporter gene (*SLC6A4)* promotor in infants.[36] Methylation of DNA is important for maintaining appropriate gene activation and silencing. Disruption of DNA methylation can alter gene expression leading to disease phenotypes. A chronic stress paradigm administered shortly before conception also produced alterations in the serotonin system.[37] Miller *et al.* found that the serotonin transporter (SERT) of depressed adults with a history of child abuse, had decreased binding potential.[39] Thus, stress during critical developmental periods alters the brain serotonin system.

Serotonin transporters & selective serotonin reuptake inhibitors

The SSRIs are widely prescribed to treat stress-related disorders. These medications inhibit SERT and thus, the reuptake of extracellular serotonin. Commonly prescribed SSRIs include citalopram, escitalopram, fluoxetine, fluvoxamine, sertraline, and others.

Studies have shown that SSRI treatment during early developmental periods rescues some of the effects of early life stress. *In utero* citalopram exposure attenuates increases in mouse forebrain serotonin levels induced by prenatal stress.[43] Early postnatal fluoxetine treatment reduced the rate of serotonin turnover (serotonin to 5-hydroxytrptamine (5-HIAA)) and elevations in mouse corticosterone levels caused by prenatal maternal stress.[38] Corticosterone in rodents and cortisol in humans is a hormone secreted by the adrenal cortex in response to stress. Oberlander *et al.* examined cortisol levels and hypothalamic-pituitary-adrenal axis (HPA) axis responsiveness to a stress challenge in 3-month-old infants exposed to prenatal SSRI.[44] Prenatal SSRI exposure decreased post-stress cortisol levels and decreased evening basal salivary cortisol levels.

Developmental fluoxetine exposure starting at postnatal day 1 rescued prenatal stress effects on hippocampal cell proliferation in both male and female rats with effects in males being more prevalent.[45] Additionally, new cell survival was also rescued by fluoxetine exposure, however, this effect was only seen in female offspring. Mice exposed to fluoxetine during the prenatal period showed reduced anxiety- and depressive-like phenotypes when exposed to continuous stress in adulthood.[29] Though there is evidence that prenatal and postnatal SSRI treatment attenuate the effects of stress later in life, the effects of concomitant maternal stress and SSRI treatment are unknown. In Chapter 2, I detail my research, which investigates the neurochemical and behavioral effects of a maternal chronic stress paradigm with concomitant SSRI treatment on postnatal and adult offspring.

Preclinical SSRI studies provide evidence in support of treating stress-related mood disorders in humans. Chronic exposure to fluvoxamine, an SSRI, rescues stress-induced increases in cortical extracellular serotonin.[30] Exposure to SSRIs increases mobility time in

the forced swim test (FST) in rodents, and repeated, but not acute, forced swim stress increases serotonin reuptake by SERT.[46] These findings suggest the role of SERT inhibition in mitigating stress-related phenotypes. Animal studies and the effectiveness of SSRIs in some patients affirm that SSRI treatment helps to mitigate the effects of stress on biological and behavioral outcomes. However, the mechanisms by which SSRIs alleviate dysphoria and other symptoms, and why SSRIs take so long to become effective are still not fully known. The SSRIs also have a number of side effects such as agitation, sleep disturbances, sexual dysfunction, serotonin syndrome, suicidal ideation, and others.[47,48]

Serotonin receptors

Due to the unknown mechanisms of action, side effects, and delayed therapeutic effects of SSRIs, additional components of the serotonin system, *e.g.*, serotonin 2A receptors ($5HT_{2A}$)[49], and other neurotransmitter systems represent potential novel drug targets for treating neuropsychiatric disorders. Serotonin receptors play roles in stress mechanisms and can serve as treatment targets *via* receptor agonists or antagonists. In rodents, stress paradigms have been found to desensitize somatodendritic $5HT_{1A}$ receptors and decrease the potency of $5HT_{1A}$ agonists.[50-54] Fontaine *et al.* reported that stress decreased serotonin 1B receptor ($5HT_{1B}$) stimulation thus decreasing serotonin transmission in the nucleus accumbens (NAc).[32] Furthermore, serotonin 2C receptor ($5HT_{2C}$) mRNA is increased after acute and chronic stress.[55] These transcriptional increases are correlated with stress-induced increases in corticosterone levels. Additionally, $5HT_{2C}$ agonists increase stress related hormones, *i.e.,* cortisol, adrenocorticotropic hormone (ACTH), and prolactin, in humans.[56]

Serotonin and the HPA axis

Serotonin system interactions with the HPA axis have been explored as another possible mechanism underlying stress-related disorders. The HPA axis connects the hypothalamus, pituitary gland, and adrenal glands in the body's response to stress. Animal studies have uncovered the importance of HPA axis activation by serotonin *via* the stimulation of corticotrophin-releasing factor (CRF) release, which triggers ACTH release and increased corticosteroid secretion.[31,33,57] Acute and chronic stress increase brain serotonin.[58-61] Studies have demonstrated that increased serotonin is caused by stimulating TPH, the rate-limiting enzyme in serotonin synthesis.[59-61] The increase in serotonin is predicted to increase the sensitivity of cortisol inhibition of CRF, a negative feedback control in the hypothalamus.[62] Therapeutics aimed at reversing the effects of stress on the HPA axis either in conjunction with SSRIs or alone could be used to treat stress-related disorders.

Kappa opioid receptors

Another system implicated in stress and stress-related disorders is the kappa opioid receptor (KOR) system. The endogenous kappa opioid system has received interest as a target for novel anxiety and depression therapeutics.[15,16] Studies have shown that KOR agonists induce dysphoric mood states, a core symptom of anxiety and depressive disorders in humans, and aversion in rodents.[19-21] The KORs are G-protein-coupled receptors (GPCRs) of the $G_{i/o}$ subtype, which are inhibitory GPCRs. Inhibitory GPCRs hyperpolarize neurons reducing the likelihood of firing action potentials and subsequent neurotransmitter release.[63]

The endogenous neuropeptide dynorphin activates KORs. Dynorphin is produced from its precursor prodynorphin (PDYN). Dynorphin is released under stressful

conditions[64,65] and is a mediator of the dysphoric component of stress.[66] Limbic regions were shown to have increased dynorphin immunoreactivity after immobilization or forced swim stress.[67] McLaughlin *et al.* showed that disruption of the prodynorphin gene, using a transgenic mouse model, protected mice from increased immobility after forced swim stress exposure.[68]

KOR activation and inhibition during stress

Pharmacologic studies have demonstrated that KOR activation occurs in stress-related phenotypes. Agonists such as Salvinorin A (SalvA), U50,488, and U69,593 induce an aversive phenotype in condition place aversion.[66,69-72] The KOR agonist, U50,488, potentiates cocaine-induced conditioned place preference similar to stress.[72] The KOR agonists were also found to elicit depressive-like phenotypes in the forced swim test.[73]

Antagonist and knockout studies also provide evidence for a role for KORs in stress. The most common KOR antagonist investigated is norbinaltorphimine (norBNI). Acting as a high-affinity competitive antagonist, norBNI is selective for KORs while having much lower affinity for mu and delta opioid receptors.[74] The antidepressant-like effects of KOR antagonists have been characterized in the forced swim test.[73] Intracerebroventricular (i.c.v) injection of norBNI decreased immobility in the force swim test in a dose-dependent manner. Prodynorphin knockout (Pdyn-/-) mice and mice administered norBNI do not display a forced swim stress-induced analgesia phenotype.[68] McLaughlin *et al.* found that forced swim stress potentiated cocaine conditioned place preference (CPP). Treatment of stressed mice with norBNI attenuates the stress-induced potentiation of the cocaine CPP. Antagonism of KORs, KOR gene knockout, or prodynorphin gene knockout blocked swim-stress-induced immobility in the forced swim test.[67,68,73,75] Land *et al.* demonstrated that norBNI blocks CRF-

induced conditioned place aversion and CRF-induced anxiety-like responses.[66,76] Together, these studies make a strong case for inhibiting KOR activation during or after stress to attenuate KOR-induced stress effects.

Early life stress & kappa opioid receptors

As discussed, exposure to early life stress is a risk factor for developing psychiatric disorders in adulthood.[1] Early life stress not only impacts the serotonin system, it disrupts the functioning of the KOR system. Maternal deprivation stress, a severe early life stressor in which pups are separated from their mothers and siblings for 24 hours, caused an increase in dynorphin-A peptide density and decreased KOR mRNA within the lateral habenula (LHb), a brain region implicated in reward/aversion, depressive-like phenotypes, and stress.[77] Increases in dynorphin-A, one of the dynorphin peptides, could increase KOR activation. Chang *et al.* found that neonatal exposure to a predator odor induced brain region and time-dependent changes in KOR mRNA levels in brain sections from female but not male mice.[78] On postnatal day 3, female stressed mice had decreased KOR mRNA in the NAc but not in the amygdala. However, by postnatal day 33, no differences in KOR mRNA levels were observed between control and stressed groups. While decreases in KOR mRNA levels did not persist into adulthood, reductions during an important developmental time point could have impacted the development of other interacting brain systems. The coordinated effects of changes in the brain during development could alter behavioral outcomes in adulthood.

Lutz *et al.* found decreased KOR mRNA levels in the anterior insula of patients who died by suicide and had a history of childhood abuse.[79] Decreased receptor mRNA does not necessarily correlate with decreased numbers of KORs due to the complex regulation of protein translation. Further research is needed to determine how changes in KOR mRNA are

related to KOR receptor expression. Nonetheless, the disruption of the KOR system by stress during development impacts susceptibility to stress and neuropsychiatric disorders later in life.

Along with KOR mRNA, early life stress also affects KOR receptor sensitivity. Early postnatal maternal deprivation stress desensitized LHb neuronal firing in response to U50,488 in adolescence.[77] By contrast, Karkhanis *et al.* found that social isolation stress enhanced the inhibitory effects U50,488 on dopamine neurons in the NAc compared to control animals.[80] Here, the half-maximal effective concentration (EC_{50}) of U50,488 was significantly decreased in animals who underwent social isolation stress. Overall, early life stress has an impact on the development of KOR system function. Nonetheless, how developmental disruption of the KOR system affects adult behavioral phenotypes needs to be understood more deeply.

Kappa opioid receptors & the HPA axis

Like the serotonin system, the KOR system regulates the HPA axis. The KOR-HPA axis hypothesis stems from the expression of KORs and dynorphin in regions implicated in stress responses, *e.g.,* amygdala, prefrontal cortex, and hypothalamus.[81] Activation of KORs, either through stress-induced dynorphin release or agonist administration increases corticosterone levels in rodents and cortisol in humans.[82-84] In contrast, corticosterone levels are reduced in Pdyn-/- mice and in wildtype mice treated with the KOR antagonist norBNI. Furthermore, Pdyn knockout attenuates stress-induced increases in corticosterone.[85] The HPA axis is regulated by KORs *via* CRF. Both stress and CRF injection increase phosphor-KOR immunoreactivity, a marker for KOR activation.[66,86] Radioimmunoassay studies also show that CRF induces dynorphin release.[87,88]

KOR antagonists as a treatment option

Due to the copious findings showing that KOR antagonists block the effects of stress and the dysphoric components of stress, these antagonists are being investigated for the treatment of stress-related psychiatric disorders.[66,68,73,76,82-84] Nonetheless, discovery and clinical trial approval for KOR antagonists have not yet been successful. The development of KOR antagonist treatments is hindered by the unusually long half-life of known antagonists. For example, the prototypical KOR antagonist used in pre-clinical research, norBNI, blocks the effects of KOR agonists for up to a month.[89] A newer antagonist, JDtic, has inhibitory effects that last up to 11 days.[90]

While JDtic has a shorter duration of action than norBNI, it is still not optimal for human clinical trials. Drugs with long half-lives (multiple days) pose safety risks, especially when their safety profile is unknown in humans. An adverse reaction could last as long as (or longer than) the drug is in the body, which could be days to weeks for JDtic or norBNI, respectively. Depending on the severity of an adverse reaction, prolonged adverse effects would be dangerous for patients, particularly without pharmacologic avenues for reversal. Surprisingly the mechanisms behind the long durations of action of KOR antagonists are still largely unknown, though there is evidence that they occur in part due to activation and phosphorylation of c-jun N-terminal kinase (JNK).[91,92]

To date, two Phase I clinical trials have explored the safety of KOR antagonists.[93,94] One trial, using JDtic, failed Phase I.[94] The other, using LY2456302, a newly developed KOR antagonist from Eli Lilly, passed Phase I and is currently moving forward in Phase II to test efficacy in treating psychiatric disorders.[93] Despite the difficulties described above, KOR antagonists are still believed to have the potential as treatments for stress-related disorders.

Further research, however, is needed to determine whether suitable drug candidates can be discovered for use in humans.

Interplay of kappa opioid receptors and serotonin in stress & dysphoria

Neurochemical systems do not act independently but instead are highly interconnected.[95,96] For example, research connects the kappa opioid and dopaminergic systems in the context of stress-related disorders.[20,80,97-99] Evidence also exists supporting the roles of the serotonin and kappa opioid receptor systems individually in stress responses and stress-related disorders, wherein commonalities suggest connections between the KOR and serotonin systems. For instance, both systems are affected by early life stress, involved in HPA axis regulation by stress and are at work in overlapping brain regions. Literature supporting the interplay of the KOR and serotonin systems in stress and dysphoria is growing.[46,67,72,97,100-102] Nonetheless, some of this research is contradictory.

Microdialysis and fast scan cyclic voltammetry (FSCV) have been used to show that activation of KORs causes decreases in dopamine levels in the NAc.[72,103-105] By contrast, the effects of KOR activation on the serotonin system are less well studied and inconclusive. In one study, Schindler *et al.* found that stress or U50,488 administration increase SERT function in synaptosomes in a manner attenuated by prior norBNI administration.[46] In contrast, Sundaramurthy *et al.* found *ex vivo* that serotonin reuptake is decreased in a dose-dependent manner after the administration of the KOR agonists U50,488 or U69,593.[106]

Research on serotonin transmission upon KOR activation is furthermore at odds. Tao *et al.* reported decreases in serotonin efflux in the ventral striatum (vST) and DRN after

U50,488 infusion into the rat DRN.[101,102] However, two other studies saw no changes in serotonin levels. The first study analyzed serotonin levels in the NAc of rats after intraperitoneal administration of Salvinorin A (SalvA), a potent kappa agoinst.[72] A second study involved U69,593 infusion into the hippocampus.[107] Together, these studies illustrate the need for further research characterizing the effects of KOR activation on serotonin transmission and SERT activity, and the mechanism of these effects.

Serotonin has been found to affect PDYN mRNA levels. Di Benedetto *et al.* found that SSRI administration increased prodynorphin mRNA in the hypothalamus, but decreased levels in the caudate putamen and NAc.[108] Pharmacologic depletion of serotonin using *para*-chloroamphetamine (PCA) decreased PDYN mRNA levels in the hypothalamus, caudate putamen, NAc, and hippocampus.[108] D'Addario *et al.* reported that serotonin depletion by PCA reversed the effects of the KOR agonist U69,593 on PDYN mRNA levels but only in the hippocampus.[109] Under control conditions, administration of U69,593 decreased PDYN mRNA. However, PCA-treated rats show increased PYDN mRNA after U69,593 administration. Overall, these results show that increases in serotonin increase PDYN mRNA, while depletion of serotonin decreases PDYN mRNA levels. Due to prodynorphin being the precursor for dynorphin synthesis, the regulation of PDYN mRNA by serotonin is thought to regulate the production of dynorphin. Dynorphin levels regulate corticosterone levels, KOR activation, and stress-induced behavioral phenotypes. As a result, we hypothesize that a feedback pathway exists wherein serotonin directly affects the transcription of PDYN mRNA connecting the two systems in stress related disorders.

Behaviorally, the dysphoric component of stress is studied using conditioned place aversion in animals. In one study, mice with constitutive loss of SERT expression (SERT-/-)

showed a loss of KOR-induced place aversion suggesting that SERT is involved in the mechanism of KOR-induced aversion.[46] In contrast, our group observed that SERT wildtype (SERT+/+) mice as well as SERT-/- mice showed context-dependent place aversion to U50,488 in a longer training conditioned place aversion task (Gilman, unpublished). Moreover, Ehrich *et al.* found that for place aversion to occur, KOR activation is required in both serotonin and dopamine neurons.[97]

Conditional deletion of KORs from SERT-expressing neurons attenuated stress-induced potentiation of cocaine place preference.[32] In addition, $5HT_{1B}$ receptors are reported to be increased in prodynorphin-expressing cells after chronic swim stress. Land *et al.* studied KOR-induced place aversion in KOR-/-mice.[100] The KOR-/- mice showed loss of KOR-induced aversion; restoration of KOR expression *via* lentiviral gene delivery into the DRN was sufficient to rescue aversion. The aversive phenotype was blocked by the injection of norBNI into the NAc. The findings of Land *et al.* suggest that serotonergic neurons projecting from the DRN to the NAc play a key role in CPA.

The contradictions in current research may stem from differences in experimental conditions across studies. These differences include the species studied, drug type, dose, route of administration, brain region investigated, type of stress, etc. Despite the contradictions across studies, the body of research supports the hypothesis that an interaction between the KOR and serotonin systems exists. Further studies to understand the mechanisms of KOR modulation of serotonin pertaining to the dysphoric components of stress and mood disorders are warranted.

Conclusions

The intersection between the serotonin and kappa opioid receptor systems is an important avenue for future research regarding the etiology of neuropsychiatric disorders where stress is a risk factor and for the development of new therapeutics. More research is needed to uncover the mechanisms of stress in these disorders, specifically focusing on the interplay between the KOR and serotonin systems. My thesis work contributes to this ongoing research by focusing on how stress and KOR activation affect the serotonin system. In chapter 2, I describe my studies on a link between SERT and KOR activity in an animal model of *in utero* stress exposure. In chapter 3, I describe my studies examining the effects of local and systemic activation of KORs on extracellular serotonin levels in the NAc and hippocampus.

References

1. Cirulli, F.; Laviola, G.; Ricceri, L., Risk factors for mental health: translational models from behavioural neuroscience. *Neurosci Biobehav Rev* **2009,** *33* (4), 493-7.

2. Steptoe, A.; Kivimaki, M., Stress and cardiovascular disease: an update on current knowledge. *Annu Rev Public Health* **2013,** *34*, 337-54.

3. Kuo, W. C.; Bratzke, L. C.; Oakley, L. D.; Kuo, F.; Wang, H.; Brown, R. L., The association between psychological stress and metabolic syndrome: A systematic review and meta-analysis. *Obes Rev* **2019,** *20* (11), 1651-1664.

4. Soung N.K., K. B. Y., Psychological stress and cancer. *J Anal Sci Technol* **2015,** *6*.

5. Smith, K. E.; Pollak, S. D., Early life stress and development: potential mechanisms for adverse outcomes. *J Neurodev Disord* **2020,** *12* (1), 34.

6. Mukhara, D.; Banks, M. L.; Neigh, G. N., Stress as a Risk Factor for Substance Use Disorders: A Mini-Review of Molecular Mediators. *Front Behav Neurosci* **2018,** *12*, 309.

7. Andersen, S. L., Stress, sensitive periods, and substance abuse. *Neurobiology of Stress* **2019,** *10*, 100140.

8. Understanding the Facts:Anxiety and depression. adaa.org.

9. Asnis, G. M.; Kohn, S. R.; Henderson, M.; Brown, N. L., SSRIs versus non-SSRIs in post-traumatic stress disorder: an update with recommendations. *Drugs* **2004,** *64* (4), 383-404.

10. Cipriani, A.; Furukawa, T. A.; Salanti, G.; Chaimani, A.; Atkinson, L. Z.; Ogawa, Y.; Leucht, S.; Ruhe, H. G.; Turner, E. H.; Higgins, J. P. T.; Egger, M.; Takeshima, N.; Hayasaka, Y.; Imai, H.; Shinohara, K.; Tajika, A.; Ioannidis, J. P. A.; Geddes, J. R., Comparative Efficacy and Acceptability of 21 Antidepressant Drugs for the Acute Treatment of Adults With Major Depressive Disorder:

A Systematic Review and Network Meta-Analysis. *Focus (American Psychiatric Publishing)* **2018,** *16* (4), 420-429.

11. Yang, H.; Sampson, M. M.; Senturk, D.; Andrews, A. M., Sex- and SERT-mediated differences in stimulated serotonin revealed by fast microdialysis. *ACS Chemical Neuroscience* **2015,** *6* (8), 1487-501.

12. Hiemke, C.; Hartter, S., Pharmacokinetics of selective serotonin reuptake inhibitors. *Pharmacol Ther* **2000,** *85* (1), 11-28.

13. Al-Harbi, K. S., Treatment-resistant depression: therapeutic trends, challenges, and future directions. *Patient Preference and Adherence* **2012,** *6*, 369-88.

14. Rush, A. J.; Warden, D.; Wisniewski, S. R.; Fava, M.; Trivedi, M. H.; Gaynes, B. N.; Nierenberg, A. A., STAR*D: revising conventional wisdom. *CNS Drugs* **2009,** *23* (8), 627-47.

15. Berrocoso, E.; Sanchez-Blazquez, P.; Garzon, J.; Mico, J. A., Opiates as antidepressants. *Current Pharmaceutical Design* **2009,** *15* (14), 1612-22.

16. Reindl, J. D.; Rowan, K.; Carey, A. N.; Peng, X.; Neumeyer, J. L.; McLaughlin, J. P., Antidepressant-like effects of the novel kappa opioid antagonist MCL-144B in the forced-swim test. *Pharmacology* **2008,** *81* (3), 229-35.

17. Jacobson, M. L.; Browne, C. A.; Lucki, I., Kappa Opioid Receptor Antagonists as Potential Therapeutics for Stress-Related Disorders. *Annu Rev Pharmacol Toxicol* **2020,** *60*, 615-636.

18. Cahill, C. M.; Taylor, A. M.; Cook, C.; Ong, E.; Moron, J. A.; Evans, C. J., Does the kappa opioid receptor system contribute to pain aversion? *Frontiers in Pharmacology* **2014,** *5*, 253.

19. Chappell, P. B.; Leckman, J. F.; Scahill, L. D.; Hardin, M. T.; Anderson, G.; Cohen, D. J., Neuroendocrine and behavioral effects of the selective kappa agonist spiradoline in Tourette's syndrome: a pilot study. *Psychiatry Research* **1993,** *47* (3), 267-80.

20. Chefer, V. I.; Backman, C. M.; Gigante, E. D.; Shippenberg, T. S., Kappa opioid receptors on dopaminergic neurons are necessary for kappa-mediated place aversion. *Neuropsychopharmacology* **2013,** *38* (13), 2623-31.

21. Pfeiffer, A.; Brantl, V.; Herz, A.; Emrich, H. M., Psychotomimesis mediated by kappa opiate receptors. *Science* **1986,** *233* (4765), 774-6.

22. Altieri, S.; Singh, Y.; Sibille, E., Serotonergic Pathways in Depression. In *Neurobiology of Depression*, CRC Press: 2011; Vol. 20115633, pp 143-170.

23. Altieri, S. C.; Yang, H.; O'Brien, H. J.; Redwine, H. M.; Senturk, D.; Hensler, J. G.; Andrews, A. M., Perinatal vs genetic programming of serotonin states associated with anxiety. *Neuropsychopharmacology* **2015,** *40* (6), 1456-70.

24. Holmes, A.; Murphy, D. L.; Crawley, J. N., Abnormal behavioral phenotypes of serotonin transporter knockout mice: parallels with human anxiety and depression. *Biological Psychiatry* **2003,** *54* (10), 953-9.

25. Mohammad-Zadeh, L. F.; Moses, L.; Gwaltney-Brant, S. M., Serotonin: a review. *J Vet Pharmacol Ther* **2008,** *31* (3), 187-99.

26. Varnas, K.; Halldin, C.; Hall, H., Autoradiographic distribution of serotonin transporters and receptor subtypes in human brain. *Hum Brain Mapp* **2004,** *22* (3), 246-60.

27. Nautiyal, K. M.; Hen, R., Serotonin receptors in depression: from A to B. *F1000Res* **2017,** *6*, 123.

28. Hannon, J.; Hoyer, D., Molecular biology of 5-HT receptors. *Behav Brain Res* **2008,** *195* (1), 198-213.

29. Avitsur, R.; Grinshpahet, R.; Goren, N.; Weinstein, I.; Kirshenboim, O.; Chlebowski, N., Prenatal SSRI alters the hormonal and behavioral responses to stress in female mice: Possible role for glucocorticoid resistance. *Horm Behav* **2016,** *84*, 41-9.

30. Dazzi, L.; Seu, E.; Cherchi, G.; Biggio, G., Chronic administration of the SSRI fluvoxamine markedly and selectively reduces the sensitivity of cortical serotonergic neurons to footshock stress. *Eur Neuropsychopharmacol* **2005,** *15* (3), 283-90.

31. Firk, C.; Markus, C. R., Review: Serotonin by stress interaction: a susceptibility factor for the development of depression? *J Psychopharmacol* **2007,** *21* (5), 538-44.

32. Fontaine, H. M.; Silva, P. R.; Neiswanger, C.; Tran, R.; Abraham, A. D.; Land, B. B.; Neumaier, J. F.; Chavkin, C., Stress decreases serotonin tone in the nucleus accumbens in male mice to promote aversion and potentiate cocaine preference via decreased stimulation of 5-HT1B receptors. *Neuropsychopharmacology* **2022,** *47* (4), 891-901.

33. Fuller, R. W., Serotonin receptors involved in regulation of pituitary-adrenocortical function in rats. *Behav Brain Res* **1996,** *73* (1-2), 215-9.

34. Caspi, A.; Sugden, K.; Moffitt, T. E.; Taylor, A.; Craig, I. W.; Harrington, H.; McClay, J.; Mill, J.; Martin, J.; Braithwaite, A.; Poulton, R., Influence of life stress on depression: moderation by a polymorphism in the 5-HTT gene. *Science* **2003,** *301* (5631), 386-9.

35. Kendler, K. S.; Kuhn, J. W.; Vittum, J.; Prescott, C. A.; Riley, B., The interaction of stressful life events and a serotonin transporter polymorphism in the prediction of episodes of major depression: a replication. *Arch Gen Psychiatry* **2005,** *62* (5), 529-35.

36. Devlin, A. M.; Brain, U.; Austin, J.; Oberlander, T. F., Prenatal exposure to maternal depressed mood and the MTHFR C677T variant affect SLC6A4 methylation in infants at birth. *PLoS One* **2010,** *5* (8), e12201.

37. Huang, Y.; Xu, H.; Li, H.; Yang, H.; Chen, Y.; Shi, X., Pre-gestational stress reduces the ratio of 5-HIAA to 5-HT and the expression of 5-HT1A receptor and serotonin transporter in the brain of foetal rat. *BMC Neurosci* **2012,** *13*, 22.

38. Ishiwata, H.; Shiga, T.; Okado, N., Selective serotonin reuptake inhibitor treatment of early postnatal mice reverses their prenatal stress-induced brain dysfunction. *Neuroscience* **2005,** *133* (4), 893-901.

39. Miller, J. M.; Kinnally, E. L.; Ogden, R. T.; Oquendo, M. A.; Mann, J. J.; Parsey, R. V., Reported childhood abuse is associated with low serotonin transporter binding in vivo in major depressive disorder. *Synapse* **2009,** *63* (7), 565-73.

40. Miyagawa, K.; Tsuji, M.; Fujimori, K.; Saito, Y.; Takeda, H., Prenatal stress induces anxiety-like behavior together with the disruption of central serotonin neurons in mice. *Neurosci Res* **2011,** *70* (1), 111-7.

41. St-Pierre, J.; Laurent, L.; King, S.; Vaillancourt, C., Effects of prenatal maternal stress on serotonin and fetal development. *Placenta* **2016,** *48 Suppl 1*, S66-S71.

42. Van den Hove, D. L.; Lauder, J. M.; Scheepens, A.; Prickaerts, J.; Blanco, C. E.; Steinbusch, H. W., Prenatal stress in the rat alters 5-HT1A receptor binding in the ventral hippocampus. *Brain Res* **2006,** *1090* (1), 29-34.

43. Velasquez, J. C.; Zhao, Q.; Chan, Y.; Galindo, L. C. M.; Simasotchi, C.; Wu, D.; Hou, Z.; Herod, S. M.; Oberlander, T. F.; Gil, S.; Fournier, T.; Burd, I.; Andrews, A. M.; Bonnin, A., In

Utero Exposure to Citalopram Mitigates Maternal Stress Effects on Fetal Brain Development. *ACS Chem Neurosci* **2019,** *10* (7), 3307-3317.

44. Oberlander, T. F.; Grunau, R.; Mayes, L.; Riggs, W.; Rurak, D.; Papsdorf, M.; Misri, S.; Weinberg, J., Hypothalamic-pituitary-adrenal (HPA) axis function in 3-month old infants with prenatal selective serotonin reuptake inhibitor (SSRI) antidepressant exposure. *Early Hum Dev* **2008,** *84* (10), 689-97.

45. Rayen, I.; Gemmel, M.; Pauley, G.; Steinbusch, H. W.; Pawluski, J. L., Developmental exposure to SSRIs, in addition to maternal stress, has long-term sex-dependent effects on hippocampal plasticity. *Psychopharmacology (Berl)* **2015,** *232* (7), 1231-44.

46. Schindler, A. G.; Messinger, D. I.; Smith, J. S.; Shankar, H.; Gustin, R. M.; Schattauer, S. S.; Lemos, J. C.; Chavkin, N. W.; Hagan, C. E.; Neumaier, J. F.; Chavkin, C., Stress produces aversion and potentiates cocaine reward by releasing endogenous dynorphins in the ventral striatum to locally stimulate serotonin reuptake. *The Journal of Neuroscience* **2012,** *32* (49), 17582-96.

47. Ferguson, J. M., SSRI Antidepressant Medications: Adverse Effects and Tolerability. *Prim Care Companion J Clin Psychiatry* **2001,** *3* (1), 22-27.

48. Cascade, E.; Kalali, A. H.; Kennedy, S. H., Real-World Data on SSRI Antidepressant Side Effects. *Psychiatry (Edgmont)* **2009,** *6* (2), 16-8.

49. Dong, C.; Ly, C.; Dunlap, L. E.; Vargas, M. V.; Sun, J.; Hwang, I. W.; Azinfar, A.; Oh, W. C.; Wetsel, W. C.; Olson, D. E.; Tian, L., Psychedelic-inspired drug discovery using an engineered biosensor. *Cell* **2021,** *184* (10), 2779-2792 e18.

50. Laaris, N.; Le Poul, E.; Laporte, A. M.; Hamon, M.; Lanfumey, L., Differential effects of stress on presynaptic and postsynaptic 5-hydroxytryptamine-1A receptors in the rat brain: an in vitro electrophysiological study. *Neuroscience* **1999,** *91* (3), 947-58.

51. Lanfumey, L.; Mongeau, R.; Cohen-Salmon, C.; Hamon, M., Corticosteroid-serotonin interactions in the neurobiological mechanisms of stress-related disorders. *Neurosci Biobehav Rev* **2008,** *32* (6), 1174-84.

52. Lanfumey, L.; Pardon, M. C.; Laaris, N.; Joubert, C.; Hanoun, N.; Hamon, M.; Cohen-Salmon, C., 5-HT1A autoreceptor desensitization by chronic ultramild stress in mice. *Neuroreport* **1999,** *10* (16), 3369-74.

53. Man, M. S.; Young, A. H.; McAllister-Williams, R. H., Corticosterone modulation of somatodendritic 5-HT1A receptor function in mice. *J Psychopharmacol* **2002,** *16* (3), 245-52.

54. Leitch, M. M.; Ingram, C. D.; Young, A. H.; McQuade, R.; Gartside, S. E., Flattening the corticosterone rhythm attenuates 5-HT1A autoreceptor function in the rat: relevance for depression. *Neuropsychopharmacology* **2003,** *28* (1), 119-25.

55. Holmes, M. C.; French, K. L.; Seckl, J. R., Modulation of serotonin and corticosteroid receptor gene expression in the rat hippocampus with circadian rhythm and stress. *Brain Res Mol Brain Res* **1995,** *28* (2), 186-92.

56. Klaassen, T.; Riedel, W. J.; van Praag, H. M.; Menheere, P. P.; Griez, E., Neuroendocrine response to meta-chlorophenylpiperazine and ipsapirone in relation to anxiety and aggression. *Psychiatry Res* **2002,** *113* (1-2), 29-40.

57. Lefebvre, H.; Contesse, V.; Delarue, C.; Feuilloley, M.; Hery, F.; Grise, P.; Raynaud, G.; Verhofstad, A. A.; Wolf, L. M.; Vaudry, H., Serotonin-induced stimulation of cortisol secretion

from human adrenocortical tissue is mediated through activation of a serotonin4 receptor subtype. *Neuroscience* **1992,** *47* (4), 999-1007.

58. Adell, A.; Garcia-Marquez, C.; Armario, A.; Gelpi, E., Chronic stress increases serotonin and noradrenaline in rat brain and sensitizes their responses to a further acute stress. *J Neurochem* **1988,** *50* (6), 1678-81.

59. Davis, S.; Heal, D. J.; Stanford, S. C., Long-lasting effects of an acute stress on the neurochemistry and function of 5-hydroxytryptaminergic neurones in the mouse brain. *Psychopharmacology (Berl)* **1995,** *118* (3), 267-72.

60. De Kloet, E. R.; Kovacs, G. L.; Szabo, G.; Telegdy, G.; Bohus, B.; Versteeg, D. H., Decreased serotonin turnover in the dorsal hippocampus of rat brain shortly after adrenalectomy: selective normalization after corticosterone substitution. *Brain Res* **1982,** *239* (2), 659-63.

61. De Kloet, E. R.; Versteeg, D. H.; Kovacs, G. L., Aldosterone blocks the response to corticosterone in the raphe-hippocampal serotonin system. *Brain Res* **1983,** *264* (2), 323-7.

62. Nuller, J. L.; Ostroumova, M. N., Resistance to inhibiting effect of dexamethasone in patients with endogenous depression. *Acta Psychiatr Scand* **1980,** *61* (2), 169-77.

63. Grudt, T. J.; Williams, J. T., Opioid receptors and the regulation of ion conductances. *Reviews in the Neurosciences* **1995,** *6* (3), 279-86.

64. Chavkin, C.; James, I. F.; Goldstein, A., Dynorphin is a specific endogenous ligand of the kappa opioid receptor. *Science* **1982,** *215* (4531), 413-5.

65. Nabeshima, T.; Katoh, A.; Wada, M.; Kameyama, T., Stress-induced changes in brain Met-enkephalin, Leu-enkephalin and dynorphin concentrations. *Life Sci* **1992,** *51* (3), 211-7.

66. Land, B. B.; Bruchas, M. R.; Lemos, J. C.; Xu, M.; Melief, E. J.; Chavkin, C., The dysphoric component of stress is encoded by activation of the dynorphin kappa-opioid system. *The Journal of Neuroscience* **2008,** *28* (2), 407-14.

67. Shirayama, Y.; Ishida, H.; Iwata, M.; Hazama, G. I.; Kawahara, R.; Duman, R. S., Stress increases dynorphin immunoreactivity in limbic brain regions and dynorphin antagonism produces antidepressant-like effects. *Journal of Neurochemistry* **2004,** *90* (5), 1258-68.

68. McLaughlin, J. P.; Marton-Popovici, M.; Chavkin, C., Kappa opioid receptor antagonism and prodynorphin gene disruption block stress-induced behavioral responses. *The Journal of Neuroscience* **2003,** *23* (13), 5674-83.

69. Cunningham, C. L.; Gremel, C. M.; Groblewski, P. A., Drug-induced conditioned place preference and aversion in mice. *Nature Protocols* **2006,** *1* (4), 1662-70.

70. Prus, A. J.; James, J. R.; Rosecrans, J. A., Chapter 4 Conditioned Place Preference. 18.

71. Shippenberg, T. S.; Rea, W., Sensitization to the behavioral effects of cocaine: modulation by dynorphin and kappa-opioid receptor agonists. *Pharmacology Biochemistry and Behavior* **1997,** *57* (3), 449-55.

72. Carlezon, W. A., Jr.; Beguin, C.; DiNieri, J. A.; Baumann, M. H.; Richards, M. R.; Todtenkopf, M. S.; Rothman, R. B.; Ma, Z.; Lee, D. Y.; Cohen, B. M., Depressive-like effects of the kappa-opioid receptor agonist salvinorin A on behavior and neurochemistry in rats. *Journal of Pharmacology and Experimental Therapeutics* **2006,** *316* (1), 440-7.

73. Mague, S. D.; Pliakas, A. M.; Todtenkopf, M. S.; Tomasiewicz, H. C.; Zhang, Y.; Stevens, W. C., Jr.; Jones, R. M.; Portoghese, P. S.; Carlezon, W. A., Jr., Antidepressant-like effects of

kappa-opioid receptor antagonists in the forced swim test in rats. *Journal of Pharmacology and Experimental Therapeutics* **2003,** *305* (1), 323-30.

74. Bethea, C. L.; Centeno, M. L.; Cameron, J. L., Neurobiology of stress-induced reproductive dysfunction in female macaques. *Mol Neurobiol* **2008,** *38* (3), 199-230.

75. Newton, S. S.; Thome, J.; Wallace, T. L.; Shirayama, Y.; Schlesinger, L.; Sakai, N.; Chen, J.; Neve, R.; Nestler, E. J.; Duman, R. S., Inhibition of cAMP response element-binding protein or dynorphin in the nucleus accumbens produces an antidepressant-like effect. *J Neurosci* **2002,** *22* (24), 10883-90.

76. Bruchas, M. R.; Land, B. B.; Chavkin, C., The dynorphin/kappa opioid system as a modulator of stress-induced and pro-addictive behaviors. *Brain Res* **2010,** *1314*, 44-55.

77. Simmons, S. C.; Shepard, R. D.; Gouty, S.; Langlois, L. D.; Flerlage, W. J.; Cox, B. M.; Nugent, F. S., Early life stress dysregulates kappa opioid receptor signaling within the lateral habenula. *Neurobiol Stress* **2020,** *13*, 100267.

78. Chang, L.; Kigar, S. L.; Ho, J. H.; Cuarenta, A.; Gunderson, H. C.; Baldo, B. A.; Bakshi, V. P.; Auger, A. P., Early life stress alters opioid receptor mRNA levels within the nucleus accumbens in a sex-dependent manner. *Brain Res* **2019,** *1710*, 102-108.

79. Lutz, P. E.; Gross, J. A.; Dhir, S. K.; Maussion, G.; Yang, J.; Bramoulle, A.; Meaney, M. J.; Turecki, G., Epigenetic Regulation of the Kappa Opioid Receptor by Child Abuse. *Biol Psychiatry* **2018,** *84* (10), 751-761.

80. Karkhanis, A. N.; Rose, J. H.; Weiner, J. L.; Jones, S. R., Early-Life Social Isolation Stress Increases Kappa Opioid Receptor Responsiveness and Downregulates the Dopamine System. *Neuropsychopharmacology* **2016,** *41* (9), 2263-74.

81. Crowley, N. A.; Kash, T. L., Kappa opioid receptor signaling in the brain: Circuitry and implications for treatment. *Prog Neuropsychopharmacol Biol Psychiatry* **2015,** *62*, 51-60.

82. Hayes, A. G.; Stewart, B. R., Effect of mu and kappa opioid receptor agonists on rat plasma corticosterone levels. *Eur J Pharmacol* **1985,** *116* (1-2), 75-9.

83. Iyengar, S.; Kim, H. S.; Wood, P. L., Kappa opiate agonists modulate the hypothalamic-pituitary-adrenocortical axis in the rat. *J Pharmacol Exp Ther* **1986,** *238* (2), 429-36.

84. Ur, E.; Wright, D. M.; Bouloux, P. M.; Grossman, A., The effects of spiradoline (U-62066E), a kappa-opioid receptor agonist, on neuroendocrine function in man. *Br J Pharmacol* **1997,** *120* (5), 781-4.

85. Wittmann, W.; Schunk, E.; Rosskothen, I.; Gaburro, S.; Singewald, N.; Herzog, H.; Schwarzer, C., Prodynorphin-derived peptides are critical modulators of anxiety and regulate neurochemistry and corticosterone. *Neuropsychopharmacology* **2009,** *34* (3), 775-85.

86. Bruchas, M. R.; Land, B. B.; Aita, M.; Xu, M.; Barot, S. K.; Li, S.; Chavkin, C., Stress-induced p38 mitogen-activated protein kinase activation mediates kappa-opioid-dependent dysphoria. *The Journal of Neuroscience* **2007,** *27* (43), 11614-23.

87. Nikolarakis, K. E.; Almeida, O. F.; Herz, A., Stimulation of hypothalamic beta-endorphin and dynorphin release by corticotropin-releasing factor (in vitro). *Brain Res* **1986,** *399* (1), 152-5.

88. Song, Z. H.; Takemori, A. E., Stimulation by corticotropin-releasing factor of the release of immunoreactive dynorphin A from mouse spinal cords in vitro. *Eur J Pharmacol* **1992,** *222* (1), 27-32.

89. Spanagel, R.; Shippenberg, T. S., Modulation of morphine-induced sensitization by endogenous kappa opioid systems in the rat. *Neurosci Lett* **1993,** *153* (2), 232-6.

90. Van't Veer, A.; Yano, J. M.; Carroll, F. I.; Cohen, B. M.; Carlezon, W. A., Jr., Corticotropin-releasing factor (CRF)-induced disruption of attention in rats is blocked by the kappa-opioid receptor antagonist JDTic. *Neuropsychopharmacology* **2012,** *37* (13), 2809-16.

91. Bruchas, M. R.; Yang, T.; Schreiber, S.; Defino, M.; Kwan, S. C.; Li, S.; Chavkin, C., Long-acting kappa opioid antagonists disrupt receptor signaling and produce noncompetitive effects by activating c-Jun N-terminal kinase. *J Biol Chem* **2007,** *282* (41), 29803-11.

92. Reichard, K. L.; Newton, K. A.; Rivera, Z. M. G.; Sotero de Menezes, P. M.; Schattauer, S. S.; Land, B. B.; Chavkin, C., Regulation of Kappa Opioid Receptor Inactivation Depends on Sex and Cellular Site of Antagonist Action. *Mol Pharmacol* **2020,** *98* (5), 548-558.

93. Buda, J. J.; Carroll, F. I.; Kosten, T. R.; Swearingen, D.; Walters, B. B., A Double-Blind, Placebo-Controlled Trial to Evaluate the Safety, Tolerability, and Pharmacokinetics of Single, Escalating Oral Doses of JDTic. *Neuropsychopharmacology* **2015,** *40* (9), 2059-65.

94. Lowe, S. L.; Wong, C. J.; Witcher, J.; Gonzales, C. R.; Dickinson, G. L.; Bell, R. L.; Rorick-Kehn, L.; Weller, M.; Stoltz, R. R.; Royalty, J.; Tauscher-Wisniewski, S., Safety, tolerability, and pharmacokinetic evaluation of single- and multiple-ascending doses of a novel kappa opioid receptor antagonist LY2456302 and drug interaction with ethanol in healthy subjects. *J Clin Pharmacol* **2014,** *54* (9), 968-78.

95. Dagher, M.; Perrotta, K. A.; Erwin, S. A.; Hachisuka, A.; Iyer, R.; Masmanidis, S. C.; Yang, H.; Andrews, A. M., Optogenetic Stimulation of Midbrain Dopamine Neurons Produces Striatal Serotonin Release. *ACS Chem Neurosci* **2022,** *13* (7), 946-958.

96. Niederkofler, V.; Asher, T. E.; Dymecki, S. M., Functional Interplay between Dopaminergic and Serotonergic Neuronal Systems during Development and Adulthood. *ACS Chemical Neuroscience* **2015,** *6* (7), 1055-1070.

97. Ehrich, J. M.; Messinger, D. I.; Knakal, C. R.; Kuhar, J. R.; Schattauer, S. S.; Bruchas, M. R.; Zweifel, L. S.; Kieffer, B. L.; Phillips, P. E.; Chavkin, C., Kappa Opioid Receptor-Induced Aversion Requires p38 MAPK Activation in VTA Dopamine Neurons. *The Journal of Neuroscience* **2015,** *35* (37), 12917-31.

98. Ebner, S. R.; Roitman, M. F.; Potter, D. N.; Rachlin, A. B.; Chartoff, E. H., Depressive-like effects of the kappa opioid receptor agonist salvinorin A are associated with decreased phasic dopamine release in the nucleus accumbens. *Psychopharmacology (Berl)* **2010,** *210* (2), 241-52.

99. Van't Veer, A.; Carlezon, W. A., Jr., Role of kappa-opioid receptors in stress and anxiety-related behavior. *Psychopharmacology (Berl)* **2013,** *229* (3), 435-52.

100. Land, B. B.; Bruchas, M. R.; Schattauer, S.; Giardino, W. J.; Aita, M.; Messinger, D.; Hnasko, T. S.; Palmiter, R. D.; Chavkin, C., Activation of the kappa opioid receptor in the dorsal raphe nucleus mediates the aversive effects of stress and reinstates drug seeking. *Proceedings of the National Academy of Sciences* **2009,** *106* (45), 19168-73.

101. Tao, R.; Auerbach, S. B., Opioid receptor subtypes differentially modulate serotonin efflux in the rat central nervous system. *Journal of Pharmacology and Experimental Therapeutics* **2002,** *303* (2), 549-56.

102. Tao, R.; Auerbach, S. B., mu-Opioids disinhibit and kappa-opioids inhibit serotonin efflux in the dorsal raphe nucleus. *Brain Research* **2005,** *1049* (1), 70-9.

103. Pirino, B. E.; Spodnick, M. B.; Gargiulo, A. T.; Curtis, G. R.; Barson, J. R.; Karkhanis, A. N., Kappa-opioid receptor-dependent changes in dopamine and anxiety-like or approach-avoidance behavior occur differentially across the nucleus accumbens shell rostro-caudal axis. *Neuropharmacology* **2020,** *181*, 108341.

104. Tejeda, H. A.; Natividad, L. A.; Orfila, J. E.; Torres, O. V.; O'Dell, L. E., Dysregulation of kappa-opioid receptor systems by chronic nicotine modulate the nicotine withdrawal syndrome in an age-dependent manner. *Psychopharmacology (Berl)* **2012,** *224* (2), 289-301.

105. Maisonneuve, I. M.; Archer, S.; Glick, S. D., U50,488, a kappa opioid receptor agonist, attenuates cocaine-induced increases in extracellular dopamine in the nucleus accumbens of rats. *Neurosci Lett* **1994,** *181* (1-2), 57-60.

106. Sundaramurthy, S.; Annamalai, B.; Samuvel, D. J.; Shippenberg, T. S.; Jayanthi, L. D.; Ramamoorthy, S., Modulation of serotonin transporter function by kappa-opioid receptor ligands. *Neuropharmacology* **2017,** *113*, 281-292.

107. Yoshioka, M.; Matsumoto, M.; Togashi, H.; Smith, C. B.; Saito, H., Opioid receptor regulation of 5-hydroxytryptamine release from the rat hippocampus measured by in vivo microdialysis. *Brain Research* **1993,** *613* (1), 74-9.

108. Di Benedetto, M.; D'Addario, C.; Collins, S.; Izenwasser, S.; Candeletti, S.; Romualdi, P., Role of serotonin on cocaine-mediated effects on prodynorphin gene expression in the rat brain. *J Mol Neurosci* **2004,** *22* (3), 213-22.

109. D'Addario, C.; Di Benedetto, M.; Izenwasser, S.; Candeletti, S.; Romualdi, P., Role of serotonin in the regulation of the dynorphinergic system by a kappa-opioid agonist and cocaine treatment in rat CNS. *Neuroscience* **2007,** *144* (1), 157-64.

CHAPTER 2

Prenatal citalopram exposure promotes resilience in male offspring exposed to maternal stress

The information in this chapter is in preparation for submission and adapted here.

Merel Dagher*, Sara E. Christiansen*, Katie A. Perrotta, Olena Lukoyanova, Audrey Nashner, Weiye Dai, Julia C. Brock, Alexandre Bonnin, and Anne M. Andrews

*Co-first author

Abstract

Mood and anxiety disorders are highly prevalent during pregnancy and can lead to adverse maternal and offspring outcomes. Selective serotonin reuptake inhibitors are the most common medications used to treat mood and anxiety disorders. Both human and animal studies suggest that serotonin signaling plays an important role in the vulnerability to and manifestation of stress-associated affective disorders. Moreover, the serotonin system is an early orchestrator of brain development. In this study, pregnant mice underwent chronic, unpredictable stress during the latter two-thirds of their pregnancies using ethologically relevant and/or mild stressors. Some of the mice received the serotonin-selective reuptake inhibitor antidepressant citalopram (Celexa) concomitantly in their drinking water. After birth, brain tissue serotonin levels at three developmentally relevant timepoints for serotonin system maturation were measured in the offspring. A subset of the adult offspring was assessed for long-term behavioral effects of *in utero* exposure to stress and/or citalopram. Finally, male adult offspring underwent microdialysis in the ventral hippocampus to investigate neurochemical effects. Offspring of stressed mothers had higher serotonin tissue levels and protein concentrations in the forebrain at postnatal day seven compared to control animals. Male adult offspring displayed greater anxiety-like behavior and stress responsiveness than sex-matched control mice. These effects were rescued in male mice whose mothers were administered citalopram. No changes were observed in basal or stimulated ventral hippocampal extracellular serotonin levels during adulthood. Yet, male adults exposed to *in utero* stress had increased kappa opioid receptor agonist-induced serotonin release in the presence of serotonin transporter blockade, which was attenuated by *in utero* exposure to citalopram. These findings suggest prenatal stress

negatively impacts neurochemical and behavioral outcomes in offspring that persist into adulthood, which could be reversed with concomitant SSRI treatment during pregnancy.

*Author Contributions: M.D. and S.E.C. contributed equally to this work. S.E.C. was the primary contributor for HPLC neurochemical and microdialysis experiments. M.D. was the primary contributor for the CUS paradigm, and all behavioral experiments. Experiments were designed by M.D., S.E.C., K.A.P., A.B., and A.M.A. and carried out by M.D., S.E.C., K.A.P., O.L., A.N., W.D., and J.B. Data Analyses were carried out by M.D., S.E.C., K.A.P., and W.D. The article was written by M.D., S.E.C., K.A.P., and A.M.A. with input from all authors.

Introduction

According to the Center for Disease Control (CDC), one in seven women of reproductive age is prescribed medication for mood or anxiety disorders. Estimates of perinatal depression or anxiety range from 5-25%.[1] Approximately 3% of pregnant women with mood or anxiety disorders take medication for the treatment of their mood or anxiety disorder.[2] The safety of antidepressant use during pregnancy remains contested due to incomplete knowledge of how exposure affects fetal development and long-term outcomes. By contrast, untreated maternal mood and anxiety disorders have known adverse health outcomes for offspring.[3-5] Epidemiological studies have shown that untreated mood or anxiety disorders during pregnancy increase risk for similar disorders in offspring.[6,7] In fact, this risk doubles when compared to offspring who were not exposed to maternal depressive or anxiety disorders during pregnancy.[8]

The most commonly prescribed medications for treating depression and anxiety are the selective serotonin reuptake inhibitors (SSRIs).[9] The SSRIs are in FDA categories C or D of pregnancy medications because animal studies have identified some potential risks of SSRIs.[10,11] Furthermore, epidemiological studies show associations between prenatal SSRI exposure and physiological and cognitive dysfunction.[12-14] However, due to the lack of randomized control trials, risk-benefit profiles of the SSRIs have not been investigated in the absence of confounding variables, *e.g.*, maternal disorder severity.[15-17] The benefits of minimizing the effects of untreated maternal mood and anxiety disorders may outweigh the potential effects of SSRIs on offspring.[18,19]

In humans, stress is a risk factor for developing mood and anxiety disorders.[20-23] In mice, exposure to prenatal stress produced increased anxiety-like behavior that was

associated with increased numbers of serotonin neurons in the dorsal raphe nucleus(DRN).[24] *In utero* stress exposure with concomitant SSRI treatment has been less well studied. One study showed that SSRI treatment in rodents during the early, but not late, postnatal period attenuated changes induced by prenatal stress in terms of HPA axis response, hippocampal serotonin levels, and synaptic density.[25] Another study showed that treatment of dams with the SSRI fluoxetine starting on postnatal day one attenuated maternal stress effects on offspring.[26] Velasquez *et al.* previously showed that administration of citalopram during an *in utero* maternal stress paradigm reversed the effects of stress on serotonin levels in fetuses at embryonic day 17.[27] We hypothesized that the effects of citalopram in mitigating adverse stress effects would carry into postnatal development and have prolonged protective effects throughout development and into adulthood.

Interactions between the kappa opioid receptor (KOR) and serotonin systems have been identified in stress, anxiety, and depression research.[28] Land *et. al* utilized an antibody against phosphorylated KORs and determined that stress induced dynorphin release and KOR activation in the dorsal raphe, nucleus accumbens, hippocampus, and ventral tegmental area.[29] Repeated forced swim stress or KOR agonist administration increased ventral striatum SERT surface expression. Increased SERT surface expression was attenuated by microinjection of the KOR antagonist, norBNI, into the DRN but not the nucleus accumbens.[30] This finding suggests that KOR activation within the dorsal raphe mediates SERT surface expression during stressful events. Moreover, constitutive gene deletion of one (SERT+/-) or both (SERT-/-) SERT alleles prevented KOR-agonist induced conditioned place aversion (CPA).[31]

Here, we investigated the effects of concomitant maternal stress and citalopram administration on offspring during the early postnatal period and adulthood. We hypothesized that increased serotonin levels in early postnatal forebrain tissue of offspring born to stressed dams would be attenuated in offspring concomitantly exposed to citalopram. Moreover, we hypothesized that adult offspring born to stressed dams would display increased anxiety-related behavior, which would be rescued by maternal SSRI administration. Finally, we hypothesized adult offspring born to stress mothers would have increased basal and stimulated serotonin levels in the ventral hippocampus (vHPC).

Methods

Animals

Timed-pregnant CD-1 mice (*N*=75 purchase, 73 were pregnant) were purchased from Charles River Laboratories (Hollister, CA) were studied. The dams were 12-24 weeks old at the beginning of pregnancy. Dams were either singly housed (stressed groups) or housed in groups of 2-4 mice per cage until embryonic day 17 (E17). All dams were singly housed at E18 until their offspring were weaned at postnatal day 21 (P21). Dams that received citalopram were dosed *via* drinking water. Citalopram hydrobromide (TCI America Cat#2370) was dissolved in 1.5% sucrose (260 mg/L).[32] Oral concentrations were based on concentrations producing antidepressant effects in mice.[33,34] This dose was found to produce blood serum levels of CIT that fall within the human therapeutic range(30-200ng/mL[35]) and crosses placental barrier to fetus.[32] Each water bottle was filled with ~200 mL citalopram solution and was changed every three days. Control and CUS only groups received plain drinking water. Water bottles for all groups were weighed daily to monitor liquid intake. Food and water were available *ad libitum* throughout the study, except for E16, when all dams were food-deprived for 22-24 h for the novelty suppressed feeding (NSF) test.

After weaning, offspring were housed in 2-5 same-sex siblings per cage. The light-dark cycle (12/12 h) was set to lights on at 0730 h (ZT0) in the colony room. The same light schedule was maintained in the rooms where behavior tests and microdialysis were carried out. The Association for Assessment and Accreditation of Laboratory Animal Care International has fully accredited UCLA. All animal care and use met the requirements of the NIH Guide for the Care and Use of Laboratory Animals, revised 2011. The UCLA Chancellor's

Animal Research Committee (Institutional Animal Care and Use Committee) preapproved all procedures.

Maternal chronic unpredictable stress paradigm

Experiments were carried out in six different cohorts of mice over four years. In the first cohort only control and maternal chronic unpredictable stress (CUS) groups were studied. Latter cohorts included control, CUS, CUS plus citalopram (CUS+CIT), and CIT. Initial cohorts only contained control and CUS groups to determine if stress induced embryonic changes in serotonin[32] persisted in postnatal development. The first half of cohorts were used for offspring tissue and behavioral testing, while the latter half were used for offspring behavior testing and microdialysis.

Timed pregnant female mice arrived on E7 and were exposed to chronic unpredictable stress from E8 through E14, equivalent to the post-conception day 22-64 in humans.[36] On E8, pregnant females in the stress groups were restrained, their ears were clipped for identification, and they were given an intraperitoneal (ip) saline injection as initial stressors. The maternal CUS paradigm was carried out as previously described[32] and is detailed in **Table S2.1**. Mice in the stressed groups were singly housed throughout the duration of the stress paradigm. On E9, stress dams were exposed to a 1% 2,4,5-trimethylthiazole (Sigma Aldrich #W332518) in water (v/v), a volatile component of fox urine, which was placed on a nestlet square (200 μL) on the wire lid of their cage for 15 min. On E10, dams in the stress group were exposed to constant light overnight from ZT12-24. On E11, stressed dams were placed in a 3.81 cm in diameter plastic restraint tube for 30 min.[37] On E12, they were exposed to constant white noise (70 dB) overnight from ZT12-24. The cage of each stressed dam was tilted at a 45° angle on E13 for the duration of

the light cycle (ZT0-12). On E14, stress dams were exposed to 83g of sani chip cage bedding saturated with 400 mL water overnight from ZT12-24. On E15-17, all pregnant females, irrespective of group, underwent the following behavior tests, which were also stressors: open field test (OFT; E15), forced swim test (FST; E16), and the novelty suppressed feeding test (NSF; E17).

Postnatal dissection and tissue collection

Offspring brains for neurochemical analyses were collected on P7, P14, and P21. At each postnatal developmental timepoint, 1-3 pups were randomly selected from each litter with fewer pups taken from smaller litters. The random selection process involved spreading out the pile of pups to pick ones in different areas of the nest as to not bias based on litter dynamics, *i.e.* not only picking pups from top of pile. The pups were weighed, their sex was identified, if possible, and they were transported individually to the procedure room. Pups were immediately sacrificed *via* decapitation without anesthesia. Their brains were rapidly removed and placed briefly in deionized water. The following brain regions were collected at P7: forebrain, midbrain, and hindbrain.[32] At P14 and P21, frontal cortex, hypothalamus, hippocampus, brain stem, striatum, and the intact remaining hemisphere were collected. Brain tissue samples were placed in Eppendorf tubes and immediately frozen on dry ice before storage in a -80° C freezer.

Tissue Sample Analysis

All analyses were performed using an Amuza HTEC-500 integrated HPLC system (Amuza Corporation, San Diego, CA) with an Amuza Insight autosampler for injecting standards and brain tissue extracts. Chromatographic separation for monoamine neurotransmitters and metabolites was attained using an Agilent Poroshell 120 column

(SB-C18, 3.0 mm × 100 mm, 2.7 μm particle size). Mobile phase for neurotransmitters consisted of 0.1 M monochloroacetic Acid (Sigma #402923), 0.2-0.4 g/L octanesulfonic acid (Acros #41636), pH 2.6, 50 mg/L EDTA·Na_2 (Sigma #03682), 0.01% triethylamine (EMD TX1200) and 5-10% acetonitrile (EMD AX0145) in water purified *via* a Milli-Q Synthesis A10 system (EMD Millipore Corporation, Billerica, MA).

Amino acid analyses employed a Phenomenex Kinetex LC Column (C18, 100 mm × 3 mm, 2.6 μm particle size, #00D-4462-Y0) column. The amino acid mobile phase consisted of 0.05-0.2 M sodium phosphate monobasic (Fluka #17844), 50 mg/L EDTA·Na_2 (Sigma #03682), pH 7.3-7.5, and 20-25% MeOH (EMD #MMX04751) in water purified *via* a Milli-Q Synthesis A10 system.

Column temperatures were maintained at 21-35 °C. The volumetric flow rates were 300-525 μL/min. Electrochemical detection was performed using an Amuza pure graphite (PG) working electrode with an applied potential of +600 mV *vs.* a Ag/AgCl reference electrode. Standards were prepared for serotonin (Sigma #H9523), 5-hydroxyindoleacetic acid 5-HIAA (Sigma # H8876), norepinephrine (Sigma # A9512), dopamine (Sigma # H8502), 3,4-dihydroxyphenylacetic acid (DOPAC) (Sigma #850217), homovanillic acid (HVA) (Sigma # H1252), phenylalanine (Sigma #78019), tryptophan (Sigma #51145), tyrosine (Sigma #93829), valine (Sigma #94619), isoleucine (Sigma #12752), and leucine (Sigma #L8000) in ice-cold sonication solution (0.1 M glacial acetic acid and 1 mg/mL EDTA-Na_2). Standard curves, which were run with each group of samples, encompassed physiological concentration ranges (31-500 nM). Chromatographic run times were 12-18 min for neurotransmitters and 20-25 min for amino acids.

Behavior tests

Elevated Plus Maze

The elevated plus maze (EPM) was used to assess avoidance of anxiogenic spaces.[38,39] A single maze was used throughout the study with two opposing open arms (30 cm length × 5 cm width), two opposing closed arms (30 cm length × 5 cm width × 15 cm height), and with a center (5 cm × 5 cm) zone connecting the arms. The maze was raised 38.5 cm from the floor. The open arms had a 0.5-cm lip around the edges of the arms to prevent animals from falling. The closed arms had clear Plexiglas walls for even light levels across all arms. The floor of the maze was black Plexiglas. During testing, mice that were naïve to the apparatus were placed on the center platform facing a closed arm and allowed to explore the maze freely for 5 min. The maze was cleaned with Accel solution and dried between same-sex mice. When switching between male and female mice, the apparatus was cleaned with 70% ethanol solution followed by Accel solution.

Behavior was recorded and analyzed using the ANYmaze behavioral tracking system (Stoelting Co., Wood Dale, IL). Parameters quantified included latency to first open arm entry, open arm distance, closed arm distance, %open arm time, %closed arm time, %open arm distance, %closed arm distance, total distance traveled and speed. Time in the closed or open arms were analyzed as a percentage of total arm time excluding time spent in the center zone of the maze. Likewise, distance traveled in the open or closed arms were analyzed as a percentage of total arm distance excluding the distance traveled in the center zone of the maze.

Open Field Test

Locomotor activity in an open field test (OFT) was assessed using ANYmaze. Open field arenas were 50 cm × 50 cm with 40-cm walls. The center area was defined by a 22 cm × 22 cm central square. Animals were considered in the center after 60% of the body entered the center area. Mice were placed in a corner of the open field and allowed to freely explore for 30 min. Total distance traveled (m) and the ratio of center distance to total distance were determined. Additionally, time spent exploring the center region was analyzed. The open field arenas were thoroughly cleaned with Accel solution and 70% ethanol and allowed to dry between mice.

Forced Swim Test

The forced swim test (FST) was carried out as previously described with minor modifications.[27] Briefly, each mouse was placed in a clear glass cylinder containing autoclaved room temperature water (22±1 °C) at a depth of 15 cm. Immobility was tracked using ANYMaze software during 6-min swim sessions. Afterward, mice were transferred to a warm environment while their fur dried before being returned to their home cages. Cylinders were emptied, cleaned with Accel solution, and refilled with fresh water between mice. Time spent immobile during the last 4 min of each 6 min trial was summed.

Novelty Suppressed Feeding

The novelty suppressed feeding (NSF) test measures latency to eat in a novel environment and is performed by adapting previously used procedures.[40] Mice were weighed, singly housed, and then fasted for 22-24 h prior to NSF testing. Mice were weighed again before testing. Mice that lost >13% of their body weight within the fasting period were excluded from testing and immediately provided free access to food and water in their home

cages. The 13% cut-off was determined empirically by testing different fasting protocols in CD-1 mice.

The latency for mice to bite a pellet in the home cage they were fasted in was determined first.[41] Once the mice took a bite of the pellet or 5 min had passed, whichever occurred first, the mice were then transferred to the novel arena. Mice were placed at the edge of the novel arena that had a food pellet secured on a brightly lit white platform. The rest of the arena was dark and covered. The latency for mice to bite the pellet in the novel arena was then determined. After the mice bit the pellet or 10 min elapsed, they were transferred to a clean cage with free access to food and water. A subset of mice were transferred back to their fasting cages with one pellet of food. The pellets were weighed prior to and 10 min after mice were given free access to the food pellet to determine food intake. Mice were then transferred to a clean cage with free access to food and water.

Microdialysis

Male offspring (*N*=25) undergoing microdialysis were implanted with guide cannulas at 3-6 months of age. Surgeries were carried out under aseptic conditions with isoflurane anesthesia, and carprofen and bupivacaine as systemic and local analgesics, on a KOPF Model 1900 Stereotaxic Alignment System (KOPF, Tujunga, CA). A CMA/7 guide cannula (Harvard Apparatus #CMAP000138) for a microdialysis probe was implanted with the tip in the vHPC (AP -3.6 mm, ML ±3.2 mm, DV -1.5 mm from Bregma). Each guide cannula was secured to the skull with Bosworth Trim II (Henry Schein #2509679). Animals recovered from surgery for at least three days before microdialysis. Following each surgery, mice were given twice daily carprofen injections (5 mg/kg, 1 mg/mL, subcutaneously) for the first three days.

On the night before the first testing (ZT10-12), each mouse was transferred to the testing room in its home cage where a CMA/7 microdialysis probe (2 mm length, 6 kDa cutoff, metal free, CMA8010772) was inserted into the guide cannula. Subjects were placed into a new, smaller cage that had bedding from their home cage. Artificial cerebrospinal fluid (aCSF) (147 mM NaCl (Fluka #73575), 3.5 mM KCl (Fluka #05257), 1.0 mM $CaCl_2$ (Aldrich #499609), 1.0 mM NaH_2PO_4 (Fluka #17844), 2.5 mM $NaHCO_3$ (Fluka #88208), 1.2 mM $MgCl_2$ (Aldrich #449172), pH 7.3 ± 0.03 was continuously perfused through the probe *via* a liquid swivel (375/D/22QM, Instech Laboratories Inc., Plymouth Meeting, PA) at 0.3 μL/min for 14-16 h to stabilize the tissue around the probe. Subjects were tethered to the liquid swivel but otherwise could move freely in their home cages during the entirety of testing.

Microdialysis experiments were carried out between ZT1-8 as previously described.[42-44] Basal dialysate samples were collected from ZT1-2, followed by three high K+ stimulations each lasting 5 min, separated by an hour of aCSF infusion from ZT2-5. After the last high K+ stimulation, animals were either (1) perfused with 10 μM citalopram into the vHPC for 2 h, (2) systemically injected with 10 mg/kg, ip, U50,588H (Sigma-Aldrich #D8040) or U69,593 (Sigma-Aldrich #U103), then perfused with 10 μM citalopram into the vHPC for 2 h, or (3) perfused with 10 μM citalopram into the vHPC for 2 h followed by an ip injection of 10 mg/kg U50,588 or U69,593.

Doses for citalopram, U50,588, and U69,593 were determined empirically through pilot experiments. Citalopram was perfused at a concentration of 10 μM into the ventral hippocampus. The U50,588 dose was determined in a conditioned place aversion behavioral assay, where 10 mg/kg ip was found to induce the greatest aversion to the drug-paired side

in male mice. Due to issues with manufacturer availability of U50,588, the kappa opioid agonist U69,593 at 10 mg/kg ip was substituted for U50,588 in the last *N*=7 mice.

Analysis of microdialysis samples was performed immediately after collection of each sample, *i.e.*, online, using an Amuza HTEC-500 integrated HPLC system (Amuza Corporation, San Diego, CA) equipped with an Amuza Insight autosampler used for injecting standards and an Amuza EAS-20s online autoinjector for collecting and injecting dialysate samples. Chromatographic separation was achieved using an Amuza PP-ODS III column (4.6 mm ID × 30 mm length, 2 μm particle diameter) and a phosphate-buffered mobile phase with 14.89 g/L NaH_2PO_4 (Fluka #17844), 1.02 g/L Na_2HPO_4 (Thermo Scientific AC448160050), 2% MeOH (EMD #MX0475), 50 mg/L EDTA·Na_2 (Sigma #03682), and 600 mg/L sodium decanesulfonate (TCI #I0348) in Optima LC/MS grade water (Fisher Scientific CAS# 7732-18-5).

The column temperature was maintained at 25 °C. The volumetric flow rate was 500 μL/min. Electrochemical detection was performed using an Amuza WE-3G graphite working electrode with an applied potential of +450 mV *vs.* a Ag/AgCl reference electrode. Dopamine (Sigma #H8502) and serotonin (Sigma #H9523) standards were prepared in a 1:1 mixture of mobile phase and aCSF. Standard curves, which were verified weekly, encompassed physiological concentration ranges (31pM-10 nM). All online dialysate samples were collected at 5 min intervals at a dialysate flow rate of 2.5 μL/min and injected immediately onto the HPLC system for analysis. The ES280 PowerChrom Chromatography Data System (CDS) Software (eDAQ, Denistone East, Australia) was used to collect, display, and analyze all chromatographic peaks.

Statistical analysis

Statistical analyses were carried out using Prism, v.9.3.0 (GraphPad Inc., La Jolla, CA). Data are expressed as group means ± SEMs with $P<0.05$ considered statistically significant.

Results

Maternal physiological and behavioral outcomes

A general experimental overview is shown in **Figure 2.1**. Timed-pregnant dams arrived on embryonic day 7 (E7) when they were randomly assigned to one of four groups. Dams in the stress groups (CUS, CUS+CIT) underwent a chronic unpredictable stress paradigm from E8 through E14 (**Fig. 2.1A, Table S2.1**). All dams then underwent the open field, forced swim, and novelty suppressed feeding tests during E15-E17. The results of all statistical analyses are shown in **Table S2.2**.

No physiological differences were observed in dams belonging to the different treatment groups (**Fig. S2.1**). All dams had similar pregnancy-related weight gains regardless of group (**Fig. S2.1A,B**). Daily water consumption was similar regardless of the presence of CIT in the drinking water in the CUS+CIT and CIT groups compared to the control and CUS groups (**Fig. 2.1C**). Moreover, average litter sizes (**Fig. 2.1D**) and early postnatal pup weights (**Fig. S2.2**) were not affected by stress, citalopram, or their combination. Significant correlations between litter size and pup weights at postnatal days 7 and 14 were observed (**Fig. S2.2**) and were similar across treatments.

On E15, dams in the CUS and CUS+CIT groups showed increases in OFT distance traveled and perambulation speed during the first 5 min of the test where mice show the highest activity levels indicative of novelty-associated exploration (**Fig. S2.3A,B**). Dams in the CUS groups exhibited a selective increase in cumulative total distance traveled over the 30-min test period, accompanied by increases in cumulative center zone distance traveled and peripheral zone speed (**Fig. S2.3C-E**). Additional parameters determined in the anxiogenic center zone did not differ across groups (**Fig. S2.3F-I**).

On E16 dams underwent FST for 6 min. No maternal group differences were observed over the full 6 min session nor in the last 4 min. On E17, no maternal group differences were observed in either home cage or novel arena latencies to feed in the NSF test (**Fig. S2.4A,C**). However, pregnancy, regardless of maternal treatment group, was associated with a reduced latency to feed in the home cage and novel arena when compared to nonpregnant female offspring (**Fig. S2.4B,D**). Dams in the CUS group also took significantly less time to take a first bite of a food pellet in the novel arena compared to nonpregnant adult female CUS-group offspring (**Fig. S2.4C**).

Postnatal tissue analysis

One or two mice per treatment group were randomly selected for tissue neurotransmitter analysis at three different early postnatal timepoints (**Fig. 2.1B**). Brains from postnatal day 7, 14, and 21 (P7, P14, and P21, respectively) pups were analyzed regionally. At P7, brains were sectioned into forebrain, midbrain, and hindbrain due to their small size. At P14 and P21, larger brains enabled dissection of frontal cortex, hippocampus, and striatum. At P7, serotonin, norepinephrine, and dopamine levels normalized for tissue protein levels for forebrain, midbrain, and hindbrain showed no significant differences in control *vs.* CUS groups (**Fig. 2.2A-C**). In midbrain, a significant decrease in the major metabolite of serotonin, 5-hydroxyindoleacetic acid (5-HIAA), was observed in pups exposed to prenatal stress. In hindbrain, an increase in the dopamine metabolite homovanillic acid (HVA) but not 3,4-dihydroxyphenylacetic acid (DOPAC) was observed in pups exposed to prenatal stress. When we examined tissue protein concentrations used to normalized neurotransmitter levels (as a proxy for tissue wet weight), we observed selective increases in protein levels in forebrain in CUS mice compared to controls at P7 (**Fig. 2.2D-F**). Analysis

of raw nanomolar concentration show pups exposed to prenatal stress had increased serotonin, HIAA, and norepinephrine in the forebrain, but not midbrain or hindbrain (**Fig. 2.2G-I**). Concomitant treatment of citalopram to stress dams rescued the prenatal stress induced increases in serotonin in the forebrain of P7 offspring (**Fig. 2.2J**). No differences were observed in P14 or P21 brains.

Adult offspring behavior

At three months of age, offspring were assessed for anxiety- and depressive-like phenotypes using four widely used behavior tests; EPM, OFT, FST, and NSF. Behavior tests were completed in the order from least to most stressful. No group differences were observed in the EPM (**Fig. S2.5**). *In utero* citalopram treatment altered OFT behavior in male adult offspring (**Fig. 2.3**). Distance traveled in the arena was significantly reduced in the CIT group compared to all other groups for male offspring, but not in females (**Fig. 2.3A-C**). For the entire duration of testing, exposure to *in utero* CIT significantly decreased center entries, center distance compared to entire arena, and center time in males compared to controls (**Fig. 2.3D-F**). The first five minutes was analyzed alone since this is when the arena is most novel and anxiogenic. Within the first 5 min of testing, *in utero* CIT exposure irrespective of stress decreased center entries and time spent in the center zone in males, but not females (**Fig. 2.3G,I**).

In the FST, prenatal stress significantly decreased immobility time in males, but not females (**Fig. 2.4B**), compared to controls. Concomitant treatment of CIT rescued the stress induced decreases in immobility in males. In females, immobility time was increased in the CUS+CIT group compared to control and CUS groups. Irrespective of sex or group,

immobility time increased across the test duration. Group differences were seen during the last four minutes of the test (**Fig. 2.4C, D**).

The last behavior test performed was the NSF. Adult offspring were fasted for 24 h before undergoing the NSF test. Mice that lost more than 13% body weight were excluded from the study. Interestingly, male offspring born to stressed mothers had the highest percentage of exclusion, with almost 50% of the group excluded (**Fig. 2.5A**). No significant pre-fast weight differences were seen between groups of each sex (**Fig. 2.5B**). Prenatal stress significantly increased the ratio between latency to feed in novelty arena compared to the home cage in male adult offspring but not females (**Fig. 2.5C**). Treatment with CIT attenuated the effects of stress on the ratio between latency to feed in novelty arena compared to home cage. To determine if these effects were due to decreased appetite, a subset of mice were given a pre-weighed pellet of food and allowed to eat for 10 min post NSF testing in their home cage. At the end of the 10 min period, food pellets were weighed again to determine amount eaten. No differences were observed between groups for amount of food eaten after 10 min (**Fig. 2.5D**).

Adult offspring neurochemistry

The adult offspring for microdialysis experiments were separated into three paradigms, in which the order of pharmacological agents administered was varied to test different hypotheses To assess the effects of prenatal stress and SSRI treatment on adult offspring neurochemistry, male adult offspring underwent microdialysis. Only males were used for microdialysis, as behavior data pointed to males being more susceptible to the effects of prenatal stress than females. The ventral hippocampus (vHPC) was targeted due to its involvement in anxiety responses and dense innervation from serotonin neurons (**Fig.**

S2.7A). Peaks were identified and quantified based on standard curves (**Fig. S2.7B**) and peaks were confirmed *in vivo* with infusion of serotonin and dopamine (**Fig. S2.7C, D**). No differences in basal or stimulated extracellular serotonin levels were observed (**Fig. 2.6A-C**). No differences in basal extracellular dopamine levels were observed (**Fig. 2.6D, E**), however the CUS group had higher stimulated dopamine levels compared to control and CUS+CIT groups (**Fig. 2.6F**).

To probe potential mechanisms of stress-induced behavioral changes, 8-OH-DPAT injections were given to male and female adult offspring to determine differences in 5HT1A receptor activity. No differences were seen and thus not probed further in microdialysis experiments (**Fig. S2.6**). Citalopram was perfused into the vHPC to determine differences in SERT activity. Moreover, KOR agonists were injected to assess a link between the serotonin system and kappa system. After basal and stimulated levels of both neurotransmitter, 10 uM citalopram was infused for 2 h then a KOR-agonist was injected (U50,488 or U69,593, 10 mg/kg, i.p.) and dialysate samples were collected for additional 1.5 h while CIT was perfused (**Fig. 2.7A, D**).

A significant effect of CIT infusion and KOR agonist was observed, but not for *in utero* treatment on dopamine concentrations (**Fig. 2.7E, F**). As expected, KOR activation decreased dopamine levels, however unexpectedly, CIT perfusion also decreased dopamine levels. A significant effect of treatment and drug on serotonin concentrations were observed (**Fig. 2.7B, C**). To ensure that CIT was not causing increased serotonin release over longer durations, we infused CIT for more than 3 hr (**Fig. S2.9**). While we did observe a significant correlation between serotonin concentration over the longer perfusion period, the increase was less than 1 nM, confirming that larger increases in serotonin levels were the result of

KOR agonist injection. Stress potentiated the increase in serotonin levels induced by KOR activation, which is rescued in the CUS+CIT group (**Fig. 2.7B**). To test if these results were dependent on SERT blockade, the KOR agonist was injected prior to CIT perfusion. Decreases in dopamine levels were seen, however, no differences in serotonin levels were observed post KOR injection without SERT blockade (**Fig. S2.8**).

Discussion

Our study points to the long-term benefits of treating dams experiencing stressful pregnancies with SSRIs as a way to mitigate adverse outcomes in offspring health. We found that stress induced developmental changes in offspring protein, neurotransmitter, and amino acid tissue levels in early postnatal development. Stress induced increases in serotonin levels were rescued in offspring whose mothers were concomitantly treated with citalopram *in* utero. While these effects were no longer observed by postnatal day 14 or 21, their impacts on behavior were seen in adulthood. We found that male, but not female, animals born to stressed mothers displayed increased anxiety and depressive-like behavior. Moreover, we found that stressed males were more susceptible to stress challenges, *i.e.*, overnight fasting, than females. These adverse behavioral phenotypes were rescued in animals whose mothers were concomitantly treated with citalopram *in utero*.

Lastly, we assayed neurochemical changes in adult male mice. While we did not see changes in basal or stimulated serotonin release, we did find pharmacological-induced changes in neurochemistry. Male mice born to stressed mothers showed higher serotonin concentrations in the vHPC in response to citalopram administration with and without the presence of kappa opioid receptor activation. These effects were rescued in the male mice whose mothers had been treated with citalopram *in utero*.

Our results add to the existing expansive literature on the adverse effects of maternal stress during pregnancy. Importantly, our results also highlight the long-term benefits of pharmacological treatments of stress experienced by pregnant mothers. The decision to take medication during pregnancy is influenced by many factors, which include severity of maternal disorder, type of medication, and other complications. However, contrary to social

perception that all medications during pregnancy are harmful to the developing fetus, our results show that SSRIs do not cause changes litter size, fetal birth weight, or viability, and are efficacious in mitigating the effects of maternal stress in a mouse model.

While we probed the vHPC, many other brain regions are implicated in the adverse effects of stress, particularly cortical regions such as the prefrontal cortex (PFC). Moreover, KOR receptor expression and localization on cell populations, *i.e.*, dopaminergic neurons, and involvement of the kappa system in stress responses point to an expansive system with much to be uncovered. Future experiments should focus on specifically probing neurochemical pathways, *i.e.*, MRN → vHPC and MRN → PFC, to understand how the brain adapts to prenatal stress exposure. Moreover, future experiments may isolate the effects of prenatal stress from postnatal maternal care, as maternal care is an important influencer of offspring development.

In sum, we showed that untreated maternal stress during pregnancy has prolonged developmental effects that impacts long-term offspring health. This study fills an important gap in previous literature in answering how long-term behavioral and neurochemical effects are impacted given adverse *in utero* exposures. Importantly, our study strongly points to the safety and efficacy of citalopram, a commonly prescribed SSRI, in attenuating adverse neurochemical and behavioral effects induced by stress. Finally, we show an important link between stress-reactivity and the integral role of the serotonin and kappa systems in mediating responses to stress.

Figures

Figure 2.1

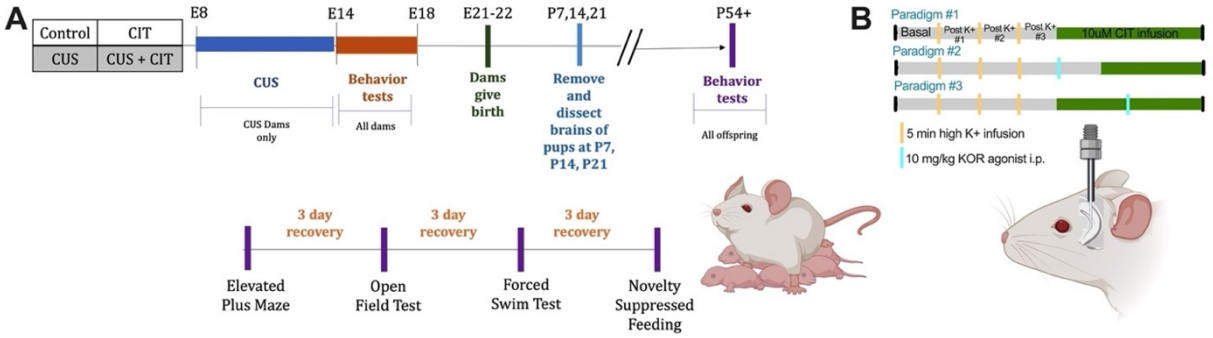

Figure 2.1: Overview of experimental paradigms. A. Timeline of *in utero* exposure and subsequent postnatal and behavior testing schedules. **B.** Timelines for different microdialysis paradigms. Aspects of this figure were created using Biorender.com.

Figure 2.2

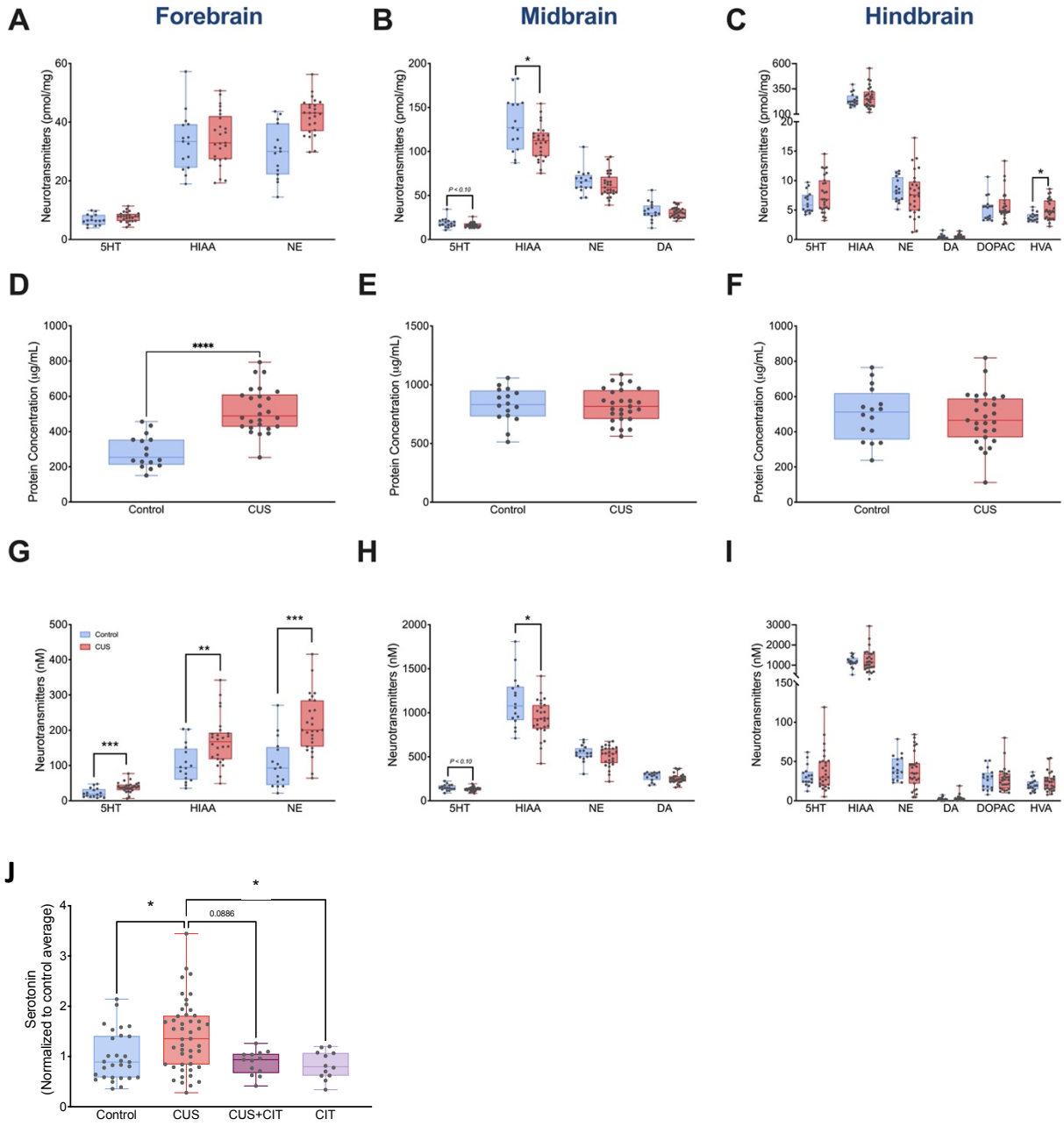

Figure 2.2: Postnatal day 7 tissue analysis shows increased neurotransmitters and protein concentration for stressed pups. Normalized **A.** forebrain, **B.** midbrain, and **C.** hindbrain neurotransmitter tissue levels. **D**. Protein concentrations are significantly increased at P7 in the forebrain of stressed pups, but not the **E.** midbrain or **F.** hindbrain. Non-normalized neurotransmitter tissue levels show significant increases in pups born to stressed mothers in **G.** forebrain, but not **H.** midbrain or **I.** hindbrain. Concomitant treatment with CIT rescues maternal stress induced increases in serotonin in **J.** forebrain. *P<0.05, **P<0.01, ***P<0.001 Abbreviations: Serotonin (5HT), 5-Hydroxyindolacetic acid (HIAA), norepinephrine (NE), dopamine

Figure 2.3

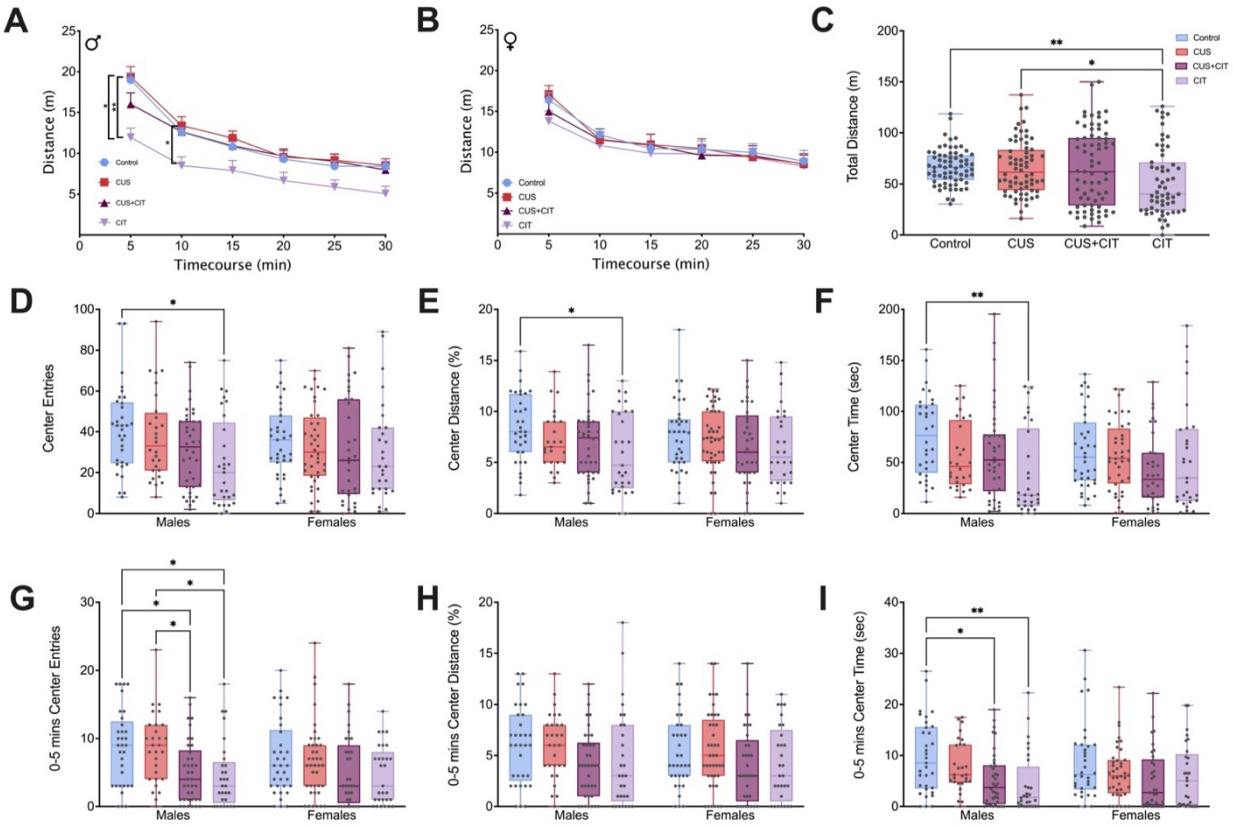

Figure 2.3: *In utero* citalopram exposure changes OFT behavior in male adult offspring. *In utero* treatment differences in distance traveled in first five and ten minutes in **A.** males, but not **B.** females. Significant effect of **C.** *in utero* treatment on total distance traveled between control and CIT groups and CUS and CIT groups. **D-F.** Center zone parameters for full 30 min OFT time course show significant changes in CIT group on **D.** number of entries into the center zone, **E.** distance travelled in the center zone compared to the entire arena, and **F.** time spent in the center zone. No changes were observed in females. **G-**I. Significant decreases of *in utero* CIT exposure on **G.** number of center entries, and **I.** time spent in the center zone, but not **H.** percent center distance during first 5 min of test. No changes were observed in females. *P<0.05, **P<0.01, ***P<0.001

Figure 2.4

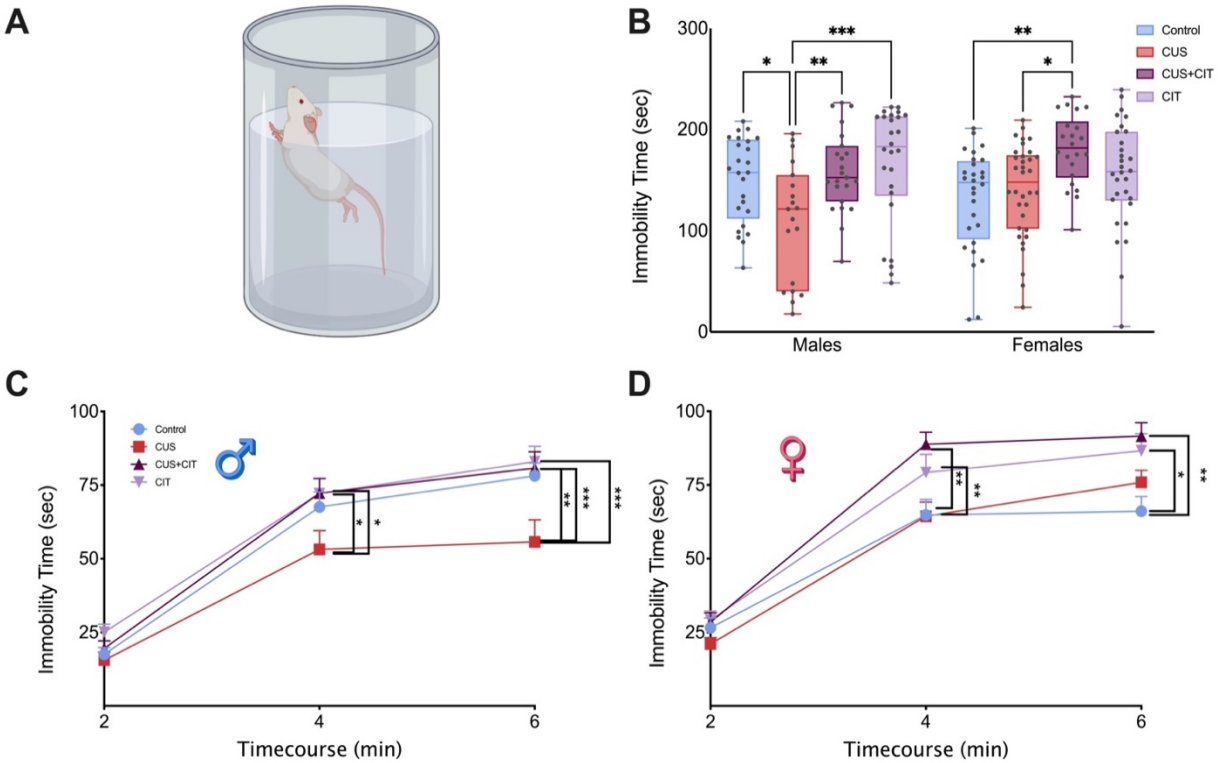

Figure 2.4: Adult offspring force swim test A. Cartoon of FST behavioral apparatus (Biorender.com). **B.** *In utero* CUS exposure significantly reduces immobility time of male adult offspring; these reductions are rescued in the CUS+CIT male group. *In utero* CUS+CIT significantly increases immobility time in female adult offspring, compared to control and CUS groups. Immobility time is summed over the last 4 minutes of the FST. **C.** Male and **D.** female immobility time course shows significant effects of treatment and time. *P<0.05, **P<0.01,

Figure 2.5

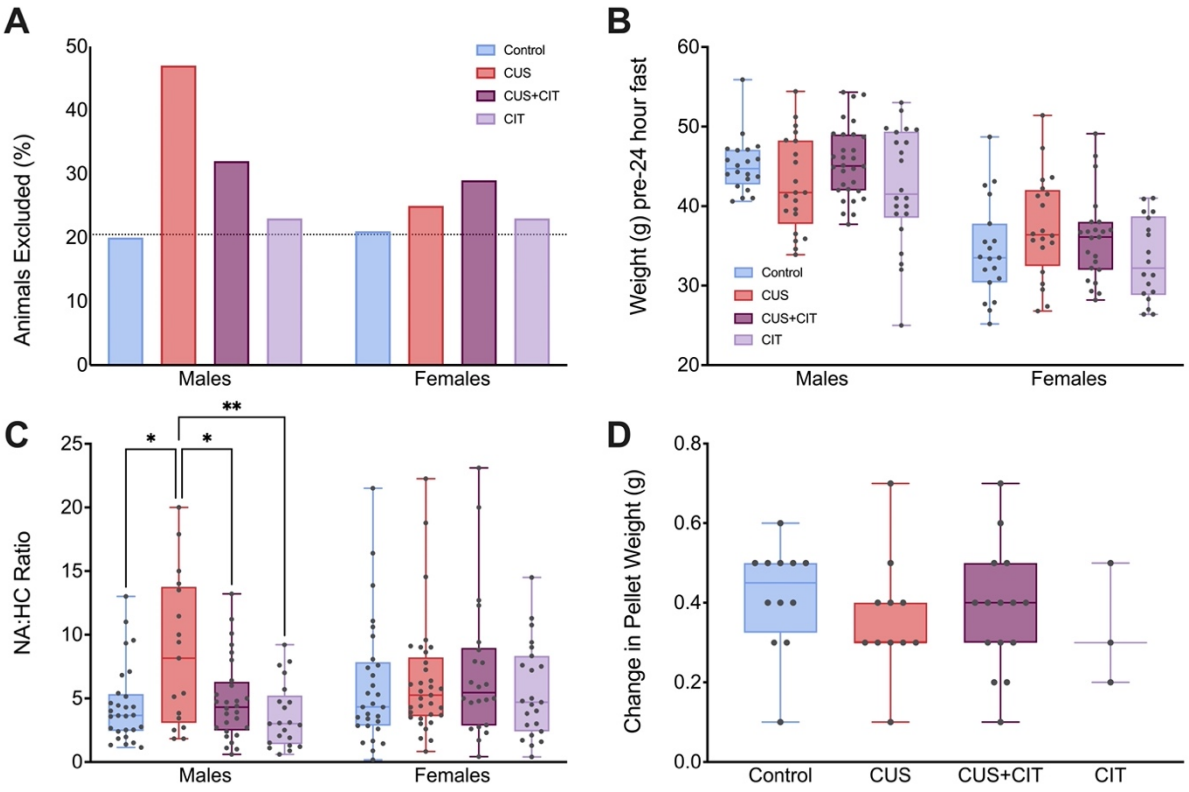

Figure 2.5: Adult offspring novelty suppressed feeding test A. Percentages of animals excluded based on percent body weight loss. Adult male CUS animals were excluded at twice the rate of other groups. **B.** No differences in body weights between treatment groups of the same sex pre-24 hour fast. **C.** Significant effect of treatment in male adult offspring on ratio between latency to feed in novelty area compared to the home cage. No difference in **D.** change in pellet weight 10 min after testing corresponding to amount of food eaten. *P<0.05, **P<0.01

Figure 2.6

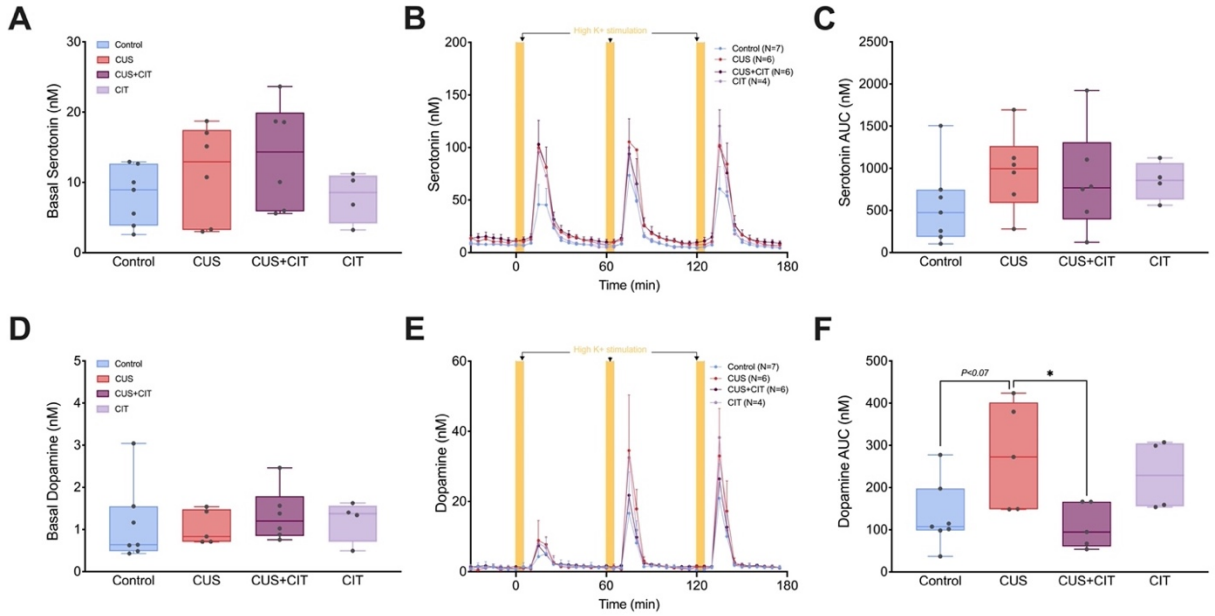

Figure 2.6: No basal extracellular serotonin or dopamine differences in adult offspring exposed to prenatal stress. Basal serotonin (**A**) and dopamine (**D**) levels in adult offspring. Microdialysis time course of extracellular serotonin (**B**) and dopamine (**E**). The yellow bars indicate 120 µM potassium stimulation (5 min). Serotonin (**C**) and dopamine high potassium (**F**) stimulated release quantified by area under the curve. *P<0.05,

Figure 2.7

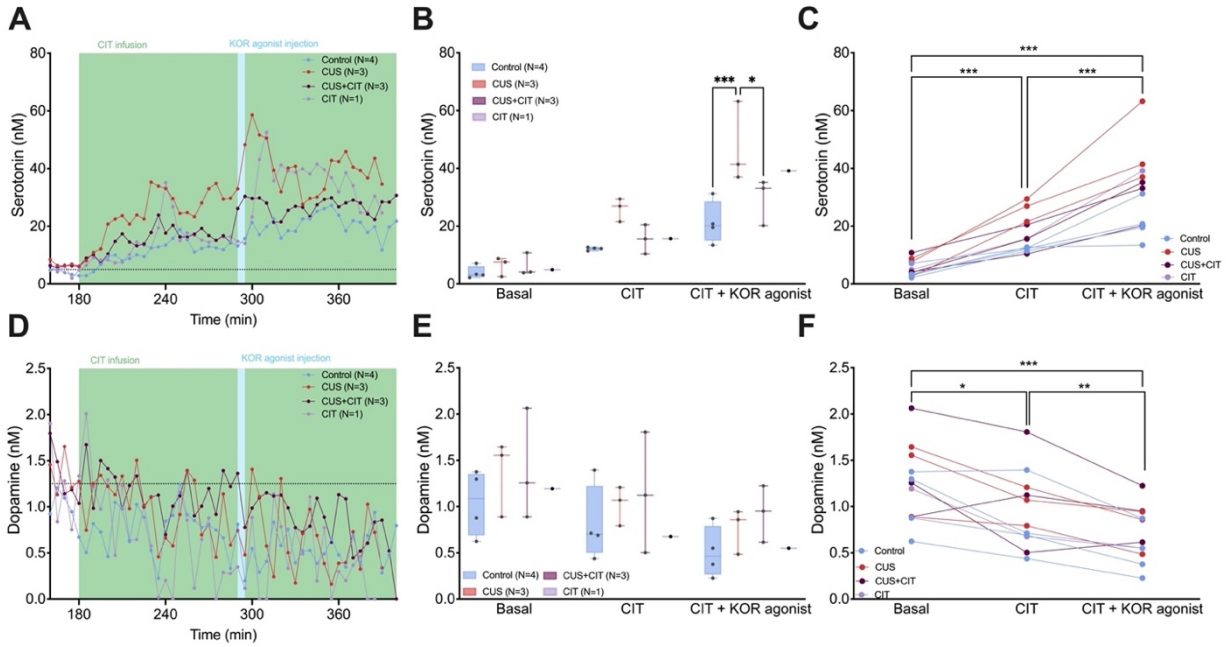

Figure 2.7: Decreases in dopamine and increases in serotonin, post concomitant CIT and KOR agonist. A. Time course before and after CIT infusion and KOR agonist injection for serotonin concentrations. Significant effect of **B.** treatment, and **C.** drug on serotonin concentrations. **D.** Time course before and after CIT infusion and KOR agonist injection for dopamine concentrations. Significant effect of **F.** CIT infusion and agonist injection, but not **E.** *in utero* treatment on dopamine concentrations. *P<0.05, **P<0.01, ***P<0.001, ****P<0.0001

Table S2.1

Monday	Tuesday	Wednesday	Thursday	Friday	Saturday	Sunday
	E7: timed-pregnant dams arrived; CUS dams placed into individual cages	**E8 10 am:** ears clipped, 5-min restraint, saline injection, and brief transportation stress	**E9 12 pm**: 15-min fox urine odor exposure	**E10 4:30 pm-7 am:** overnight light	**E11 10 am-12 pm:** 30-min restraint in tubes	**E12 4 pm-7 am:** overnight static noise (70dB)
E13 8 am-4 pm: 45° cage tilt	**E14 4:30 pm-7 am:** overnight wet bedding	**E15 6 pm-10 pm:** OFT test	**E16 12 pm-2:30 pm:** FST test; **7 pm**: begin fast for NSF	**E17 5 pm-7 pm:** NSF test		

Table S2.1: Maternal chronic unpredictable stress paradigm

Figure S2.1

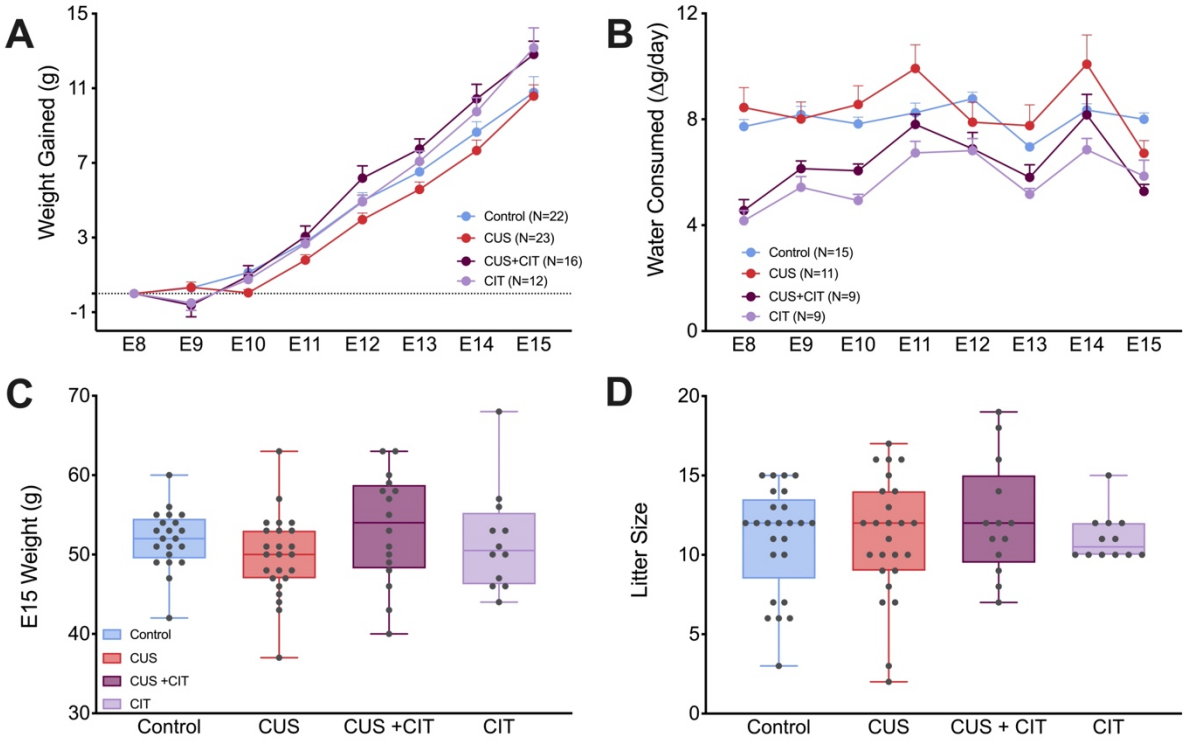

Figure S2.1: Maternal measures. A. Maternal weight gains over the course of pregnancy were similar regardless of group. **B.** There were no differences dam weights at E15 across groups. **C.** Water consumption across groups by day. The drinking water for the CUS+CIT and CIT groups contained 1.5% sucrose to mask the taste of the drug. **D.** Litter sizes were not different across groups.

Figure S2.2

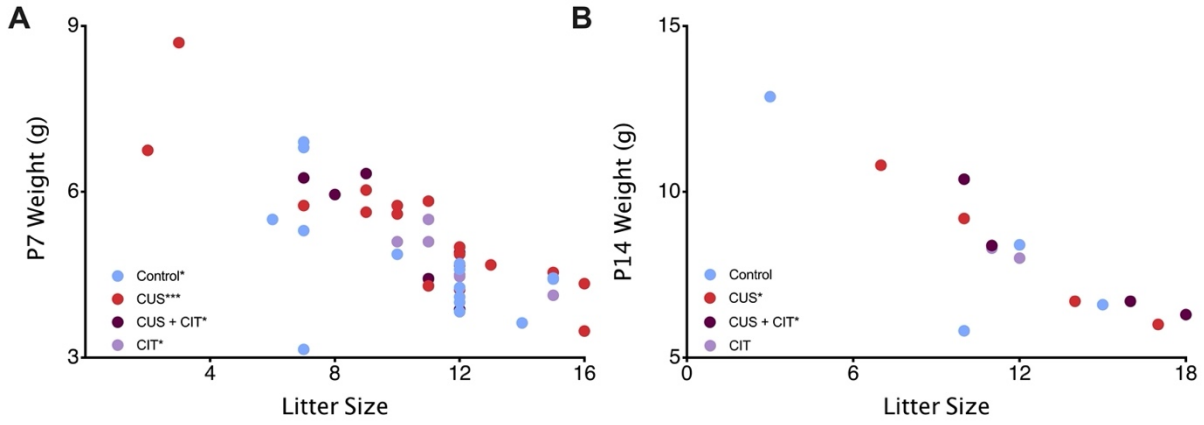

Figure S2.2: Correlations between liter size and postnatal weights. Pup weights were negatively correlated with litter size, as expected and regardless of group, on **A.** postnatal day 7 (P7) and **B.** postnatal day 14 (P14).

Figure S2.3

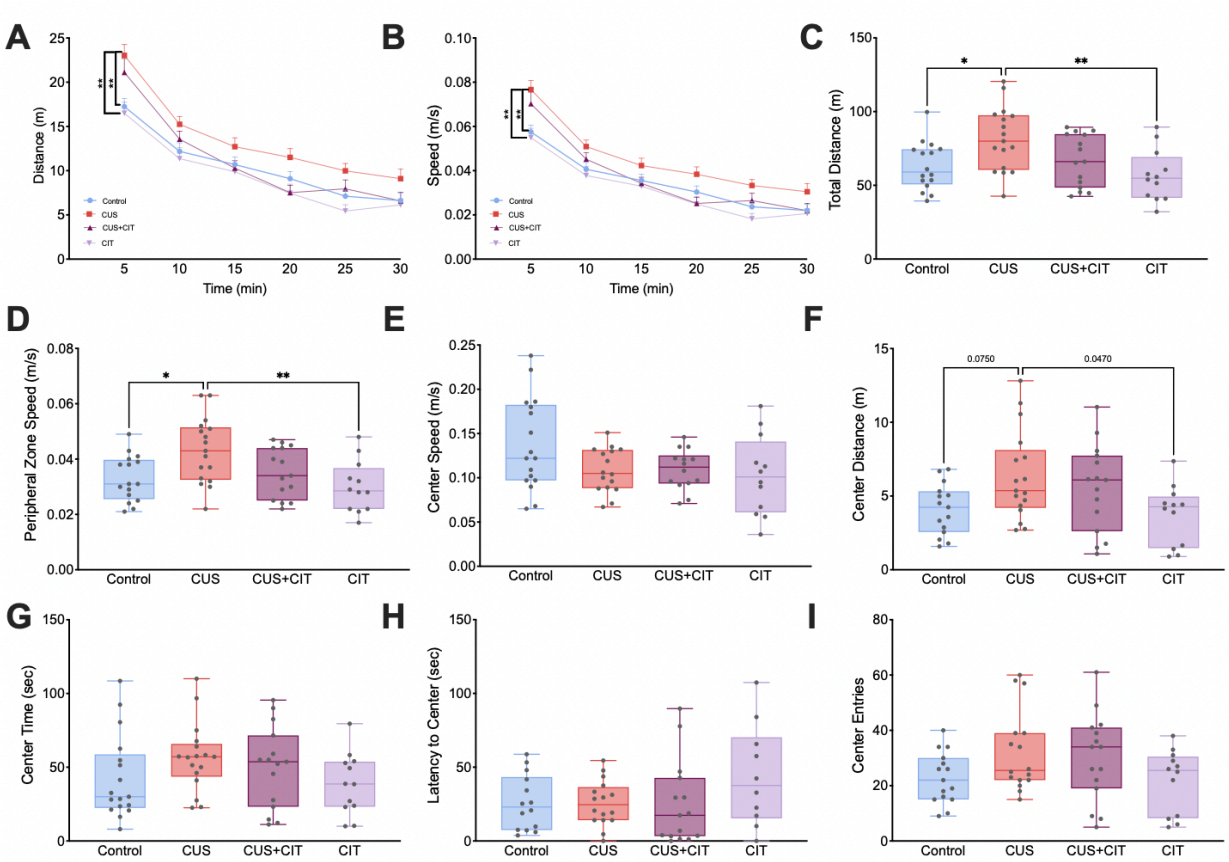

Figure S2.3: Maternal open field test (OFT) on E15. A. Distance traveled during the initial 5-min exploratory period was increased in dams from both groups exposed to chronic unpredictable stress (CUS) during pregnancy. **B.** Likewise, speed during the first 5-min was increased in CUS and CUS+CIT groups. **C.** Cumulative distance traveled was increased in CUS dams. **D.** The CUS group also showed Increased peripheral zone speed, **E.** but not center zone speed. **F.** A trend toward increased distance traveled in the center zone was also observed in the CUS group. **G-I.** No differences were observed in other center zone parameters. *P<0.05 and **P<0.01.

Figure S2.4

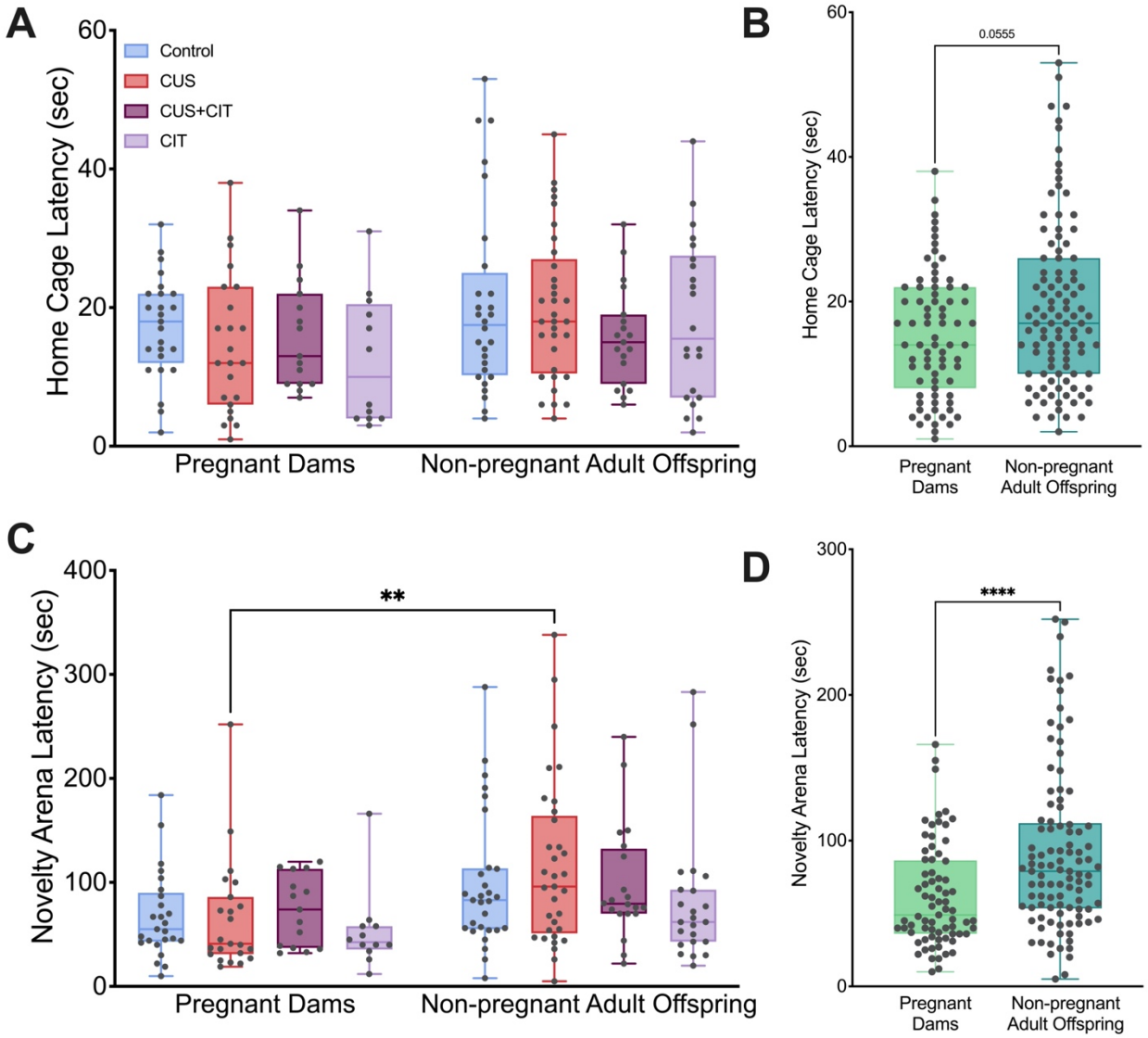

Figure S2.4: Maternal novelty suppressed feeding test on E17. A. No changes in home cage latency to feed occurred between maternal groups. **B.** There was a trend toward a decrease in home cage latency to feed between pregnant (collapsed on treatment group) and non-pregnant female mice. **C.** The latency to feed in the novel arena was not significantly different across maternal groups and was shorter in CUS mothers vs. their adult female offspring. **D.** Pregnancy generally decreased the latency to feed in the novel arena. ***P*<0.01 and ****P*<0.001.

Figure S2.5

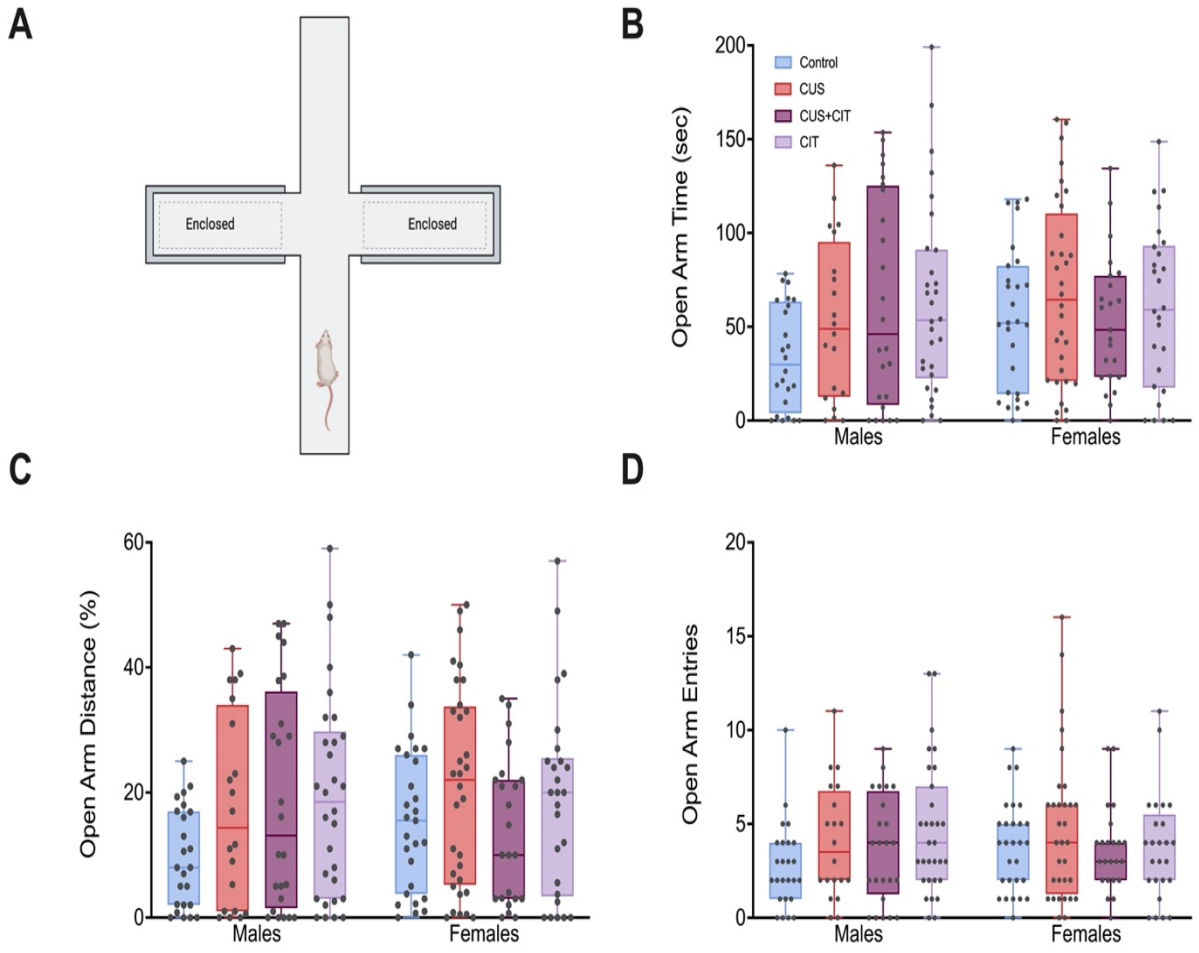

Figure S2.5: No changes in the EPM of 3-month-old adult offspring. A. Cartoon of EPM behavioral apparatus (Biorender.com) **B-D.** No changes in open arm parameters between groups or sex-specific differences.

Figure S2.6

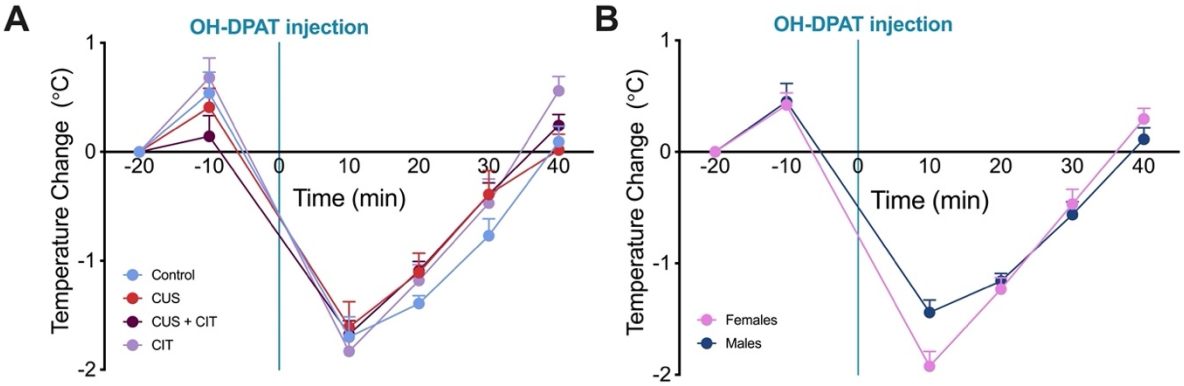

Figure S2.6: No changes in the temperature after 5HT1A agonist. No temperature changes by **A.** treatment or by **B**. sex after 8-OH-DPAT i.p. injection.

Figure S2.7

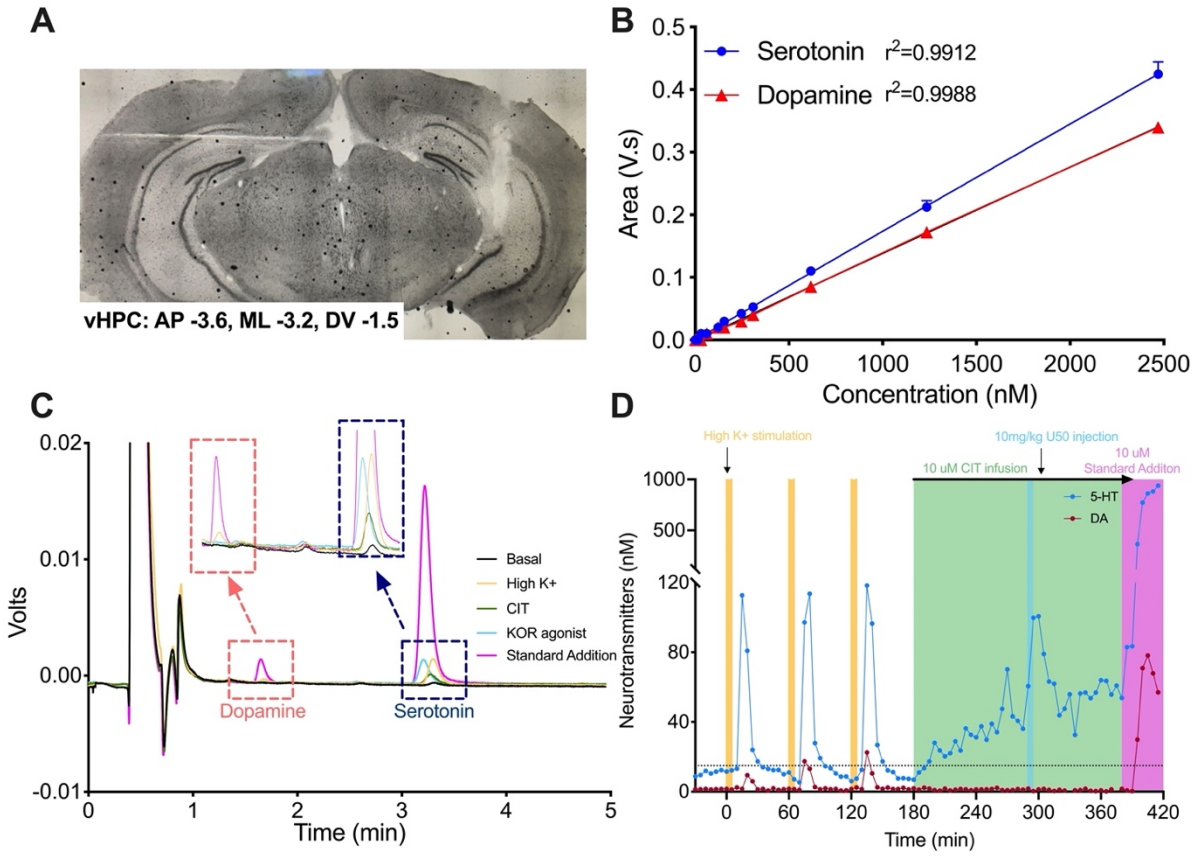

Figure S2.7: Microdialysis probe and peak verification. A. Cresyl violet image showing microdialysis cannula and probe localization to the ventral hippocampus. **B.** Standard curves for dopamine and serotonin used to quantify analyte concentrations. A standard curve was run each week prior to microdialysis experiments N=6/analyte. **C.** Overlay of five chromatograms from a representative mouse showing dopamine and serotonin peaks before (basal) and after pharmacological manipulations to verify peak identities. **D.** Time course from the same mouse in C.

Figure S2.8

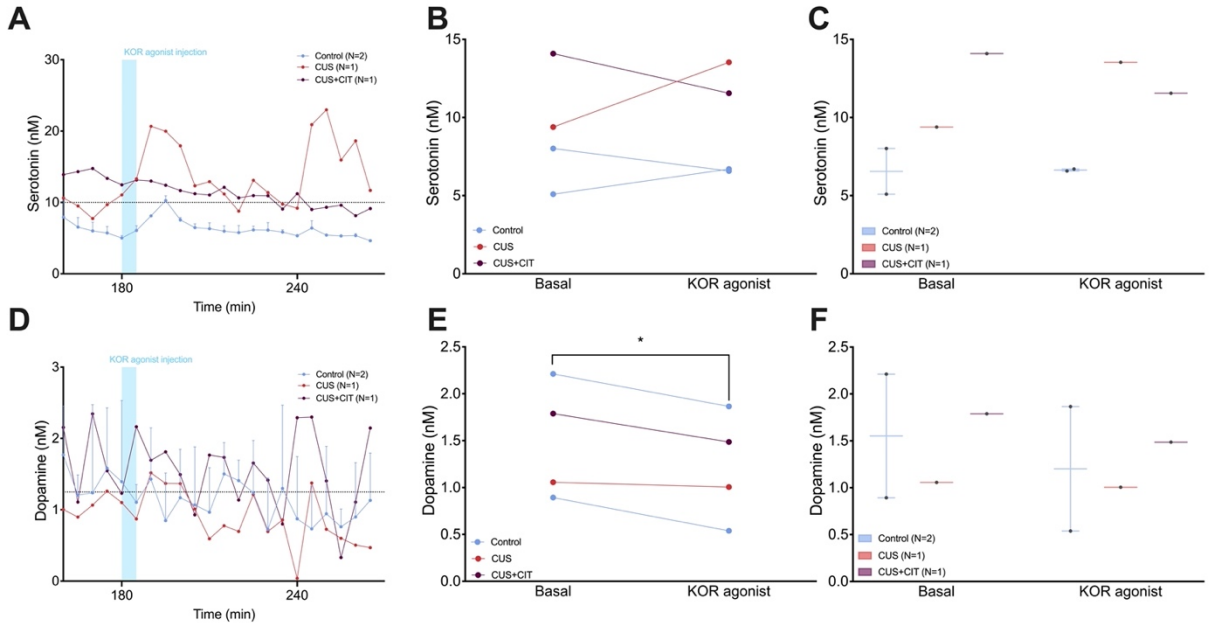

Figure S2.8: Decreases in dopamine, but not serotonin, post KOR agonist i.p. injection. A. Time course before and after KOR agonist injection for serotonin concentrations. No effect of **B.** KOR injection or **C.** *in utero* treatment on serotonin concentrations. **D.** Time course before and after KOR agonist injection for dopamine concentrations. Significant effect of **E.** KOR injection, but not **C.** *in utero* treatment on dopamine concentrations. *P<0.05

Figure S2.9

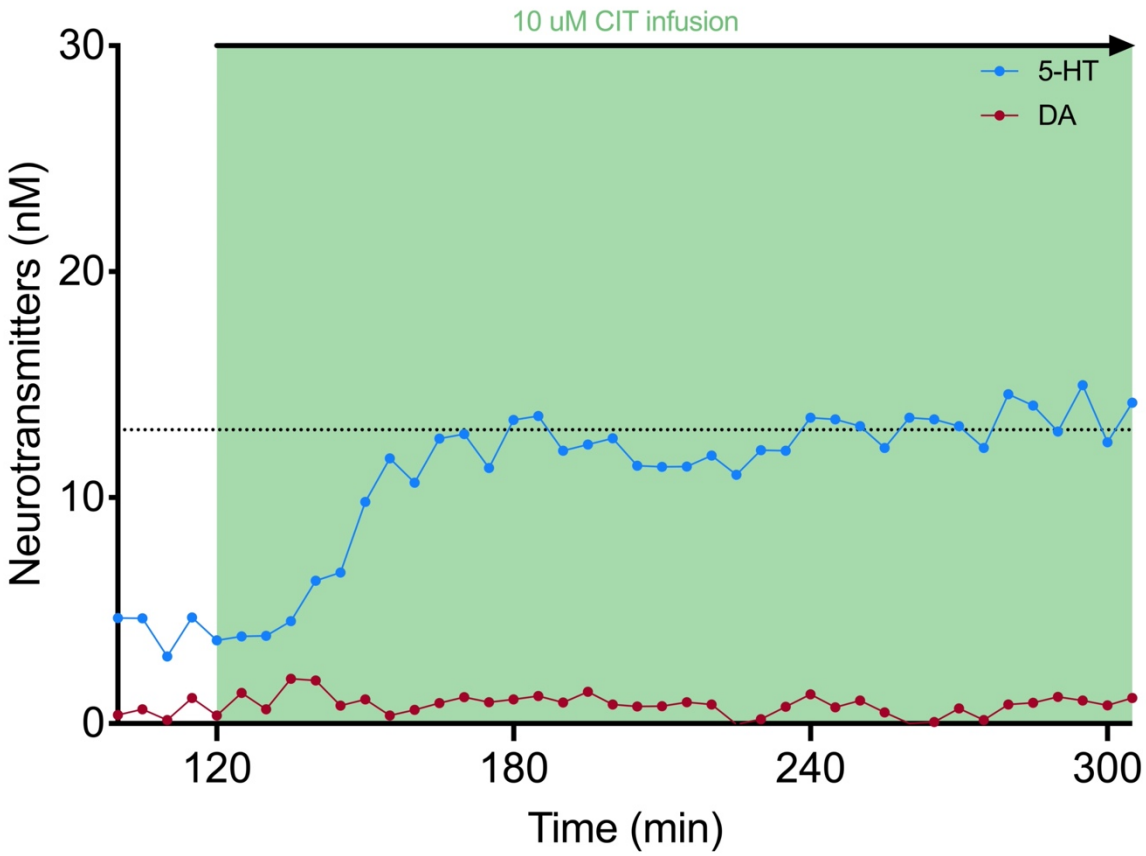

Figure S2.9: Stable serotonin levels after three hr of CIT infusion. Serotonin concentrations remained stable during longer infusion of CIT. Time course is taken from N=1 animal that underwent basal collection and two high K+ potassium stimulations. Each point represents a 5 min sample. Points pre-120 min are neurotransmitter concentrations post-high K+ #2 and pre-CIT infusion. Infusion of CIT began at 120 min (or 2 hours into microdialysis testing day) and continued until 310 min, for a duration of three hr and 10 min.

Table S2.2

Figure	Comparison	Test and result
Figure 2A	***Pup forebrain neurotransmitters (pmol/mg) between treatment***	Serotonin: *Unpaired t-test; P<0.08* HIAA: Unpaired t-test; P>0.05 Norepinephrine: ***Unpaired t-test; P<0.001***
Figure 2B	***Pup midbrain neurotransmitters (pmol/mg) between treatment***	Serotonin: Mann-Whitney test; P>0.05 HIAA: ***Unpaired t-test; P<0.05*** Norepinephrine: Mann-Whitney test; P>0.05 Dopamine: Unpaired t-test; P>0.05
Figure 2C	***Pup hindbrain neurotransmitters (pmol/mg) between treatment***	Serotonin: Unpaired t-test; P>0.05 HIAA: Unpaired t-test; P>0.05 Norepinephrine: Unpaired t-test; P>0.05 Dopamine: Mann-Whitney test; P>0.05 DOPAC: Mann-Whitney test; P>0.05 HVA: ***Unpaired t-test; P<0.05***
Figure 2D	***Pup forebrain protein concentrations between treatment***	***Unpaired t-test; P>0.001***
Figure 2E	Pup midbrain protein concentrations between treatment	Unpaired t-test; P>0.05
Figure 2F	Pup hindbrain protein concentrations between treatment	Unpaired t-test; P>0.05
Figure 2G	***Pup forebrain neurotransmitters (nM) between treatment***	***Serotonin: Unpaired t-test; P<0.001*** ***HIAA: Unpaired t-test; P<0.01*** ***Norepinephrine: Unpaired t-test; P<0.001***
Figure 2H	***Pup midbrain neurotransmitters (nM) between treatment***	*Serotonin: Unpaired t-test; P<0.08* HIAA: ***Unpaired t-test; P<0.05*** Norepinephrine: Unpaired t-test; P>0.05 Dopamine: Mann-Whitney test; P>0.05
Figure 2I	Pup hindbrain neurotransmitters (nM) between treatment	Serotonin: Unpaired t-test; P>0.05 HIAA: Unpaired t-test; P>0.05 Norepinephrine: Unpaired t-test; P>0.05 Dopamine: Unpaired t-test; P>0.05 DOPAC: Unpaired t-test; P>0.05 HVA: Unpaired t-test; P>0.05
Figure 3A	***Male distance traveled across time***	***Two-way ANOVA*** ***Time x treatment*** — ***F (15, 605) = 3.81; P<0.001*** ***Time*** — ***F (2.6, 315) = 221; P<0.001*** ***Treatment*** — ***F (3, 121) = 4.89; P<0.01*** ***Subject*** — ***F (121, 605) = 21.1.; P<0.001***

Figure 3B	***Female distance traveled across time***	***Two-way ANOVA*** Time x treatment: F (15, 675) = 1.15; P>0.05 ***Time: F (5, 675) = 88.4; P<0.001*** Treatment: F (3, 135) = 4.89; P>0.05 ***Subject: F (135, 675) = 24.0.; P<0.001***
Figure 3C	***Total distance traveled between treatments***	***Kruskal-Wallis test; P<0.001***
Figure 3D	***Entries into center zone***	***Two-way ANOVA*** Interaction: F (3, 256) = 0.68; P>0.05 Sex: F (1, 256) = 0.06; P>0.05 ***Treatment: F (3,256) = 6.33; P<0.001***
Figure 3E	***% center distance in OFT***	***Two-way ANOVA*** Interaction: F (3, 258) = 0.50; P>0.05 Sex: F (1, 258) = 0.08; P>0.05 ***Treatment: F (3,258) = 2.96; P<0.05***
Figure 3F	***Time spent in the center zone***	***Two-way ANOVA*** Interaction: F (3, 256) = 2.26; P>0.05 Sex: F (1, 256) = 0.80; P>0.05 ***Treatment: F (3,256) = 3.85; P<0.05***
Figure 3G	***Entries into center zone in first 5 min***	***Two-way ANOVA*** Interaction: F (3, 257) = 0.62; P>0.05 Sex: F (1, 257) = 1.67; P>0.05 ***Treatment: F (3,257) = 7.04; P<0.001***
Figure 3H	***% center distance in first 5 min***	***Two-way ANOVA*** Interaction: F (3, 258) = 0.06; P>0.05 Sex: F (1, 258) = 0.79; P>0.05 ***Treatment: F (3,258) = 3.52; P<0.05***
Figure 3I	***Time spent in the center zone in first 5 min***	***Two-way ANOVA*** Interaction: F (3, 256) = 0.68; P>0.05 Sex: F (1, 256) = 0.06; P>0.05 ***Treatment: F (3,256) = 6.33; P<0.001***
Figure 4B	***2-6 min immobility time in FST***	***Two-way ANOVA*** ***Interaction: F (3, 199) = 3.23; P<0.05 **** Sex: F (1, 199) = 0.70; P>0.05 ***Treatment: F (3,199) = 8.43; P<0.001***
Figure 4C	***Male immobility time across time***	***Two-way ANOVA*** ***Time x treatment: F (6, 190) = 2.42; P<0.05*** ***Time: F (1.78, 169) = 378; P<0.001*** ***Treatment: F (3, 95) = 3.68; P<0.05*** ***Subject: F (95, 190) = 5.32; P<0.001***

Figure 4D	***Female immobility time across time***	***Two-way ANOVA*** ***Time x treatment*** — ***F (6, 212) = 3.71; P<0.01*** ***Time*** — ***F (1.90, 202) = 371; P<0.001*** ***Treatment*** — ***F (3, 106) = 4.96; P<0.01*** ***Subject*** — ***F (106, 212) = 4.44; P<0.001***
Figure 5B	***Animal weights pre-NSF fast***	***Two-way ANOVA*** Interaction — F (3, 165) = 1.81; P>0.14 ***Sex*** — ***F (1, 165) = 101; P<0.001*** Treatment — F (3,165) = 1.97; P>0.12
Figure 5C	***Ratio of latency to feed in the novelty arena compared to the home cage***	***Two-way ANOVA*** ***Interaction*** — ***F (3, 193) = 2.70; P<0.05*** Sex — F (1, 193) = 2.06; P>0.15 ***Treatment*** — ***F (3,193) = 3.83; P<0.05***
Figure 5D	Pellet weight change 10 min post-NSF test	One-way ANOVA F (3, 37) = 0.38; P>0.05
Figure 6A	Serotonin basal comparison	One-way ANOVA F (3, 19) = 1.29; P>0.05
Figure 6C	Serotonin AUC comparison	One-way ANOVA F (3, 19) = 0.82; P>0.05
Figure 6D	Dopamine basal comparison	One-way ANOVA F (3, 18) = 0.19; P>0.05
Figure 6F	***Dopamine AUC comparison***	***One-way ANOVA*** ***F (3, 17) = 3.96; P<0.05***
Figure 7B, C	***Serotonin basal, CIT, and CIT+KOR comparison across treatments***	***Two-way ANOVA*** ***Drug x treatment*** — ***F (6, 14) = 4.21; P<0.05*** ***Drug*** — ***F (2, 14) = 75.44; P<0.001*** ***Treatment*** — ***F (3, 7) = 4.70; P<0.05*** ***Subject*** — ***F (7, 14) = 3.79; P<0.05***
Figure 7E, F	***Dopamine basal, CIT, and CIT+KOR comparison across treatments***	***Two-way ANOVA*** Drug x treatment — F (6, 14) = 0.19; P>0.05 ***Drug*** — ***F (2, 14) = 16.5; P<0.001*** Treatment — F (3, 7) = 0.71; P>0.05 Subject — F (7, 14) = 10.0; P>0.05

Figure S1A	***Weight change over pregnancy***	***Two-way ANOVA*** ***Time x treatment*** — ***F (21, 497) = 3.42; P<0.001*** ***Time*** — ***F (7, 497) = 578; P<0.001*** *Treatment* — *F (3, 71) = 2.64; P<0.06* ***Subject*** — ***F (71, 497) = 7.91; P<0.001***
Figure S1B	***Water consumption over pregnancy***	***Two-way ANOVA*** ***Time x treatment*** — ***F (21, 280) = 5.60; P<0.001*** ***Time*** — ***F (7, 280) = 31.6; P<0.001*** ***Treatment*** — ***F (3, 40) = 8.71; P<0.001*** ***Subject*** — ***F (40, 280) = 17.6; P<0.001***
Figure S1C	E15 dam weights	One-way ANOVA F (3, 69) = 1.33; P>0.05
Figure S1D	Litter size	One-way ANOVA F (3, 71) = 0.44; P>0.05
Figure S2A	***P7 weights and maternal liter size***	***Control: R^2 = 0.77; P<0.001*** ***CUS: R^2 = 0.68; P<0.05*** ***CUS+CIT: R^2 = 0.67; P<0.05*** ***CIT: R^2 = 0.67; P<0.05***
Figure S2B	***P14 weights and maternal liter size***	Control: R^2 = 0.70; P>0.16 ***CUS: R^2 = 0.98; P<0.05*** *CUS+CIT: R^2 = 0.87; P<0.07* CIT: too few pairs
Figure S3A	***Dam distance traveled across time***	***Two-way ANOVA*** ***Time x treatment*** — ***F (15, 280) = 2.24; P<0.01*** ***Time*** — ***F (2.6, 146) = 204; P<0.001*** ***Treatment*** — ***F (3, 56) = 4.97; P<0.01*** ***Subject*** — ***F (56, 280) = 9.19.; P<0.001***
Figure S3B	***Dam speed across time***	***Two-way ANOVA*** ***Time x treatment*** — ***F (15, 280) = 2.20; P<0.01*** ***Time*** — ***F (2.6, 146) = 203; P<0.001*** ***Treatment*** — ***F (3, 56) = 4.96; P<0.01*** ***Subject*** — ***F (56, 280) = 9.18.; P<0.001***
Figure S3C	***Dam total distance traveled in OFT***	***One-way ANOVA*** ***F (3, 56) = 4.97; P<0.01***
Figure S3D	***Dam distance traveled in center zone of OFT***	***One-way ANOVA*** ***F (3, 55) = 3.47; P<0.05***
Figure S3E	***Dam peripheral zone speed***	***One-way ANOVA*** ***F (3, 56) = 5.02; P<0.01***

Figure S3F	Dam center zone speed	*One-way ANOVA* *F (3, 55) = 2.60; P<0.07*
Figure S3G	Dam time spent in center zone	Kruskal-Wallis test; P>0.05
Figure S3H	Dam latency to enter center zone	Kruskal-Wallis test; P>0.05
Figure S3I	Dam total entries to center zone	Kruskal-Wallis test; P>0.05
Figure S4A	***Latency to feed in home cage between treatments***	***Two-way ANOVA*** Interaction: F (3, 169) = 0.65; P>0.05 ***Pregnancy: F (1, 169) = 4.87; P<0.05*** Treatment: F (3,169) = 0.99; P>0.05
Figure S4B	***Latency to feed in novelty arena between treatments***	***Two-way ANOVA*** Interaction: F (3, 172) = 0.73; P>0.05 ***Pregnancy: F (1, 172) = 13.0; P<0.001*** Treatment: F (3,172) = 1.08; P>0.05
Figure S4C	*Pregnancy effects in latency to feed in home cage*	*Mann-Whitney test; P<0.06*
Figure S4D	***Pregnancy effects in latency to feed in novelty arena***	***Mann-Whitney test; P<0.001***
Figure S5B	Dam time spent in the open arm of the EPM	Two-way ANOVA Interaction: F (3, 198) = 1.34; P>0.05 Sex: F (1, 198) = 0.75; P>0.05 Treatment: F (3,198) = 1.72; P>0.05
Figure S5C	Dam % distance traveled in open arms of the EPM	Two-way ANOVA Interaction: F (3, 198) = 1.35; P>0.05 Sex: F (1, 198) = 0.26; P>0.05 Treatment: F (3,198) = 2.42; P>0.05
Figure S5D	Dam entries to the open arms of the EPM	Two-way ANOVA Interaction: F (3, 200) = 1.19; P>0.05 Sex: F (1, 200) = 0.22; P>0.05 Treatment: F (3,200) = 1.47; P>0.05
Figure S6A	***Change in temperature after DPAT across treatment***	***Repeated measures one-way ANOVA*** Treatment: F (2.06, 10.3) = 0.96; P>0.05 ***Time: F (5, 15) = 100; P<0.001***

Figure S6B	***Change in temperature after DPAT across sex***	***Two-way ANOVA*** ***Time x Sex*** — ***F (5, 225) = 2.69; P<0.05*** ***Time*** — ***F (1, 225) = 141; P<0.001*** Sex — F (5,225) = 0.43; P>0.05 ***Subject*** — ***F (45, 225) = 1.84; P<0.01***
Figure S8B, C	Serotonin basal vs. KOR comparison across treatments	Two-way ANOVA Drug x treatment — F (2, 1) = 2.46; P>0.05 Drug — F (1, 1) = 0.35; P>0.05 Treatment — F (2, 1) = 16.2; P>0.05 Subject — F (1, 1) = 0.84; P>0.05
Figure S8E, F	***Dopamine basal vs. KOR comparison across treatments***	***Two-way ANOVA*** ***Drug x treatment*** — ***F (2, 1) = 844; P<0.05*** ***Drug*** — ***F (1, 1) = 5477; P<0.001*** Treatment — F (2, 1) = 0.11; P>0.05 ***Subject*** — ***F (7, 14) = 96977; P>0.05***
Figure S9	***Analyte concentration changes over time***	***Simple linear regression*** ***Serotonin: Y = 0.01385*X + 9.457; R^2 = 0.25*** Dopamine: Y = -0.001606*X + 1.158; R^2 = 0.02

Table S2.2: Statistical analyses for all data.

References

1. Corrigan, P. W.; Watson, A. C., Understanding the impact of stigma on people with mental illness. *World psychiatry : official journal of the World Psychiatric Association (WPA)* **2002,** *1* (1), 16-20.

2. Gavin, N. I.; Gaynes, B. N.; Lohr, K. N.; Meltzer-Brody, S.; Gartlehner, G.; Swinson, T., Perinatal depression: a systematic review of prevalence and incidence. *Obstet Gynecol* **2005,** *106* (5 Pt 1), 1071-83.

3. Hayashi, A.; Nagaoka, M.; Yamada, K.; Ichitani, Y.; Miake, Y.; Okado, N., Maternal stress induces synaptic loss and developmental disabilities of offspring. *Int J Dev Neurosci* **1998,** *16* (3-4), 209-16.

4. Peters, D. A., Maternal stress increases fetal brain and neonatal cerebral cortex 5-hydroxytryptamine synthesis in rats: a possible mechanism by which stress influences brain development. *Pharmacol Biochem Behav* **1990,** *35* (4), 943-7.

5. Talge, N. M.; Neal, C.; Glover, V.; Early Stress, T. R.; Prevention Science Network, F.; Neonatal Experience on, C.; Adolescent Mental, H., Antenatal maternal stress and long-term effects on child neurodevelopment: how and why? *J Child Psychol Psychiatry* **2007,** *48* (3-4), 245-61.

6. Deave, T.; Heron, J.; Evans, J.; Emond, A., The impact of maternal depression in pregnancy on early child development. *BJOG* **2008,** *115* (8), 1043-51.

7. Paulson, J. F.; Keefe, H. A.; Leiferman, J. A., Early parental depression and child language development. *J Child Psychol Psychiatry* **2009,** *50* (3), 254-62.

8. Pilowsky, D. J.; Wickramaratne, P. J.; Rush, A. J.; Hughes, C. W.; Garber, J.; Malloy, E.; King, C. A.; Cerda, G.; Sood, A. B.; Alpert, J. E.; Wisniewski, S. R.; Trivedi, M. H.; Talati, A.; Carlson, M. M.; Liu, H. H.; Fava, M.; Weissman, M. M., Children of currently depressed mothers: a STAR*D ancillary study. *J Clin Psychiatry* **2006,** *67* (1), 126-36.

9. Betcher, H. K.; Wisner, K. L., Psychotropic Treatment During Pregnancy: Research Synthesis and Clinical Care Principles. *J Womens Health (Larchmt)* **2020,** *29* (3), 310-318.

10. Bourke, C. H.; Stowe, Z. N.; Owens, M. J., Prenatal antidepressant exposure: clinical and preclinical findings. *Pharmacol Rev* **2014,** *66* (2), 435-65.

11. Dubovicky, M.; Belovicova, K.; Csatlosova, K.; Bogi, E., Risks of using SSRI / SNRI antidepressants during pregnancy and lactation. *Interdiscip Toxicol* **2017,** *10* (1), 30-34.

12. Croen, L. A.; Grether, J. K.; Yoshida, C. K.; Odouli, R.; Hendrick, V., Antidepressant use during pregnancy and childhood autism spectrum disorders. *JAMA Psychiatry* **2011,** *68* (11), 1104-12.

13. Harrington, R. A.; Lee, L. C.; Crum, R. M.; Zimmerman, A. W.; Hertz-Picciotto, I., Prenatal SSRI use and offspring with autism spectrum disorder or developmental delay. *Pediatrics* **2014,** *133* (5), e1241-8.

14. Oberlander, T. F.; Warburton, W.; Misri, S.; Aghajanian, J.; Hertzman, C., Neonatal outcomes after prenatal exposure to selective serotonin reuptake inhibitor antidepressants and maternal depression using population-based linked health data. *JAMA Psychiatry* **2006,** *63* (8), 898-906.

15. Molenaar, N. M.; Kamperman, A. M.; Boyce, P.; Bergink, V., Guidelines on treatment of perinatal depression with antidepressants: An international review. *Australian & New Zealand Journal of Psychiatry* **2018,** *52* (4), 320-327.

16. Gentile, S., SSRIs in Pregnancy and Lactation. *CNS Drugs* **2005,** *19* (7), 623-633.

17. Gawley, L.; Einarson, A.; Bowen, A., Stigma and attitudes towards antenatal depression and antidepressant use during pregnancy in healthcare students. *Adv Health Sci Educ Theory Pract* **2011,** *16* (5), 669-679.

18. Altieri, S. C.; Yang, H.; O'Brien, H. J.; Redwine, H. M.; Senturk, D.; Hensler, J. G.; Andrews, A. M., Perinatal vs Genetic Programming of Serotonin States Associated with Anxiety. *Neuropsychopharmacology* **2015,** *40* (6), 1456-1470.

19. Bourke, C. H.; Stowe, Z. N.; Owens, M. J., Prenatal Antidepressant Exposure: Clinical and Preclinical Findings. *Pharmacological Reviews* **2014,** *66* (2), 435-465.

20. Cirulli, F.; Laviola, G.; Ricceri, L., Risk factors for mental health: translational models from behavioural neuroscience. *Neurosci Biobehav Rev* **2009,** *33* (4), 493-7.

21. Henry, L. M.; Steele, E. H.; Watson, K. H.; Bettis, A. H.; Gruhn, M.; Dunbar, J.; Reising, M.; Compas, B. E., Stress Exposure and Maternal Depression as Risk Factors for Symptoms of Anxiety and Depression in Adolescents. *Child Psychiatry Hum Dev* **2020,** *51* (4), 572-584.

22. Herbison, C. E.; Allen, K.; Robinson, M.; Newnham, J.; Pennell, C., The impact of life stress on adult depression and anxiety is dependent on gender and timing of exposure. *Dev Psychopathol* **2017,** *29* (4), 1443-1454.

23. McLaughlin, K. A.; Conron, K. J.; Koenen, K. C.; Gilman, S. E., Childhood adversity, adult stressful life events, and risk of past-year psychiatric disorder: a test of the stress sensitization hypothesis in a population-based sample of adults. *Psychol Med* **2010,** *40* (10), 1647-58.

24. Miyagawa, K.; Tsuji, M.; Fujimori, K.; Saito, Y.; Takeda, H., Prenatal stress induces anxiety-like behavior together with the disruption of central serotonin neurons in mice. *Neurosci Res* **2011,** *70* (1), 111-7.

25. Ishiwata, H.; Shiga, T.; Okado, N., Selective serotonin reuptake inhibitor treatment of early postnatal mice reverses their prenatal stress-induced brain dysfunction. *Neuroscience* **2005,** *133* (4), 893-901.

26. Gemmel, M.; Rayen, I.; Lotus, T.; van Donkelaar, E.; Steinbusch, H. W.; De Lacalle, S.; Kokras, N.; Dalla, C.; Pawluski, J. L., Developmental fluoxetine and prenatal stress effects on serotonin, dopamine, and synaptophysin density in the PFC and hippocampus of offspring at weaning. *Developmental Psychobiology* **2016,** *58* (3), 315-327.

27. Velasquez, J. C.; Zhao, Q.; Chan, Y.; Galindo, L. C. M.; Simasotchi, C.; Wu, D.; Hou, Z.; Herod, S. M.; Oberlander, T. F.; Gil, S.; Fournier, T.; Burd, I.; Andrews, A. M.; Bonnin, A., In Utero Exposure to Citalopram Mitigates Maternal Stress Effects on Fetal Brain Development. *ACS Chemical Neuroscience* **2019,** *10* (7), 3307-3317.

28. Valentino, R. J.; Volkow, N. D., Untangling the complexity of opioid receptor function. *Neuropsychopharmacology* **2018,** *43* (13), 2514-2520.

29. Land, B. B.; Bruchas, M. R.; Lemos, J. C.; Xu, M.; Melief, E. J.; Chavkin, C., The dysphoric component of stress is encoded by activation of the dynorphin kappa-opioid system. *J Neurosci* **2008,** *28* (2), 407-14.

30. Schindler, A. G.; Messinger, D. I.; Smith, J. S.; Shankar, H.; Gustin, R. M.; Schattauer, S. S.; Lemos, J. C.; Chavkin, N. W.; Hagan, C. E.; Neumaier, J. F.; Chavkin, C., Stress Produces Aversion and Potentiates Cocaine Reward by Releasing Endogenous Dynorphins in the Ventral Striatum to Locally Stimulate Serotonin Reuptake. *J Neurosci* **2012,** *32* (49), 17582.

31. Schindler, A. G.; Messinger, D. I.; Smith, J. S.; Shankar, H.; Gustin, R. M.; Schattauer, S. S.; Lemos, J. C.; Chavkin, N. W.; Hagan, C. E.; Neumaier, J. F.; Chavkin, C., Stress produces aversion and potentiates cocaine reward by releasing endogenous dynorphins in the ventral striatum to locally stimulate serotonin reuptake. *The Journal of Neuroscience* **2012,** *32* (49), 17582-96.

32. Velasquez, J. C.; Zhao, Q.; Chan, Y.; Galindo, L. C. M.; Simasotchi, C.; Wu, D.; Hou, Z.; Herod, S. M.; Oberlander, T. F.; Gil, S.; Fournier, T.; Burd, I.; Andrews, A. M.; Bonnin, A., In Utero Exposure to Citalopram Mitigates Maternal Stress Effects on Fetal Brain Development. *ACS Chem Neurosci* **2019,** *10* (7), 3307-3317.

33. Jiao, J.; Nitzke, A. M.; Doukas, D. G.; Seiglie, M. P.; Dulawa, S. C., Antidepressant response to chronic citalopram treatment in eight inbred mouse strains. *Psychopharmacology (Berl)* **2011,** *213* (2-3), 509-20.

34. Warner-Schmidt, J. L.; Vanover, K. E.; Chen, E. Y.; Marshall, J. J.; Greengard, P., Antidepressant effects of selective serotonin reuptake inhibitors (SSRIs) are attenuated by antiinflammatory drugs in mice and humans. *Proc Natl Acad Sci U S A* **2011,** *108* (22), 9262-7.

35. Meng, Q. H.; Gauthier, D., Simultaneous analysis of citalopram and desmethylcitalopram by liquid chromatography with fluorescence detection after solid-phase extraction. *Clin Biochem* **2005,** *38* (3), 282-5.

36. Workman, A. D.; Charvet, C. J.; Clancy, B.; Darlington, R. B.; Finlay, B. L., Modeling transformations of neurodevelopmental sequences across mammalian species. *J Neurosci* **2013,** *33* (17), 7368-83.

37. Johnson, E. A.; Sharp, D. S.; Miller, D. B., Restraint as a stressor in mice: against the dopaminergic neurotoxicity of D-MDMA, low body weight mitigates restraint-induced hypothermia and consequent neuroprotection. *Brain Res* **2000,** *875* (1-2), 107-18.

38. Kirlic, N.; Young, J.; Aupperle, R. L., Animal to human translational paradigms relevant for approach avoidance conflict decision making. *Behav Res Ther* **2017,** *96*, 14-29.

39. Griebel, G.; Holmes, A., 50 years of hurdles and hope in anxiolytic drug discovery. *Nat Rev Drug Discov* **2013,** *12* (9), 667-687.

40. Samuels, B. A.; Hen, R., Novelty-Suppressed Feeding in the Mouse. In *Mood and Anxiety Related Phenotypes in Mice*, Gould, T. D., Ed. Humana Press: Totowa, NJ, 2011; Vol. 63, pp 107-121.

41. Andrews, A. M.; Cheng, X.; Altieri, S. C.; Yang, H., Bad Behavior: Improving Reproducibility in Behavior Testing. *ACS Chem Neurosci* **2018,** *9* (8), 1904-1906.

42. Dagher, M.; Perrotta, K. A.; Erwin, S. A.; Hachisuka, A.; Iyer, R.; Masmanidis, S. C.; Yang, H.; Andrews, A. M., Optogenetic Stimulation of Midbrain Dopamine Neurons Produces Striatal Serotonin Release. *ACS Chem Neurosci* **2022,** *13* (7), 946-958.

43. Sampson, M. M.; Yang, H.; Andrews, A. M., ADVANCED MICRODIALYSIS APPROACHES RESOLVE DIFFERENCES IN SEROTONIN HOMEOSTASIS AND SIGNALING. In *Compendium of In Vivo Monitoring in Real-Time Molecular Neuroscience*, WORLD SCIENTIFIC: 2017; pp 119-140.

44. Yang, H.; Thompson, A. B.; McIntosh, B. J.; Altieri, S. C.; Andrews, A. M., Physiologically relevant changes in serotonin resolved by fast microdialysis. *ACS Chemical Neuroscience* **2013,** *4* (5), 790-8.

Chapter 3

Kappa opioid receptor modulation of dopamine and serotonin

Introduction

The endogenous opioid system plays an important role in stress-related disorders.[1] The kappa, mu, and delta opioid receptors (KORs, MORs, and DORs, respectively) are the principal opioid receptors.[2,3] Unlike MOR agonists, which have high abuse liability due to their euphoric effects, KOR activation is aversive and produces dysphoria.[4] Dysphoria is a state of profound discomfort, distress, or unease[5,6] and is a common symptom of anxiety and depressive disorders, as well as during withdrawal in substance use disorders.[7]

The native neuropeptide dynorphin activates KORs. The KORs are G-protein-coupled receptors of the $G_{i/o}$ subtype. The KORs are expressed in brain regions related to anxiety, depression, and substance use disorders including the dorsal raphe nucleus (DRN), the ventral hippocampus, and the ventral striatum (vST).[8] The vST, which includes the nucleus accumbens (NAc), is involved in natural- and drug-reward-seeking behaviors and substance use disorders. This brain region also modulates pro- and anti-depressive phenotypes.[9-12] The vST receives serotonergic innervation directly from neurons in the DRN.[13] Additionally, the vST receives indirect serotonergic input *via* dense innervation of dopaminergic cell bodies in the ventral tegmental area, which project to the vST.[14,15] The KORs are highly expressed in the vST, as is their endogenous ligand dynorphin.[16,17]

Dysphoria is modeled in animals by aversive/avoidance responses in behavioral assessments. Conditioned-place aversion (CPA) is commonly used to assess aversion in mice and rats.[18,19] It still not well understood whether the serotonin system, the dopamine system, and/or their interactions mediates dysphoria. For example, Ehrich *et al.* found that for place aversion to occur, KOR activation is required in both serotonin and dopamine neurons.[20] In

contrast, Chefer *et al.* concluded that only KORs on dopaminergic neurons were necessary for place aversion.[21] However, Land *et al.* used a dopamine-deficient mouse line reporting that dopamine is not necessary for place aversion.[22]

Mice with constitutive reductions in KOR expression (KOR-/- mice) fail to produce a place aversion phenotype after KOR agonist administration. Here, restoration of KOR expression *via* non-cell specific lentiviral gene delivery into the DRN was sufficient to rescue aversion. These findings suggest that serotonin neurons projecting from the DRN to the NAc play a key role in CPA.[22] Furthermore, mice with a constitutive loss of serotonin transporter (SERT) expression, *i.e.*, SERT-/- mice, do not show KOR-induced place aversion, suggesting that SERT or altered neurotransmission associated with constitutive loss of SERT[23-25] are involved in the mechanism of KOR-induced aversion.[26] Fontaine *et. al.* demonstrated that deletion of KORs on SERT-expressing neurons prevents stress-induced potentiation of cocaine-conditioned place preference.[27] These authors also found that optogenetic inhibition of serotonin neurons projecting from DRN induces a place aversion phenotype.

Behavioral studies suggest that both the dopamine and serotonin systems are involved in aversive phenotypes. Studies have been carried out to investigate the effects of KOR activation neurochemically. Activation of KORs modulates dopamine and serotonin neurotransmission.[11,20-22,26,27] The majority of research investigating the role of KORs in mood, anxiety, and stress-related disorders have implicated the dopamine system.[21,28-30] Microdialysis studies have shown that activation of KORs causes decreases in dopamine levels in the NAc.[30-33] Drugs of abuse increase dopamine levels in the NAc and contribute to rewarding effects.[34] The opposite effect that KOR has on dopamine transmission compared to drugs of abuse suggests a mechanism for producing aversive states. However, given that

the dopamine and serotonin systems are interconnected,[35,36] we hypothesize that KOR activation modulates these systems synergistically. Nevertheless, few studies have looked at the interactions between the dopamine and serotonin systems after KOR activation.

Although behavioral studies implicate the serotonin system in KOR-induced aversion, the effects of KOR activation on the basal and stimulated serotonin levels in the vST and DRN remain under-studied and inconclusive. Tao *et al.* found decreases in serotonin efflux in the vST and DRN after perfusion of the KOR agonist U50,488 into the DRN in rats.[37,38] They also found decreased serotonin efflux in the vST after perfusion of U50,488 into the vST. Therefore, showing activation of KOR in the cell body region of DRN and in the terminal region of vST. By contrast, Carlezon and colleagues observed no changes in serotonin levels in the NAc after intraperitoneal injection of Salvinorin A (SalvA), a highly potent KOR agonist.[31,39]

In addition to mesolimbic brain regions, the hippocampus (HPC) has been studied in the context of anxiety, depression, stress, and antidepressant medications,[40] making the HPC a region of interest in KOR-serotonin interaction studies. Yoshioka *et al.* perfused U69,593, another KOR agonist, into rat ventral hippocampus and observed no changes in basal or stimulated serotonin levels by microdialysis.[39] However, Grilli *et al.* found that SalvA or U69,593 blunted K^+-stimulated the release of serotonin from hippocampal synaptosomes.[41] These and other contradictions in the literature illustrate the need for further research characterizing the effects of KOR activation, particularly on serotonin neurotransmission.

Concurrent analyses of the dopamine and serotonin systems are needed to understand the mechanisms of KOR activation as they pertain to dysphoria and other behavioral effects. Here, I used *in situ* hybridization and microdialysis to investigate the

relationship between the dopamine, serotonin, and kappa opioid receptor systems. Based on previous literature and the known mechanisms of action of $G_{i/o}$ GPCRs, I hypothesized that systemic and local administration of the KOR agonist U50,488 would decrease basal and stimulated levels of extracellular serotonin and dopamine. Examining stimulated release, in addition to basal levels, is important for investigating the stimulus-responsivity of neurotransmitter release.

Materials & Methods

Animals and Treatment

Mice were obtained from The Jackson Laboratory (C57BL/6J, JAX stock no. 000664) or generated at the University of California, Los Angeles (UCLA) from an ePet^{cre} line (B6.Cg-Tg(Fev-cre)1Esd/J, JAX stock no. 012712) on a C57Bl/6J background *via* female carrier and male non-carrier matings. The Association for Assessment and Accreditation of Laboratory Animal Care International has fully accredited UCLA. All animal care and use met the requirements of the NIH Guide for the Care and Use of Laboratory Animals, revised 2011. The UCLA Chancellor's Animal Research Committee (Institutional Animal Care and Use Committee) preapproved all procedures.

Drugs

The following drugs were obtained from Sigma Aldrich: (+/-)-trans-U-50488 methane sulfonate salt (Cat# D8040), (-)-trans-(1S,2S)-U-50488 hydrochloride hydrate (Cat# U111), and clozapine *N* oxide (CNO) (Cat# C0832). Citalopram hydrobromide was obtained from TCI America (Cat#2370).

RNAscope

In situ hybridization was carried out using RNAscope® (Advanced Cell Diagnostics Inc., Newark, CA) and a fresh-frozen V2 protocol as previously described[36] to colocalize mRNA for SERT, KOR, vesicular glutamate transporter 3 (VGlut3), and vesicular GABA transporter (Vgat) in dorsal raphe neurons. Four mice were sacrificed by cervical dislocation without isoflurane. Their brains were removed, cryoprotected, and frozen. One section per mouse was used for analyses. The sections spanned different areas of the DRN with some being

more rostral and some more caudal. Coronal sections were cut at 20-µm on a cryostat at -15-20 °C and mounted on poly-L-lysine-coated slides (Fisher Scientific, Cat #12-550-15).

In situ hybridization probes were as follows: *Sert* (Mm-Slc6a4 Cat#315851) channel 1, *Oprk1* (Mm-Oprk1 Cat#316111-C2) channel 2, *Vglut3* (Mm-Slc32a1 Cat#319191-C3) channel 3, or *Vgat* (Mm-Slc17a8-C3 Cat# 431261-C3) channel 3. Opal dyes 520, 570, and 690 were paired with each probe, respectively (Cat# FP1487A, FP1488A, FP1497A). ProLong™ Diamond Antifade Mountant with DAPI (Molecular Probes P36966) was added to visualize cell bodies. For *Vglut3*, one section from each of four mice was used. For *Vgat* , three sections from one of these four mice were used.

Visualization was carried out using a Leica DMI8 or Zeiss LSM800 microscope and images were processed with LAS X and Zen software. Cell nuclei in each field of view were identified by DAPI staining. The DAPI-labeled nuclei associated with puncta for one or more mRNA probes were then counted. Data are reported as percent positive cells calculated by dividing the number of cells labeled with *Sert*, *Oprk1*, and/or *Vglut3*/*Vgat* by the total number of labeled cells or by the total number of *Sert* labeled cells.

Surgical procedures

Surgeries were carried out under aseptic conditions with isoflurane anesthesia on a KOPF Model 1900 Stereotaxic Alignment System (KOPF, Tujunga, CA). The analgesic carprofen (5 mg/kg, 1 mg/mL) was given subcutaneously (sc) just prior to beginning surgery. Bupivacaine (0.05-0.1 mL) was administered as a local anesthetic under the skin prior to making incisions. Viral vector, *i.e.*, 500 nL of $\geq 1\times10^{13}$ vg/mL 7.8×10^{12}/mL pAAV-hSyn-DIO-hM4D(Gi)-mCherry was delivered into the DRN (AP-4.6 mm, ML ±1.93 mm, DV -2.75 mm from Bregma at a 40° angle) using a Nanoject II (Drummond Scientific, Broomall, PA). The

pAAV-hSyn-DIO-hM4D(Gi)-mCherry was donated by Bryan Roth (Addgene viral prep #44362-AAV9; http://n2t.net/addgene:44362;RRID:Addgene_44362).[42]

After the surgery, mice recovered for two weeks to allow for viral vector expression before experiments. Mice undergoing chemogenetics and microdialysis were implanted with a guide cannula at the same time as AAV delivery. For KOR agonist experiments, a CMA/7 guide cannula for a microdialysis probe was aimed at the vST (AP+1.00 mm, ML±1.75 mm, DV-3.10 mm from Bregma) or vHPC (AP-3.6 mm, ML±3.2 mm, DV-1.5 mm from Bregma). Each guide cannula was secured to the skull with Trim II Dental Cement (Keystone) and an anchor screw. After surgery, mice were given daily carprofen injections (5 mg/kg, 1 mg/mL, sc) for three days.

Microdialysis

Microdialysis experiments were carried out in male mice as previously described between ZT1-8.[23,24,36] Basal samples were collected during ZT1-2, followed by three high K^+ perfusions to stimulate neurotransmitter release (ZT2-5) each lasting 5 min and separated by an hour of aCSF perfusion. After the last high K^+ stimulation, animals received an intraperitoneal (i.p.) injection of U50,588H (10 mg/kg, 3 mL/kg). The injection solution concentration was based on the salt MW. The pH was adjusted to 7.4, and solutions were sterilized by filtration through 0.22 μm syringe filters (Millipore, Billerica, MA). The systemic U50,588 dose was determined in a conditioned place aversion assay, where 10 mg/kg induced the greatest aversion to the drug-paired side in male mice.

For intracerebral drug administration, basal samples were collected from ZT1-2 followed by perfusion of U50,588 into the vST from lowest to highest concentrations for 90 min each. The U50,588 solutions perfused during microdialysis were prepared in regular

aCSF at concentrations between 10-1000 μM. In experiments using the SSRI citalopram, 10 mM citalopram was prepared in regular aCSF alone and in combination with 500 μM U50,588. For chemogenetic experiments, an injection of clozapine-*N*-oxide (CNO, 1 mg/kg, ip, 10 mL/kg) was administered following the collection of basal dialysate samples.

All analyses were performed using an Amuza HTEC 500 integrated HPLC system (Amuza Corporation, San Diego, CA) with an Amuza Insight autosampler for injecting standard samples and an Amuza EAS 20s online autoinjector for collecting and injecting dialysate samples. Chromatographic separation was achieved using an Amuza PP ODS III column (4.6 mm ID × 30 mm length, 2 μm particle diameter) and a phosphate buffered mobile phase with 14.9 g/L NaH_2PO_4 (Fluka #17844), 1.02 g/L Na_2HPO_4 (Thermo Scientific AC448160050), 2% MeOH (EMD #MX0475), 50 mg/L EDTA·Na_2 (Sigma #03682), and 600 mg/L sodium decanesulfonate (TCI #I0348) in Optima LC/MS grade water (Fisher Scientific CAS# 7732-18-5). The column temperature was maintained at 25 °C. The volumetric flow rate was 500 μL/min.

Electrochemical detection was performed using an Amuza WE-3G graphite working electrode with an applied potential of +450 mV *vs.* a Ag/AgCl reference electrode. Dopamine (Sigma #H8502) and serotonin (Sigma #H9523) standards were prepared in a 1:1 mixture of mobile phase and regular aCSF (147 mM NaCl (Fluka #73575), 3.5 mM KCl (Fluka #05257), 1.0 mM $CaCl_2$ (Aldrich #499609), 1.0 mM NaH_2PO_4, 2.5 mM $NaHCO_3$ (Fluka #88208), 1.2 mM $MgCl_2$ (Aldrich #449172), pH 7.3 ± 0.03. Standard curves (62.5 pM−10 nM) encompassed physiological concentration ranges. The limit of detection was ≤65 pM, and the practical limit of quantification was ≤200 pM. All dialysate samples were collected online at

5-min intervals at a dialysate flow rate of 2.5 μL/min and injected immediately onto the HPLC system for analysis.

Conditioned Place Aversion

The testing room containing the conditioning chambers was equipped with low lighting. The two sides of the conditioning chamber were the same size (22 cm length × 19.8 cm width × 27 cm height) but were visually distinct *via* black-and-white checkered or diagonal stripes. Adjacent sides of the conditioning chamber were separated by a 20.7 cm wide × 30 cm high sliding partition.

The U50,488 was dissolved in 0.9% USP sodium chloride (Hospira, Lake Forest, IL). Injection solution concentrations were based on the salt MW and solutions were sterilized by filtration through 0.22 μm syringe filters (Millipore, Billerica, MA). On day 0, no injections were administered, and all mice were given free access to both sides of the conditioning chamber for 30 min to assess side biases. Experimental groups were balanced for side preferences. On days 1-8, ip injections of saline or U50,488 (2-10 mg/kg; 10 mL/kg) were administered once per day prior to placing each mouse into the paired side of the conditioning chamber. One side of the chamber was always paired with saline; the other side was paired with U50,488 in drug-treated mice or saline in saline-treated mice.

During the 8 conditioning days, access was limited for 30 min to the single side of the chamber paired with that day's treatment. Saline-treated mice received saline every day on days 1-8. Drug-treated mice received U50,488 or saline on alternating days. On day 9, mice were not injected but were placed on the center line randomly facing a side of the conditioning chamber with free access to both sides for 30 min. On day 10, drug- and saline-

treated mice were administered U50,488 or saline, respectively, prior to being placed in the apparatus with free access to both sides for 30 min.

Chambers were cleaned with DLAM-provided Accel solution and wiped dry between mice. The chambers were cleaned with ethanol and then Accel solution when switching between males and females. The time spent in each side, transitions between sides, and locomotor activity were tracked and analyzed using Any-Maze software (Stoelting Co.). Data were analyzed and plotted as a preference score defined as [Time in Test(paired) − Time in Test(unpaired)] − [Time at baseline(paired) − time at baseline(unpaired)]. The CPA paradigm and analysis were adapted from protocols used in the laboratory of Dr. Catherine Cahill at UCLA.[43,44]

Immunocytochemistry for DREADD transfection

Immunocytochemistry experiments to confirm DREADD (designer receptors exclusively activated by designer drug) transfection were carried out as described previously by Falcy *et. al.*[45] Mouse brains were cut into 35-40 μM sections targeting the DRN using a cryostat. The antibodies were from Abcam: rabbit monoclonal anti-mCherry[EPR20579] (ab213511) and donkey anti-rabbit IgG H&L with Alexa Fluor® 488 (ab150073). Both antibodies were used at a dilution of 1:1000. Antibodies were diluted in 0.3% Triton-X (Sigma Aldrich #11332481001) in 1× tris-buffered saline (TBS) (Sigma Aldrich #T5912). ProLong™ Diamond Antifade Mountant with DAPI (Molecular Probes P36966) was added to stain cell bodies. Visualization was carried out using a Leica DMI8 microscope and images were processed with LAS X software.

Data Analysis & Statistics

The microdialysis time-course data were analyzed in terms of absolute neurochemical concentrations (nM) and as precents of mean pre-drug basal neurochemical levels (%basal). The area under the curve (AUC) for each stimulation peak, defined by the four dialysate samples after the onset of stimulation, was calculated by trapezoidal integration and is reported in nM or as a percent of mean pre-drug basal levels.

Statistical analyses were carried out using Prism v.9.0.2 (GraphPad Inc., La Jolla, CA). Data are expressed as group means ± SEMs. Two-tailed *t*-tests (either unpaired or ratio paired, as appropriate) were used for two group comparisons. One-way and two-way ANOVAs were used for multiple group comparisons. Throughout, $P<0.05$ was considered statistically significant.

Results & Discussion

Identification of KOR-expressing neuronal populations in the dorsal raphe nucleus

The DRN contains a majority of the forebrain projecting serotonin neurons yet is a heterogenous brain region.[46-48] High throughput single-cell transcriptome sequencing showed that the DRN contains in addition to serotonergic neurons, neurons with dopaminergic, peptidergic, glutamatergic, and GABAergic phenotypes.[46] Fontaine *et al.* reported co-expression of *Sert* (serotonin transporter), *OPRK1* (KOR), and *Vglut3* (vesicular glutamate transporter type 3) mRNA in the DRN using RNAscope.[27] I carried out RNAscope experiments examining co-expression of *Sert, OPRK1, Vglut3*, and *Vgat* (vesicular GABA transporter) mRNA in the DRN.

First, I analyzed co-expression of *Sert, Oprk1*, and *Vglut3* in the DRN of mouse brain sections (**Fig. 3.1a**). Relative to all cells counted, ~17% expressed *Sert* alone, ~3% expressed

Oprk1 alone, and 40% expressed *Vglut3* alone. Moreover, 20% co-expressed *Sert* and *Vglut3*, 4% co-expressed *Sert* and *Oprk1*, 9% co-expressed *Vglut3* and *Oprk1*, and 6% co-expressed all three genes (**Fig. 3.1b**). In total, about 10% of DRN cell bodies co-expressed *Oprk1* and *Sert*. I further analyzed co-expression in terms of total *Sert*-positive cells (**Fig. 3.1c**). I found that 35% of all *Sert*+ cells expressed only *Sert*, 42% co-expressed only *Sert* and *Vglut3*, 9% co-expressed only *Sert* and *Oprk1*, and 13% co-expressed all three genes. Thus, I found that about 22% of *Sert*+ cells co-expressed *Oprk1* irrespective of *Vglut3*. My results differ from the single other study that also examined *Sert, Vglut3,* and *Oprk1* co-expression. Fontaine *et al.* suggests almost 100% co-expression of *Sert, Vglut3* and *Orpk1* within the DRN.[27] The difference in results could be due to slight variations in the rostral-caudal coordinates of the slices analyzed in my study and their study. Ideally, the entirety of the DRN from most rostral to most caudal would be analyzed to determine overall expression.

Next, I investigated the co-expression of *Sert, Oprk1*, and *Vgat* in the DRN of mouse brain sections (**Fig. 3.2a**). Sections came from one mouse that was also used for *Vglut3* experiments. Relative to all cells counted, ~20% expressed *Sert*, ~7% expressed *Oprk1*, and 26% expressed *Vgat* alone. Meanwhile, 5% co-expressed *Sert* and *Vgat*, 7% co-expressed *Sert* and *Oprk1*, 30% co-expressed *Vgat* and *Oprk1*, and 5% co-expressed all three genes (**Fig. 3.2b**). Similar to the analysis above for *Vglut*, about 12% of DRN cell bodies expressed *Oprk1* and *Sert*. I further analyzed co-expression in terms of total *Sert*-positive cells (**Fig. 3.2c**). I found that 60% of all *Sert*+ cells expressed only *Sert*, 14% co-expressed only *Sert* and *Vgat*, 15% co-expressed only *Sert* and *Oprk1*, and 10% co-expressed all three mRNAs. Again, I found that about 25% of *Sert*+ cells co-expressed *Oprk1* irrespective of *Vgat*.

The results of the RNAscope experiments indicated two possible modes of KOR modulation of serotonin. First, by activating KORs on serotonin neurons, dynorphin or a KOR agonist would directly inhibit serotonin release through the known $G_{i/o}$ GPCR mechanism of hyperpolarization, which decreases the probability of action potentials. I also found that *Oprk1* and *Vgat* as well as *Oprk1* and *Vglut3* mRNA were co-localized in the same cell bodies, indicating a possible mode of indirect modulation of serotonin *via* GABAergic or glutamatergic neurons. I hypothesize that these GABA+/KOR+ neurons are interneurons. Activation of KORs on GABAergic neurons inhibits GABA release, leading to the disinhibition of serotonin neurons. Disinhibition of serotonin neurons could result in increased serotonin in the extracellular space (**Fig. 3.7**). Fontaine *et al.* suggests *SERT+*DRN neurons but not *Vglut3+* neurons are responsible for the consequences of stress on cocaine CPP.[27] These data suggest these subpopulations of neurons could have differing effects upon activation or inhibition. Thus, further experiments would need to be carried out to investigate these mechanisms and to identify whether the *Vgat/Vglut3* and *Oprk1* expressing cells are interneurons or projection neurons and their role in aversion.

Effects of systemic activation of KORs on ventral striatum

Using microdialysis, I quantified basal and stimulated extracellular dopamine and serotonin levels in the vST prior to and during global activation of KORs with U50,488, a kappa agonist. Dopamine and serotonin were measured in the same dialysate samples.[24,36] Dialysate samples were collected from the vST (**Fig. 3.3a**), a brain region widely studied in the context of natural- and drug-reward-seeking behaviors, substance use disorder (SUD), and pro- and anti-depressive phenotypes.[9-11,49,50]

Standard curves were used to identify and quantify sample peaks (**Fig. 3.3b**). In agreement with the literature,[30-33] I observed significant decreases in basal dopamine levels after administration of a KOR agonist (**Fig. 3.4ab**). No differences in K^+-stimulated dopamine overflow were observed (**Fig. 3.4c**). Regarding serotonin, I observed no significant differences in basal or stimulated release after the kappa agonist was administered systemically (**Fig. 3.4d-f**). In a previous study, we found that 5-6-min K^+ stimulations caused maximal neurotransmitter release. Thus, the use of 5-min K^+ stimulations here might have obscured more subtle effects of U50,488 on stimulated dopamine and serotonin levels.

In chapter 2, I report on increased extracellular serotonin in the ventral hippocampus (vHPC) after systemic injection of a KOR agonist, U50,488, with simultaneous SSRI administration. Since I did not observe changes in serotonin in the vST after systemic administration of a KOR agonist, my combined findings suggest that KOR modulation of serotonin may be brain-region specific.

Local activation of KORs in ventral striatum and ventral hippocampus

Microdialysis is both a neurotransmitter measurement technique and a method of local delivery that enables the investigation of brain-region-specific effects of drugs. Hence, I quantified extracellular dopamine and serotonin in the vST in response to local perfusion of the kappa agonist, U50,488. For dopamine, I observed decreases in basal levels after intrastriatal U50,488 perfusion, similar to what I observed after systemic U50,488 (**Fig. 3.5a**). However, for serotonin, in contrast to systemic administration, I observed increases in basal levels after perfusion of U50,488 into the vST (**Fig. 3.5b**). Figure 5c shows an overlay of representative dialysate time courses and the dose-dependent effects of local perfusion of U50,488.

While I observed increased serotonin levels upon perfusion of a kappa agonist into the vST, Tao *et al.*, reported decreased serotonin in the vST after perfusion of U50,488 (300-1000 μM) into the DRN.[37,38] One explanation for these contrasting findings is differences in brain-region-dependent activation of KORs, *i.e.,* activation of KORs on terminals in vST *vs.* cell bodies in DRN. I hypothesize that within the vST, serotonin increases are mediated *via* activation of KORs on GABAergic neurons (medium spiny neurons), resulting in disinhibition of serotonin terminals. Meanwhile, activating KORs in the DRN might directly inhibit serotonin neurons (as described above), resulting in decreased serotonin levels in the vST. Figure 7 depicts these proposed mechanisms. I further hypothesize that activation of KORs simultaneously in the DRN and vST by systemic injection of a KOR agonist results in no net changes in vST serotonin.

In addition to vST, I perfused U50,488 into the vHPC of a prenatally stressed mouse from the chronic unpredictable stress project (see chapter 2). The *in vivo* microdialysis time course is shown in **Figure 3.6a**. Like the vST, I saw an increase in extracellular serotonin levels within the vHPC after local perfusion of 500 μM U50,488. The SSRI citalopram was also perfused concomitantly with U50,488. The increase in serotonin after the combined perfusion of U50,488 and citalopram was nearly double that of either drug alone (**Fig. 3.6b**). These preliminary data suggest that local SERT inhibition and KOR activation are additive.

Conditioned Place Aversion

The CPA and conditioned place preference (CPP) paradigms are behavioral assays commonly used in rodents to study the aversive and rewarding properties, respectively of various stimuli, *e.g.*, drugs. Human studies have demonstrated the subjective dysphoric properties of KOR agonists.[4] In rodents, KOR agonists produce context-dependent CPA.[3,21,51]

Here, experiments were carried out in male and female C57B6/J mice to determine optimal doses of U50,488 to induce CPA phenotypes. **Figure 3.8** shows the eight-day conditioning paradigm. Doses of 0, 2.5, 5, and 10 mg/kg were tested in male mice and were adapted from previous studies.[20,44] Doses were reduced (0, 2, 4, and 6 mg/kg) in female mice due observations in pilot work in SERT (+/+) mice showing that females are more sensitive to the hypolocomotor effects of higher doses of U50,488, as indicated by a lack of movement within the CPA apparatus (**Fig. 3.8b,c**).

On the context-dependent testing day (day 9), a significant dose-dependent decrease in preference score was seen in male mice (**Fig. 3.9a**, left). The same trend was observed in female mice (**Fig. 3.9b**, left). On the state-dependent testing day (day 10), mice were given an injection of U50,488 or saline corresponding to experimental or control groups, respectively. A similar trend toward decreases in preference scores was seen in male and female mice. However, there were larger individual variations in the state-dependent data, which could be associated with greater individual differences in drug responses.

The results of the state-depending testing are not what I would initially hypothesize, *i.e.*, potentiated aversion during state-dependent testing. This hypothesis stems from the idea that a combination of U50,488 and endogenous dynorphin activation of KORs will result in potentiated avoidance of the drug-paired side of the CPA apparatus A reason for the data trends could be that KOR agonists have hypolocomotive and analgesic properties.[44,52] Groups receiving higher doses of the KOR agonist displayed decreased locomotion (**Fig. 3.8bc**). If mice were sedated due to KOR activation, the ability to roam freely and avoid the "aversive" chamber would be hindered, thus, confounding data interpretation. Overall,

these results indicate that the U50,488 doses used for future studies should be 5-10 mg/kg for male mice and 4 mg/kg for female mice.

Chemogenetic inhibition of serotonin neurons during CPA

Serotonin neurons in the DRN project to the vST.[46-48] The inhibitory DREADD hM4D(Gi) was selectively expressed in serotonin neurons in the DRN using an ePET^{cre} mouse line, which restricts gene expression to *Pet-1* expressing neurons. The Pet-1 erythroblast transformation specific (ETS) factor is a precise marker for developing and adult serotonin neurons.[53] After a 2-week transduction period, immunocytochemistry was performed in brain sections to confirm successful integration and expression of the inhibitory DREADD (**Fig. 3.10a**). Although the AAV construct was tagged with an mCherry fluorescent reporter, an anti-mCherry antibody was used based on findings by Falcy *et. al.* suggesting that expression of this DREADD in neurons dampens mCherry fluorescence.[45] Poor mCherry fluorescence hinders the ability to confirm transfection. Nonetheless, I identified the DREADD expression through both mCherry and anti-mCherry antibody fluorescence with mCherry fluorescence observed only after long exposure times *i.e.,* >1 min.

Microdialysis was used to confirm the functional effectiveness of the DREADD expression to selectively inhibit serotonin release. Basal serotonin and dopamine levels were collected for one hour prior to an injection of CNO (1 mg/kg, i.p.)[54] to activate the DREADDs (**Fig. 3.10b**). Activation of inhibitory DREADDs by CNO significantly decreased extracellular serotonin levels but not dopamine levels (**Fig. 3.10c**). The decrease in serotonin but not dopamine indicates I can selectively inhibit serotonin transmission using chemogenetics.

Conclusions & Future Directions

My data show that KOR activation increases extracellular serotonin in the vST and vHPC. Systemic KOR-induced increases in serotonin are dependent on SERT inhibition, while KOR-induced increases in serotonin due to local activation occur with or without SERT inhibition.

Multiple mechanisms of action are hypothesized to be the cause of the differences in the effects of local *vs.* systemic KOR administration with and without SERT inhibition. The RNAscope data indicate a few possible mechanisms. One is a direct mechanism involving KORs on serotonergic neurons, in which KOR activation causes a hyperpolarization of neurons. A second is an indirect mechanism that involves GABAergic and glutamatergic neurons projecting to vST, causing a possible disinhibitory effect. To investigate the indirect role of GABAergic neurons, pharmacological interventions targeting GABA systemically and locally can be used to determine the role of GABAergic neurons during KOR activation and brain region specificity. I hypothesize that activating GABAergic neurons will attenuate serotonin increases observed after KOR agonist administration.

Third, is activating downstream intracellular pathways. Schindler *et al.* proposed a mechanism whereby KOR activation induces a mitogen-activated protein kinase (MAPK) dependent intracellular signaling pathway that ultimately results in the phosphorylation of SERT (and other target proteins).[26] Phosphorylation of SERT increases plasma-membrane SERT localization effectively increasing serotonin reuptake.[26,55] This would decrease extracellular serotonin, which is the opposite of what I found but would match the findings of Tao *et al.*[37,38] One way to test this theory would be to investigate extracellular levels of serotonin after KOR activation in SERT deficient mice. Another way to test this hypothesis would be to administer a p38 MAPK inhibitor prior to KOR agonist administration to

determine whether the former blocks the effects of the KOR agonist on extracellular serotonin levels.

Fourth, KORs could be modulating serotonin *via* medium spiny neurons (MSN). The D1 receptor-containing MSNs express and release dynorphin.[56-58] These D1 dynorphin-positive MSNs have been implicated in reward and aversion.[58] Soares-Cunha *et al.* showed that prolonged optical stimulation of D1 MSNs in the vST induced aversion.[58] Conversely, brief stimulation induced a place preference phenotype. These findings suggest that the same MSNs are involved in reward and aversion depending on the time frame of neuronal activation.

The D1-containing MSNs are found to constitute the majority of striatal input to serotonergic neurons in the DRN.[47] The vST MSNs projecting to the DRN were found to inhibit serotonergic signaling directly. The inhibitory effect was blocked by a GABA-A antagonist further implicating a role of GABA in this inhibitory effect.[47] While we do not know the effect of dynorphin released from these MSNs, there is a possibility of dynorphin-related regulation due to the inhibitory nature of these neurons and their projection to the DRN. Future studies should assess the effects of optogenetic or chemogenetic inhibition of D1 dynorphin-positive MSNs to determine the effects on extracellular serotonin and dopamine levels in multiple brain regions associated with dysphoria and aversion.

While my study shows that KOR activation can increase serotonin levels, further research is needed to link changes in serotonin levels after KOR activation and aversive phenotypes. Future studies should be aimed at coupling microdialysis with behavior testing. I optimized our HPLC methods to enable 5-min (or less) online dialysate sampling times in the vST for concurrent dopamine and serotonin analysis. This relatively short sampling time

will allow enough samples to be collected during the 30-min CPA behavioral test, as opposed to conventional microdialysis sampling, which is on the order of 10-20 min per sample. By analyzing brain dialysate samples during CPA, we will be able to investigate whether serotonin signaling is necessary and sufficient for the manifestation of aversive behavior, *i.e.*, the avoidance of environments paired with dysphoria-producing KOR agonists. Studies can specifically target serotonin neuron populations and subpopulations (using intersectional genetics) using optogenetics and chemogenetics to determine the necessity of increased vST extracellular serotonin in the aversive phenotype.

Based on my results showing increased serotonin after KOR activation, I hypothesize that disinhibiting serotonin neurons *via* KORs expressed on GABAergic neurons will increase extracellular serotonin and produce place aversion. My hypothesis is also supported by studies showing that giving drugs that increase extracellular serotonin cause place aversion. For example, Marona-Lewick *et al.* found that fenfluramine and 5-methoxy-6-methyl-2-aminoindane (MMAI), both known serotonin-releasing agents, induced a place aversion phenotype in rats.[59] However, these authors also found that MDMA, which is known to release serotonin, causes place preference. The drug MDMA can also cause norepinephrine and dopamine release, though not as greatly as serotonin.[59] This discrepancy in place aversion *vs.* preference associated with serotonin releasing drugs could have to do with interactions with and/or involvement of other neurotransmitters. Making multiplexed neurochemical measurements during behavioral tests will enable a better understanding of the interplay of neurotransmitter systems during complex behaviors.

Figures & Tables

Figure 3.1

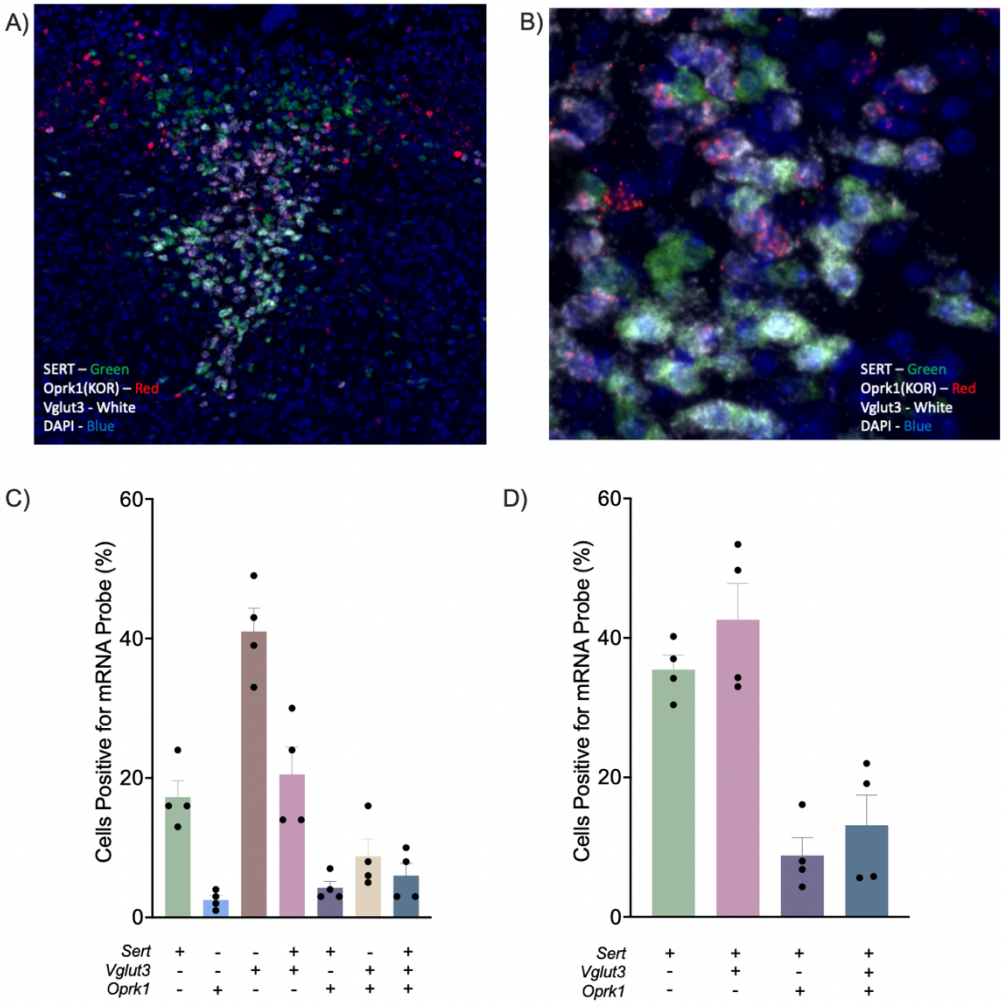

Figure 3.1: Co-expression of *Sert, Oprk1,* and *Vglut3* by RNAscope. **A.** Cell nuclei were stained with DAPI (blue). Antisense probes to localize *Sert* (green), *Oprk1* (red), and *Vglut3* (white) mRNA were visualized. To be counted, puncta for each mRNA were colocalized in the same nuclei but did not necessarily overlap. **B.** Zoomed in area to show representative individual cell types. **C.** Relative quantification of cells containing *Sert*, *Oprk1*, and *Vglut3* mRNA with respect to the total numbers of cells counted. **D.** Relative quantification of cells containing *Sert*, *Oprk1*, and *Vglut3* mRNA with respect to the total number of *Sert* expressing cell bodies counted. For C and D, data are means ± SEMs for *N*=4 mice. Each dot is the mean from n=4 brain sections/mouse.

Figure 3.2

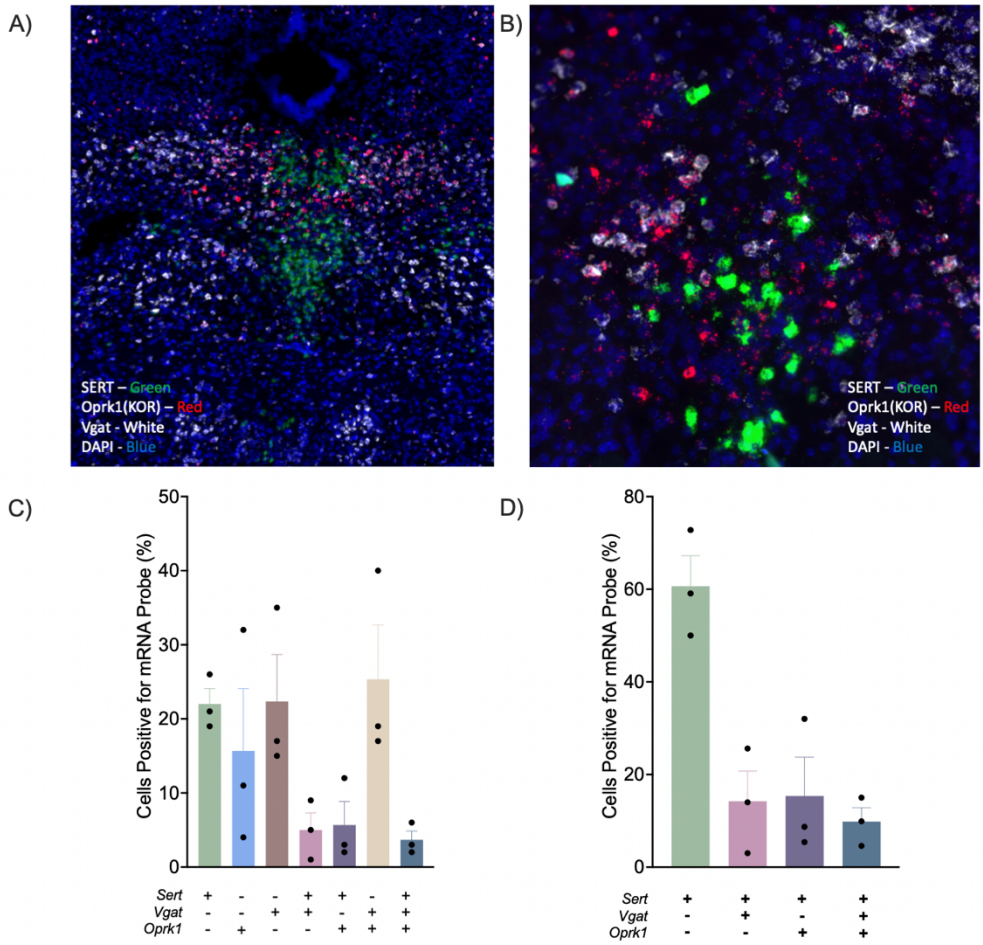

Figure 3.2: Co-expression of *Sert, Oprk1,* and *Vgat* by RNAscope. **A.** Cell nuclei were stained with DAPI (blue). Antisense probes to localize *Sert* (green), *Oprk1* (red), and *Vgat* (white) mRNA were visualized. To be counted, puncta for each mRNA were colocalized in the same nuclei but did not necessarily overlap. **B.** Zoomed in area to show representative individual cell types. **C.** Relative quantification of cells containing *Sert*, *Oprk1*, and *Vgat* mRNA with respect to the total number of cell bodies counted. **D.** Relative quantification of cells containing *Sert*, *Oprk1*, and *Vgat* mRNA with respect to the total number of *Sert* expressing cell bodies counted. In C and D, data are means ± SEMs for *N*=1 mouse; each dot is a single section (n=3 brain sections).

Figure 3.3

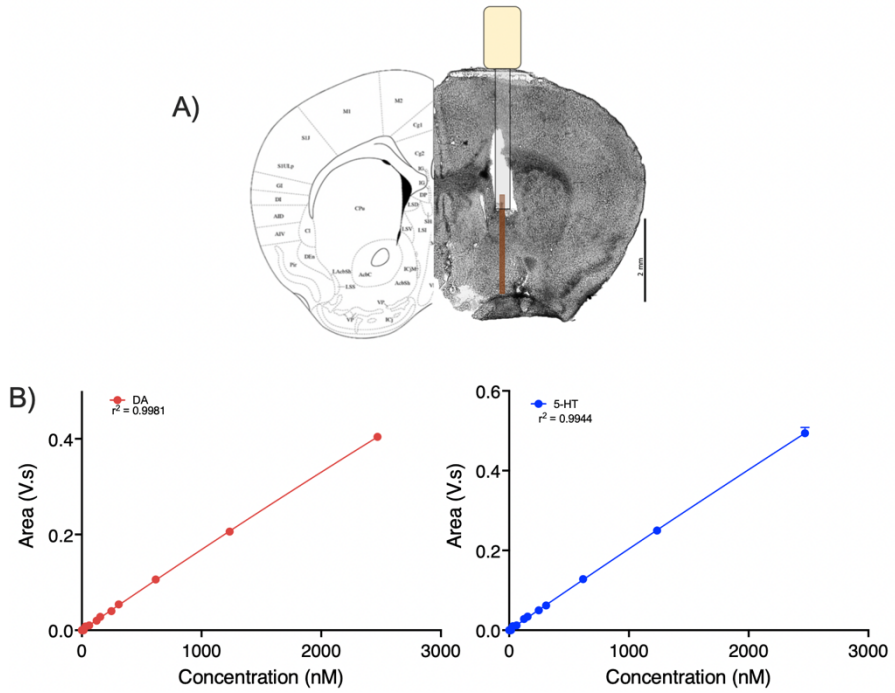

Figure 3.3: *In vivo* Microdialysis **A)** Microdialysis probe verification in the ventral striatum using cresyl violet staining aligned with Mouse Brain Atlas Fig. 21 (Paxinos, George, and Franklin. The mouse brain in stereotaxic coordinates: hard cover edition. Access Online via Elsevier, 2001.) **B)** Dopamine (left) and serotonin (right) standard curve plots by high performance liquid chromatography.

Figure 3.4

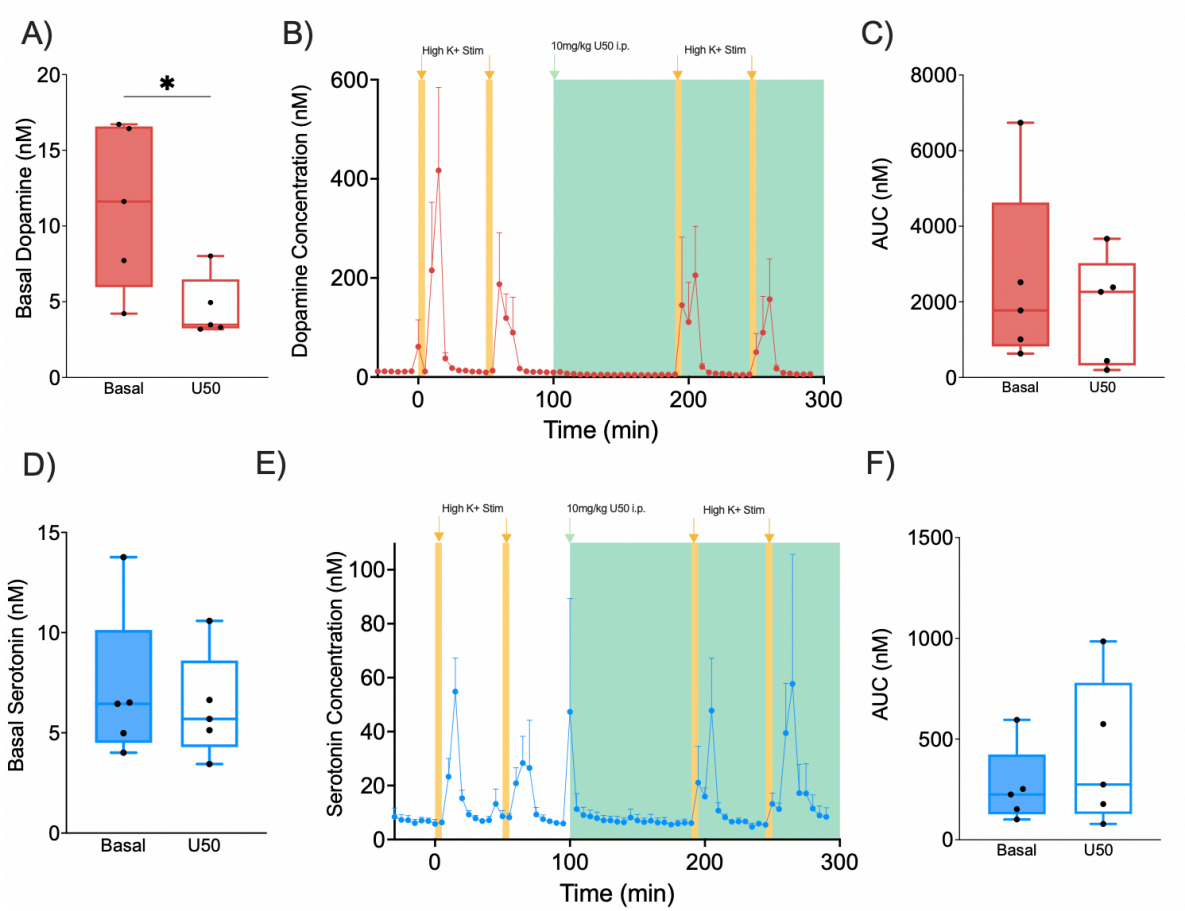

Figure 3.4: Neurochemical effects of systemic administration of a kappa agonist. **A,D)** Basal changes in dopamine (red) and serotonin (blue), respectively. **B,E)** Microdialysis time courses of dopamine and serotonin. **C, F)** Areas under the curve for high potassium stimulations (5-min each, yellow bars). Data are means ±SEMs. Each point in A,C,D,and F represents averages from one mouse. *N*=5 mice. *P<0.05.

Figure 3.5

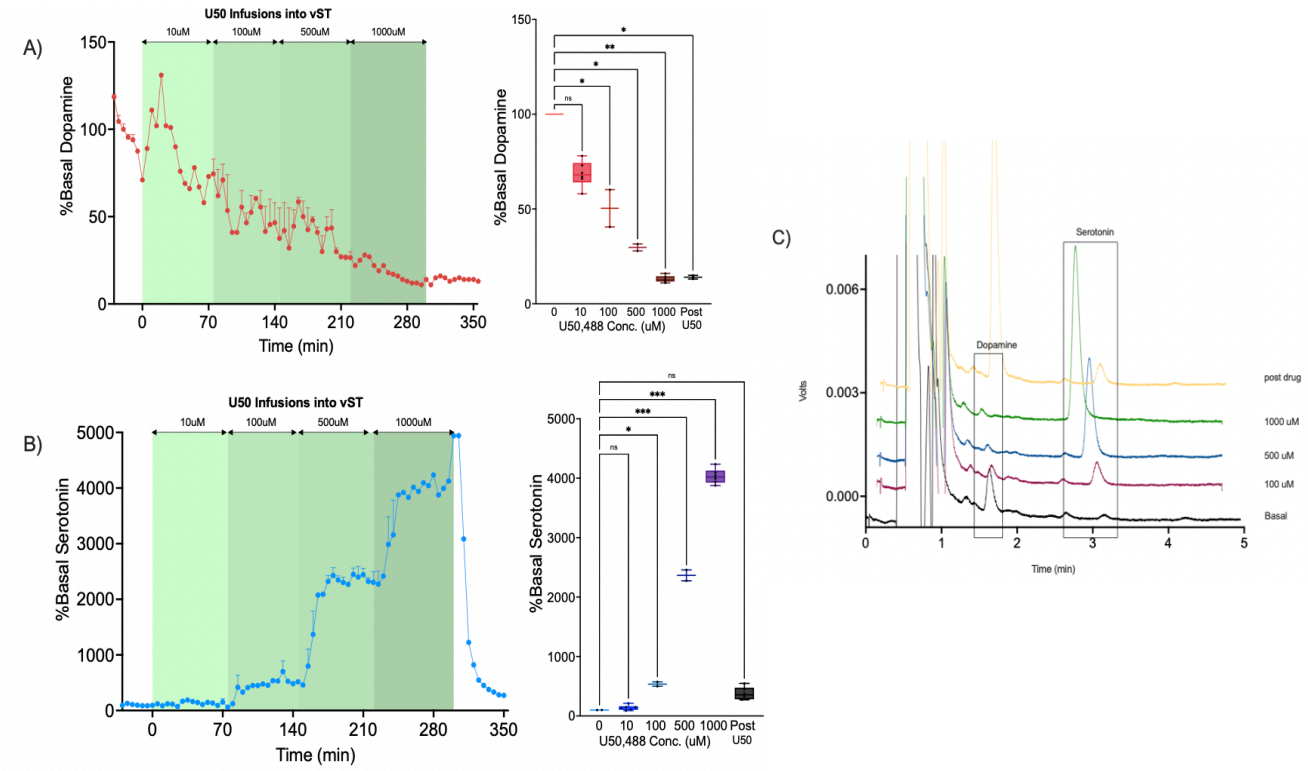

Figure 3.5: Effects of local perfusion of the kappa agonist U50,488 on neurotransmission in the ventral striatum. **A)** Percent basal dopamine levels before and after perfusion of different concentrations of U50,488. **B)** Percent basal serotonin levels before and after perfusion of U50,488. **C)** Representative microdialysis chromatograms for each infusion concentration. Data are means ± SEMs. N=2 mice. *P<0.05, **P<0.01, ***P<0.001

Figure 3.6

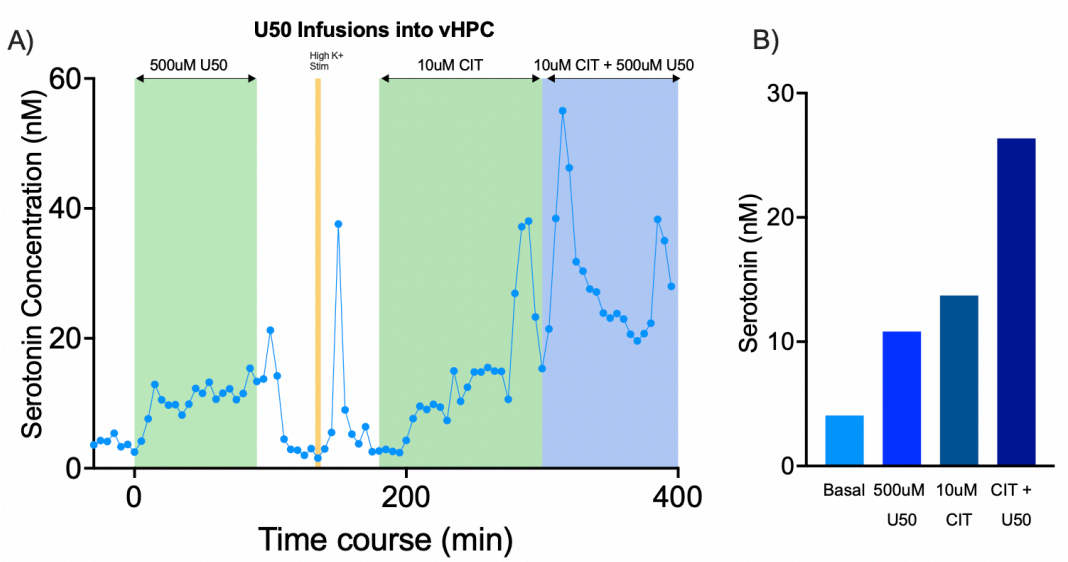

Figure 3.6: Effect of local perfusion of the kappa agonist U50,488 on serotonin neurotransmission in the ventral hippocampus. **A)** *In vivo* microdialysis time course. **B)** Serotonin levels before and after perfusion of U50,488, the SSRI citalopram, and their combination. *N*=1 mouse.

Figure 3.7

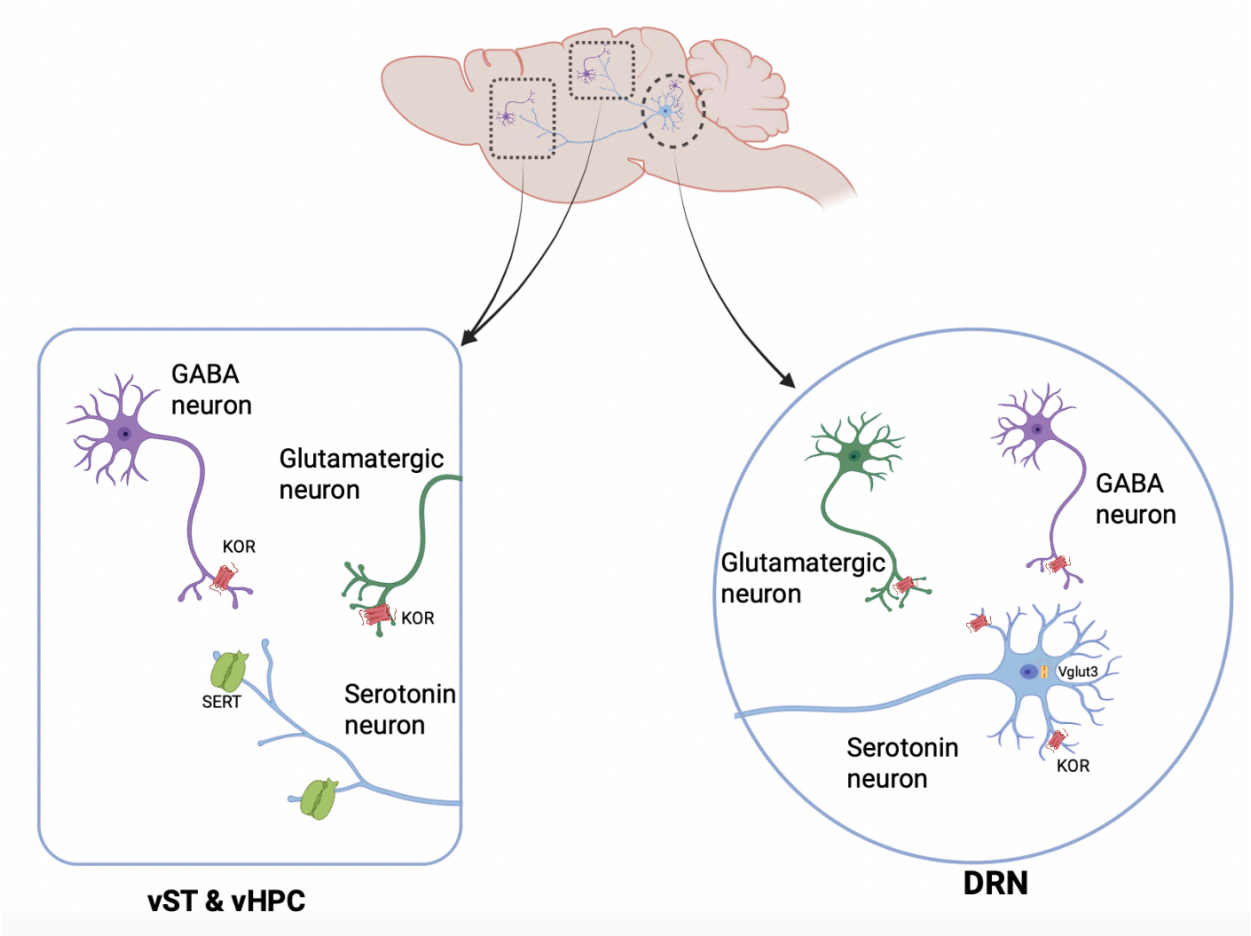

Figure 3.7: Schematic of proposed KOR, GABA, glutamate, and serotonin circuitry implicated during KOR activation. Figure was created with BioRender.com.

Figure 3.8

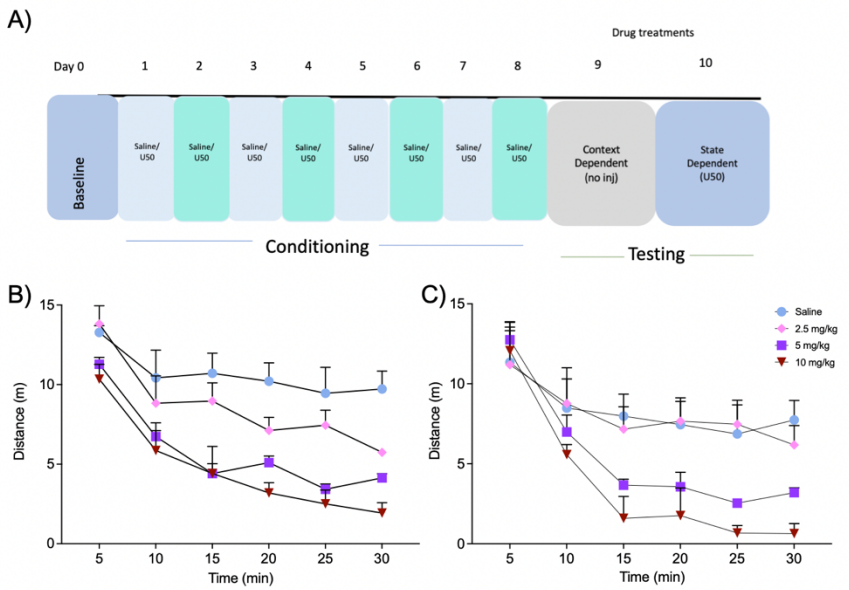

Figure 3.8: KOR-induced Conditioned Place Aversion **A)** Conditioned placed aversion paradigm. Significant effect of U50,488 dose and time on distance traveled in the testing apparatus for male **(B)** and female **(C)** mice on state-dependent testing day.

Figure 3.9

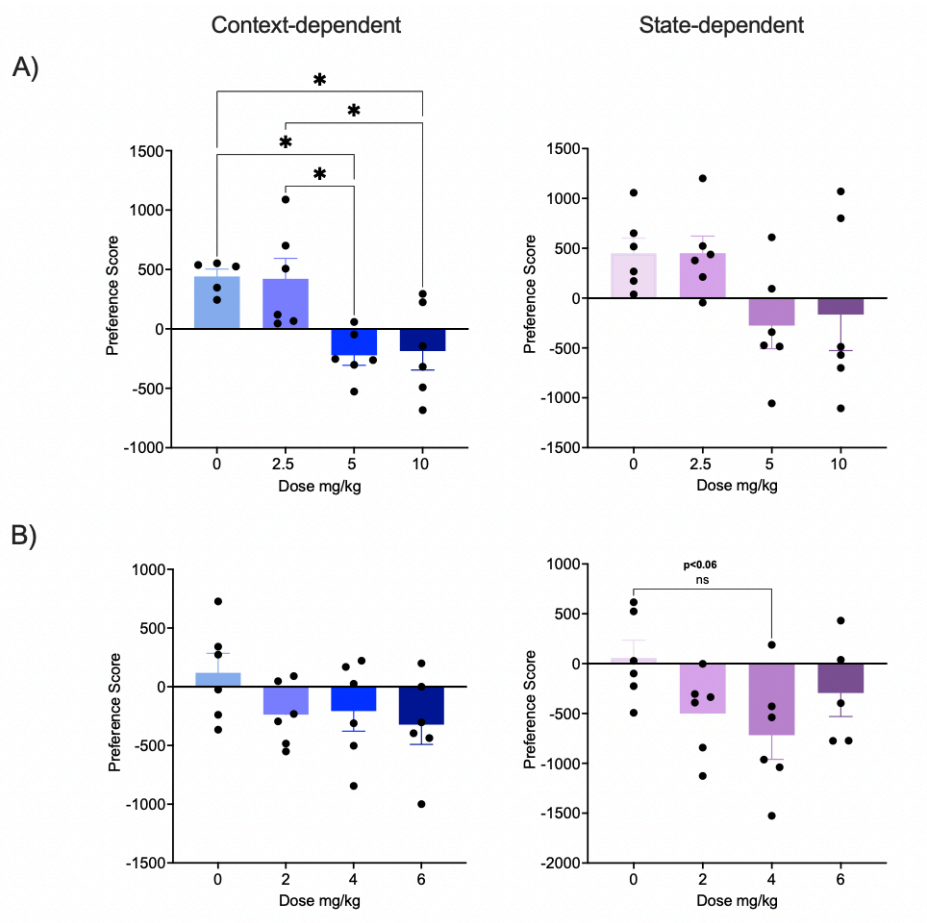

Figure 3.9: Dose response for KOR-induced conditioned place aversion. **A)** Male preference scores for context-dependent (left) and state-dependent (right) testing days. **B)** Female preference scores for context-dependent (left) and state-dependent (right) testing days. *N*=6 mice per group per sex. Data are means ± SEMs. *$P<0.05$

Figure 3.10

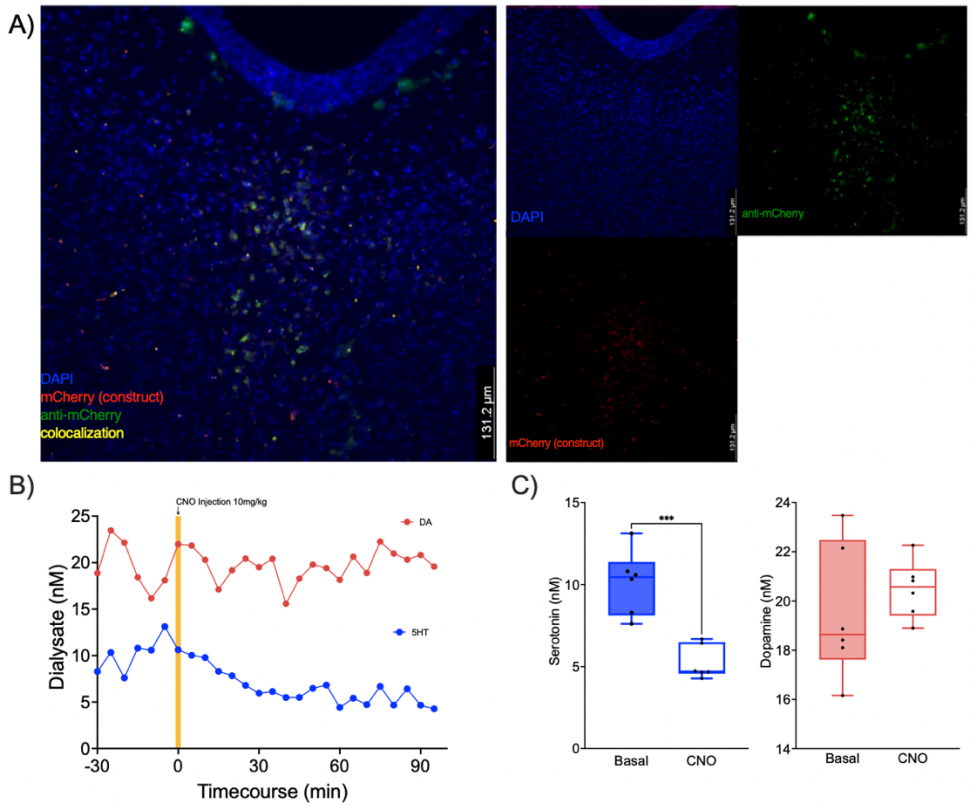

Figure 3.10: Chemogenetic inhibition of serotonin neurons. **A)** Immunocytochemistry microscopy images of a representative brain section from a mouse transfected with an inhibitory DREADD. Overlay (left), mCherry construct alone (middle), anti-mCherry antibody (right). **B)** Microdialysis time course before and after CNO injection. **C)** Basal *vs.* post-CNO. Each point represents one dialysate sample. Data are means ± SEMs. N=1 mouse. ***P<0.001

Table 3.1

Figure	Comparison	Test and Result
Figure 3.4a	***Dopamine levels (nM) between drug treatment***	***Paired t-test P<0.04***
Figure 3.4c	***Dopamine AUC levels between drug treatment***	Paired t-test P>0.05
Figure 3.4d	***Serotonin levels (nM) between drug treatment***	Paired t-test P>0.05
Figure 3.4f	***Serotonin AUC between drug treatment***	Paired t-test P>0.05
Figure 3.5a	**Percent basal dopamine levels between drug concentrations**	ANOVA summary F: 26.48 P value: 0.0110 P value summary: *
Figure 3.5b	**Percent basal serotonin levels between drug concentrations**	ANOVA summary F: 484.2 P value: 0.0001 P value summary: ***
Figure 3.9a	**Male preference scores context-dependent**	ANOVA summary F: 7.582 P value: 0.0016 P value summary: **
Figure 3.9a	**Male preference scores state-dependent**	ANOVA summary F: 2.577 P value: 0.0824 P value summary: ns
Figure 3.9b	**Female preference scores context-dependent**	ANOVA summary F: 1.541 P value: 0.2347 P value summary: ns
Figure 3.9b	**Female preference scores state-dependent**	ANOVA summary F: 2.674 P value: 0.0765 P value summary: ns
Figure 3.10c	**Chemogenetic inhibition**	***Serotonin: Unpaired t-test, P<0.001*** Dopamine: Unpaired t-test, P>0.05

References

1. Cahill, C. M.; Taylor, A. M.; Cook, C.; Ong, E.; Moron, J. A.; Evans, C. J., Does the kappa opioid receptor system contribute to pain aversion? *Front Pharmacol* **2014,** *5*, 253.

2. Knoll, A. T.; Meloni, E. G.; Thomas, J. B.; Carroll, F. I.; Carlezon, W. A., Jr., Anxiolytic-like effects of kappa-opioid receptor antagonists in models of unlearned and learned fear in rats. *Journal of Pharmacology and Experimental Therapeutics* **2007,** *323* (3), 838-45.

3. Mague, S. D.; Pliakas, A. M.; Todtenkopf, M. S.; Tomasiewicz, H. C.; Zhang, Y.; Stevens, W. C., Jr.; Jones, R. M.; Portoghese, P. S.; Carlezon, W. A., Jr., Antidepressant-like effects of kappa-opioid receptor antagonists in the forced swim test in rats. *Journal of Pharmacology and Experimental Therapeutics* **2003,** *305* (1), 323-30.

4. Pfeiffer, A.; Brantl, V.; Herz, A.; Emrich, H. M., Psychotomimesis mediated by kappa opiate receptors. *Science* **1986,** *233* (4765), 774-6.

5. Understanding the Facts:Anxiety and depression. adaa.org.

6. Cahill, C. M.; Taylor, A. M.; Cook, C.; Ong, E.; Moron, J. A.; Evans, C. J., Does the kappa opioid receptor system contribute to pain aversion? *Frontiers in Pharmacology* **2014,** *5*, 253.

7. Kaufman, J.; Charney, D., Comorbidity of mood and anxiety disorders. *Depression and Anxiety* **2000,** *12 Suppl 1*, 69-76.

8. Crowley, N. A.; Kash, T. L., Kappa opioid receptor signaling in the brain: Circuitry and implications for treatment. *Prog Neuropsychopharmacol Biol Psychiatry* **2015,** *62*, 51-60.

9. Beck, A.; Schlagenhauf, F.; Wustenberg, T.; Hein, J.; Kienast, T.; Kahnt, T.; Schmack, K.; Hagele, C.; Knutson, B.; Heinz, A.; Wrase, J., Ventral striatal activation during reward anticipation correlates with impulsivity in alcoholics. *Biological Psychiatry* **2009,** *66* (8), 734-42.

10. Corral-Frias, N. S.; Nikolova, Y. S.; Michalski, L. J.; Baranger, D. A.; Hariri, A. R.; Bogdan, R., Stress-related anhedonia is associated with ventral striatum reactivity to reward and transdiagnostic psychiatric symptomatology. *Psychological Medicine* **2015,** *45* (12), 2605-17.

11. Land, B. B.; Bruchas, M. R.; Lemos, J. C.; Xu, M.; Melief, E. J.; Chavkin, C., The dysphoric component of stress is encoded by activation of the dynorphin kappa-opioid system. *The Journal of Neuroscience* **2008,** *28* (2), 407-14.

12. Shippenberg, T. S.; Rea, W., Sensitization to the behavioral effects of cocaine: modulation by dynorphin and kappa-opioid receptor agonists. *Pharmacology Biochemistry and Behavior* **1997,** *57* (3), 449-55.

13. Hensler, J. G., Serotonergic modulation of the limbic system. *Neuroscience & Biobehavioral Reviews* **2006,** *30* (2), 203-14.

14. Han, X.; Jing, M. Y.; Zhao, T. Y.; Wu, N.; Song, R.; Li, J., Role of dopamine projections from ventral tegmental area to nucleus accumbens and medial prefrontal cortex in reinforcement behaviors assessed using optogenetic manipulation. *Metabolic Brain Disease* **2017,** *32* (5), 1491-1502.

15. Wang, H. L.; Zhang, S.; Qi, J.; Wang, H.; Cachope, R.; Mejias-Aponte, C. A.; Gomez, J. A.; Mateo-Semidey, G. E.; Beaudoin, G. M. J.; Paladini, C. A.; Cheer, J. F.; Morales, M., Dorsal Raphe Dual Serotonin-Glutamate Neurons Drive Reward by Establishing Excitatory Synapses on VTA Mesoaccumbens Dopamine Neurons. *Cell Report* **2019,** *26* (5), 1128-1142 e7.

16. Fallon, J. H.; Leslie, F. M., Distribution of dynorphin and enkephalin peptides in the rat brain. *Journal of Comparative Neurology* **1986,** *249* (3), 293-336.

17. Svingos, A. L.; Colago, E. E.; Pickel, V. M., Cellular sites for dynorphin activation of kappa-opioid receptors in the rat nucleus accumbens shell. *The Journal of Neuroscience* **1999,** *19* (5), 1804-13.

18. Cunningham, C. L.; Gremel, C. M.; Groblewski, P. A., Drug-induced conditioned place preference and aversion in mice. *Nature Protocols* **2006,** *1* (4), 1662-70.

19. Prus, A. J.; James, J. R.; Rosecrans, J. A., Chapter 4 Conditioned Place Preference. 18.

20. Ehrich, J. M.; Messinger, D. I.; Knakal, C. R.; Kuhar, J. R.; Schattauer, S. S.; Bruchas, M. R.; Zweifel, L. S.; Kieffer, B. L.; Phillips, P. E.; Chavkin, C., Kappa Opioid Receptor-Induced Aversion Requires p38 MAPK Activation in VTA Dopamine Neurons. *The Journal of Neuroscience* **2015,** *35* (37), 12917-31.

21. Chefer, V. I.; Backman, C. M.; Gigante, E. D.; Shippenberg, T. S., Kappa opioid receptors on dopaminergic neurons are necessary for kappa-mediated place aversion. *Neuropsychopharmacology* **2013,** *38* (13), 2623-31.

22. Land, B. B.; Bruchas, M. R.; Schattauer, S.; Giardino, W. J.; Aita, M.; Messinger, D.; Hnasko, T. S.; Palmiter, R. D.; Chavkin, C., Activation of the kappa opioid receptor in the dorsal raphe nucleus mediates the aversive effects of stress and reinstates drug seeking. *Proceedings of the National Academy of Sciences* **2009,** *106* (45), 19168-73.

23. Yang, H.; Sampson, M. M.; Senturk, D.; Andrews, A. M., Sex- and SERT-mediated differences in stimulated serotonin revealed by fast microdialysis. *ACS Chemical Neuroscience* **2015,** *6* (8), 1487-501.

24. Yang, H.; Thompson, A. B.; McIntosh, B. J.; Altieri, S. C.; Andrews, A. M., Physiologically relevant changes in serotonin resolved by fast microdialysis. *ACS Chemical Neuroscience*

2013, *4* (5), 790-8.

25. Mathews, T. A.; Fedele, D. E.; Coppelli, F. M.; Avila, A. M.; Murphy, D. L.; Andrews, A. M., Gene dose-dependent alterations in extraneuronal serotonin but not dopamine in mice with reduced serotonin transporter expression. *J Neurosci Methods* **2004,** *140* (1-2), 169-81.

26. Schindler, A. G.; Messinger, D. I.; Smith, J. S.; Shankar, H.; Gustin, R. M.; Schattauer, S. S.; Lemos, J. C.; Chavkin, N. W.; Hagan, C. E.; Neumaier, J. F.; Chavkin, C., Stress produces aversion and potentiates cocaine reward by releasing endogenous dynorphins in the ventral striatum to locally stimulate serotonin reuptake. *The Journal of Neuroscience* **2012,** *32* (49), 17582-96.

27. Fontaine, H. M.; Silva, P. R.; Neiswanger, C.; Tran, R.; Abraham, A. D.; Land, B. B.; Neumaier, J. F.; Chavkin, C., Stress decreases serotonin tone in the nucleus accumbens in male mice to promote aversion and potentiate cocaine preference via decreased stimulation of 5-HT1B receptors. *Neuropsychopharmacology* **2022,** *47* (4), 891-901.

28. Ebner, S. R.; Roitman, M. F.; Potter, D. N.; Rachlin, A. B.; Chartoff, E. H., Depressive-like effects of the kappa opioid receptor agonist salvinorin A are associated with decreased phasic dopamine release in the nucleus accumbens. *Psychopharmacology (Berl)* **2010,** *210* (2), 241-52.

29. Van't Veer, A.; Bechtholt, A. J.; Onvani, S.; Potter, D.; Wang, Y.; Liu-Chen, L. Y.; Schutz, G.; Chartoff, E. H.; Rudolph, U.; Cohen, B. M.; Carlezon, W. A., Jr., Ablation of kappa-opioid receptors from brain dopamine neurons has anxiolytic-like effects and enhances cocaine-induced plasticity. *Neuropsychopharmacology* **2013,** *38* (8), 1585-97.

30. Zhang, Y.; Butelman, E. R.; Schlussman, S. D.; Ho, A.; Kreek, M. J., Effects of the plant-derived hallucinogen salvinorin A on basal dopamine levels in the caudate putamen and in a

conditioned place aversion assay in mice: agonist actions at kappa opioid receptors. *Psychopharmacology (Berl)* **2005,** *179* (3), 551-8.

31. Carlezon, W. A., Jr.; Beguin, C.; DiNieri, J. A.; Baumann, M. H.; Richards, M. R.; Todtenkopf, M. S.; Rothman, R. B.; Ma, Z.; Lee, D. Y.; Cohen, B. M., Depressive-like effects of the kappa-opioid receptor agonist salvinorin A on behavior and neurochemistry in rats. *Journal of Pharmacology and Experimental Therapeutics* **2006,** *316* (1), 440-7.

32. Gehrke, B. J.; Chefer, V. I.; Shippenberg, T. S., Effects of acute and repeated administration of salvinorin A on dopamine function in the rat dorsal striatum. *Psychopharmacology (Berl)* **2008,** *197* (3), 509-17.

33. Spanagel, R.; Herz, A.; Shippenberg, T. S., Opposing tonically active endogenous opioid systems modulate the mesolimbic dopaminergic pathway. *Proceedings of the National Academy of Sciences* **1992,** *89* (6), 2046-50.

34. Nestler, E. J.; Carlezon, W. A., Jr., The mesolimbic dopamine reward circuit in depression. *Biol Psychiatry* **2006,** *59* (12), 1151-9.

35. Niederkofler, V.; Asher, T. E.; Dymecki, S. M., Functional Interplay between Dopaminergic and Serotonergic Neuronal Systems during Development and Adulthood. *ACS Chemical Neuroscience* **2015,** *6* (7), 1055-1070.

36. Dagher, M.; Perrotta, K. A.; Erwin, S. A.; Hachisuka, A.; Iyer, R.; Masmanidis, S. C.; Yang, H.; Andrews, A. M., Optogenetic Stimulation of Midbrain Dopamine Neurons Produces Striatal Serotonin Release. *ACS Chem Neurosci* **2022,** *13* (7), 946-958.

37. Tao, R.; Auerbach, S. B., Opioid receptor subtypes differentially modulate serotonin efflux in the rat central nervous system. *Journal of Pharmacology and Experimental Therapeutics* **2002,** *303* (2), 549-56.

38. Tao, R.; Auerbach, S. B., mu-Opioids disinhibit and kappa-opioids inhibit serotonin efflux in the dorsal raphe nucleus. *Brain Research* **2005,** *1049* (1), 70-9.

39. Yoshioka, M.; Matsumoto, M.; Togashi, H.; Smith, C. B.; Saito, H., Opioid receptor regulation of 5-hydroxytryptamine release from the rat hippocampus measured by in vivo microdialysis. *Brain Research* **1993,** *613* (1), 74-9.

40. Dranovsky, A.; Hen, R., Hippocampal neurogenesis: regulation by stress and antidepressants. *Biol Psychiatry* **2006,** *59* (12), 1136-43.

41. Grilli, M.; Neri, E.; Zappettini, S.; Massa, F.; Bisio, A.; Romussi, G.; Marchi, M.; Pittaluga, A., Salvinorin A exerts opposite presynaptic controls on neurotransmitter exocytosis from mouse brain nerve terminals. *Neuropharmacology* **2009,** *57* (5-6), 523-30.

42. Krashes, M. J.; Koda, S.; Ye, C.; Rogan, S. C.; Adams, A. C.; Cusher, D. S.; Maratos-Flier, E.; Roth, B. L.; Lowell, B. B., Rapid, reversible activation of AgRP neurons drives feeding behavior in mice. *J Clin Invest* **2011,** *121* (4), 1424-8.

43. Cahill, C. M.; Xue, L.; Grenier, P.; Magnussen, C.; Lecour, S.; Olmstead, M. C., Changes in morphine reward in a model of neuropathic pain. *Behav Pharmacol* **2013,** *24* (3), 207-13.

44. Liu, S. S.; Pickens, S.; Burma, N. E.; Ibarra-Lecue, I.; Yang, H.; Xue, L.; Cook, C.; Hakimian, J. K.; Severino, A. L.; Lueptow, L.; Komarek, K.; Taylor, A. M. W.; Olmstead, M. C.; Carroll, F. I.; Bass, C. E.; Andrews, A. M.; Walwyn, W.; Trang, T.; Evans, C. J.; Leslie, F. M.; Cahill, C. M., Kappa

Opioid Receptors Drive a Tonic Aversive Component of Chronic Pain. *The Journal of Neuroscience* **2019,** *39* (21), 4162-4178.

45. Falcy, B. A.; Mohr, M. A.; Micevych, P. E., Immunohistochemical amplification of mCherry fusion protein is necessary for proper visualization. *MethodsX* **2020,** *7*, 100946.

46. Huang, K. W.; Ochandarena, N. E.; Philson, A. C.; Hyun, M.; Birnbaum, J. E.; Cicconet, M.; Sabatini, B. L., Molecular and anatomical organization of the dorsal raphe nucleus. *Elife* **2019,** *8*.

47. Pollak Dorocic, I.; Furth, D.; Xuan, Y.; Johansson, Y.; Pozzi, L.; Silberberg, G.; Carlen, M.; Meletis, K., A whole-brain atlas of inputs to serotonergic neurons of the dorsal and median raphe nuclei. *Neuron* **2014,** *83* (3), 663-78.

48. Ren, J.; Isakova, A.; Friedmann, D.; Zeng, J.; Grutzner, S. M.; Pun, A.; Zhao, G. Q.; Kolluru, S. S.; Wang, R.; Lin, R.; Li, P.; Li, A.; Raymond, J. L.; Luo, Q.; Luo, M.; Quake, S. R.; Luo, L., Single-cell transcriptomes and whole-brain projections of serotonin neurons in the mouse dorsal and median raphe nuclei. *Elife* **2019,** *8*.

49. Nestler, E. J.; Carlezon, W. A., Jr., The mesolimbic dopamine reward circuit in depression. *Biological Psychiatry* **2006,** *59* (12), 1151-9.

50. Russo, S. J.; Nestler, E. J., The brain reward circuitry in mood disorders. *Nature Reviews Neuroscience* **2013,** *14* (9), 609-25.

51. Chappell, P. B.; Leckman, J. F.; Scahill, L. D.; Hardin, M. T.; Anderson, G.; Cohen, D. J., Neuroendocrine and behavioral effects of the selective kappa agonist spiradoline in Tourette's syndrome: a pilot study. *Psychiatry Research* **1993,** *47* (3), 267-80.

52. Abraham, A. D.; Schattauer, S. S.; Reichard, K. L.; Cohen, J. H.; Fontaine, H. M.; Song, A. J.; Johnson, S. D.; Land, B. B.; Chavkin, C., Estrogen Regulation of GRK2 Inactivates Kappa Opioid Receptor Signaling Mediating Analgesia, But Not Aversion. *J Neurosci* **2018,** *38* (37), 8031-8043.

53. Hendricks, T.; Francis, N.; Fyodorov, D.; Deneris, E. S., The ETS domain factor Pet-1 is an early and precise marker of central serotonin neurons and interacts with a conserved element in serotonergic genes. *J Neurosci* **1999,** *19* (23), 10348-56.

54. Teissier, A.; Chemiakine, A.; Inbar, B.; Bagchi, S.; Ray, R. S.; Palmiter, R. D.; Dymecki, S. M.; Moore, H.; Ansorge, M. S., Activity of Raphe Serotonergic Neurons Controls Emotional Behaviors. *Cell Rep* **2015,** *13* (9), 1965-76.

55. Samuvel, D. J.; Jayanthi, L. D.; Bhat, N. R.; Ramamoorthy, S., A role for p38 mitogen-activated protein kinase in the regulation of the serotonin transporter: evidence for distinct cellular mechanisms involved in transporter surface expression. *J Neurosci* **2005,** *25* (1), 29-41.

56. Nagai, T.; Yoshimoto, J.; Kannon, T.; Kuroda, K.; Kaibuchi, K., Phosphorylation Signals in Striatal Medium Spiny Neurons. *Trends Pharmacol Sci* **2016,** *37* (10), 858-871.

57. Perreault, M. L.; Hasbi, A.; Alijaniaram, M.; Fan, T.; Varghese, G.; Fletcher, P. J.; Seeman, P.; O'Dowd, B. F.; George, S. R., The dopamine D1-D2 receptor heteromer localizes in dynorphin/enkephalin neurons: increased high affinity state following amphetamine and in schizophrenia. *J Biol Chem* **2010,** *285* (47), 36625-34.

58. Soares-Cunha, C.; de Vasconcelos, N. A. P.; Coimbra, B.; Domingues, A. V.; Silva, J. M.; Loureiro-Campos, E.; Gaspar, R.; Sotiropoulos, I.; Sousa, N.; Rodrigues, A. J., Nucleus accumbens medium spiny neurons subtypes signal both reward and aversion. *Mol Psychiatry* **2020,** *25* (12), 3241-3255.

59. Marona-Lewicka, D.; Rhee, G. S.; Sprague, J. E.; Nichols, D. E., Reinforcing effects of certain serotonin-releasing amphetamine derivatives. *Pharmacol Biochem Behav* **1996,** *53* (1), 99-105.

CHAPTER 4

Optogenetic Stimulation of Midbrain Dopamine Neurons Produces Striatal Serotonin Release

Optogenetic Stimulation of Midbrain Dopamine Neurons Produces Striatal Serotonin Release. Merel Dagher, Katie A. Perrotta, Sara A. Erwin*, Ayaka Hachisuka, Rahul Iyer, Sotiris C. Masmanidis, Hongyan Yang, and Anne M. Andrews. *ACS Chemical Neuroscience* 2022 *13* (7), 946-958.DOI: 10.1021/acschemneuro.1c00715.

*published under maiden name

Introduction

Optogenetics entails expressing light-driven ionotropic receptors in neurons or other excitable cells to enable spatially and temporally restricted activation or inhibition.[4-7] Gene constructs for microbial or engineered rhodopsins packaged in viruses are used to transduce brain-region-specific gene expression following local delivery. Gene expression can be further targeted using Cre recombinase under the control of cell-type-specific promotors, in combination with Cre-activated opsin constructs.[8] Opsins produce excitatory (*e.g.,* channelrhodopsin-2, Chrimson) or inhibitory (*e.g.,* halorhodopsin, archaerhodopsin) effects on neural activity.[9-11] The discovery and use of opsins have enabled the identification of neural pathways involved in the modulation of behavior.[12-15]

Opsin-targeted cell types, however, do not operate autonomously. Dopamine and serotonin are examples of functionally interconnected neurotransmitter systems. For instance, while dopamine signaling is often associated with reward prediction error, serotonin transmission also plays a role in processing reward-associated information.[16-18] Moreover, while widely used therapeutics for mood disorders target the serotonin system,[19] the dopamine system encodes information associated with anhedonia, a core symptom of major depressive disorder.[17,20-25] Interactions between the dopamine and serotonin systems are evident in drug mechanisms of action, *e.g.,* cocaine, methamphetamine, and 3,4-methylenedioxymethamphetamine.[26-29] Thus, these systems act in concert to modulate subjective states.[30,31]

Microdialysis is a tissue sampling technique. When combined with chemical separation and detection methods, microdialysis enables the identification and quantification of neurotransmitters, metabolites, and drugs in the extracellular space.[32]

Several groups, including ours, have optimized microdialysis to monitor brain extracellular dopamine or serotonin levels *via* online coupling with fast separations by high performance liquid chromatography (HPLC) and electrochemical detection in awake mice and rats.[33-39] Dopamine and serotonin can be resolved in the same dialysate samples enabling biologically relevant changes in basal and stimulated levels of these neurotransmitters to be simultaneously monitored.[39,40]

Here, we set out to determine the magnitude of extracellular dopamine release in the dorsal striatum (dSTR) upon optogenetic stimulation of midbrain dopaminergic neurons. The excitatory opsin Chrimson was expressed under the control of the dopamine transporter promoter in mice. Optical activation of dopamine neurons has been used to study dopaminergic encoding of reward and movement.[15,41] In addition to dopamine, we observed optically induced increases in the dopamine metabolite 3-methoxytyramine (3-MT) and in serotonin levels. These findings demonstrate a functional link between the dopamine and serotonin systems in the basal ganglia. They illustrate the importance of monitoring multiple neurotransmitters simultaneously. And they suggest that opsin-induced behavioral changes may not be attributable solely to the neurotransmitter system or cell type targeted by opsin expression. That is to say, while optogenetics imparts highly selective control of specific types of neurons, brain function and behavior arise from distributed and interconnected networks.

Materials and Methods

Animal procedures

Mice were generated at the University of California, Los Angeles (UCLA) from a DAT$^{IRES\mathit{cre}}$ line (The Jackson Laboratory, stock no. 006660) on a C57Bl/6J background *via* heterozygous matings. Mice were housed in groups of 2-5 same-sex siblings prior to surgery, same-sex-sibling pairs after the first surgery to deliver viral vectors and to implant optical fibers and head bars, and singly after the second surgery to implant a microdialysis guide cannula. Food and water were available *ad libitum* throughout, with the exception of microdialysis testing days where mice were hand-fed a 2:1 sweetened condensed milk:water solution *via* pipette every 2 h.

The light-dark cycle (12/12 h) in the animal colony room was set to lights on at 0730 h (ZT0). The same light schedule was maintained in the room where microdialysis was performed. The Association for Assessment and Accreditation of Laboratory Animal Care International has fully accredited UCLA. All animal care and use met the requirements of the NIH Guide for the Care and Use of Laboratory Animals, 2011. The UCLA Chancellor's Animal Research Committee (Institutional Animal Care and Use Committee) preapproved all animal procedures.

Surgeries were carried out under aseptic conditions with isoflurane anesthesia on a KOPF Model 1900 Stereotaxic Alignment System (KOPF, Tujunga, CA). A pair of rectangular stainless steel head-bars (9 mm × 7 mm × 0.76 mm, 0.6 g each, Fab2Order, Brownsburg, IN) were attached to the sides of the skull by C&B Metabond (Parkell, Edgewood, NY) for head fixation (**Fig. 4.S1A,B**). Viral vectors, 600 nL of 7.8 × 10^{12}/mL AAV5/Syn-Flex-ChrimsonR-tdTomato (for experimental groups) or 4.4 × 10^{12}/mL AAV5/EF1a-DIO-eYFP or 3.3 ×

10^{12}/mL AAV5/EF1a-DIO-mcherry (for control subjects), were delivered unilaterally into the SN/VTA (AP-3.08 mm, ML ±1.20 mm, DV -4.00 mm from Bregma) using a Nanoject II (Drummond Scientific, Broomall, PA). A 200 μm diameter optical fiber (0.22 NA, Thorlabs, Newton, NJ) with a total length of 1 cm was lowered *via* the same track to reach the AAV injection site for optogenetic stimulation. Optical fibers were secured on the skull with C&B Metabond. The top of each optical fiber outside the skull was covered by a sleeve until coupling to a laser device for testing. All AAV Cre-dependent adeno-associated viral vectors were obtained from the University of North Carolina Vector Core (Chapel Hill, NC).

After the first surgery, animals recovered for 2-3 weeks (**Fig. 4.1B**) to allow for viral vector expression prior to guide cannula implantation for microdialysis. During recovery, subjects were acclimated to being head-fixed over the course of 6-10 training sessions, each lasting 15-30 min. A second surgery was carried out on each mouse to implant a CMA/7 guide cannula for a microdialysis probe aimed at the dSTR (AP+1.00 mm, ML±1.75 mm, DV-3.10 mm from Bregma) in the same hemisphere as the viral delivery and fiber implant site. Each guide cannula was secured to the skull with C&B Metabond. Animals recovered from the second surgery for at least three days before microdialysis. Following each surgery, mice were given daily carprofen injections (5 mg/kg, 1 mg/mL, subcutaneously) for the first three days and a combination of an antibiotic (amoxicillin, 0.25 mg/mL) and a second analgesic (ibuprofen, 0.25 mg/mL) in their drinking water for 14 days postoperatively.

Microdialysis

Virgin female mice (*N*=23) underwent microdialysis at 3-6 months of age. Microdialysis was carried out over two consecutive days for Chrimson-transfected mice (*N*=14) and one day for control mice (*N*=9). On the night before the first testing day (ZT10-12), each mouse was transferred to the testing room in its home cage and briefly anesthetized with isoflurane (1-3 min) for insertion of a CMA/7 microdialysis probe (1 mm length, 6 kDa cutoff, CMA8010771) into the guide cannula. Subjects were returned to their home cages and aCSF was continuously perfused through the probe *via* a liquid swivel (375/D/22QM, Instech Laboratories Inc., Plymouth Meeting, PA) at 2-3 μL/min for 30-60 min followed by a 0.3 μL/min flow rate for an additional 12-14 h to allow the tissue surrounding the probe to recover from acute changes associated with probe insertion. Subjects were tethered to the liquid swivel but otherwise could move freely in their home cages.

Prior to microdialysis, the tubing connecting the microdialysis probe to the liquid swivel was disconnected. The mouse was transferred from its home cage and mounted to the head-fixed stage *via* its head-bars in the same testing room. The microdialysis probe was connected between the microdialysis syringe pump and the online autoinjector. The aCSF was perfused at 1.8 uL/min throughout each testing day, and samples were collected at 5-min intervals. Subjects were habituated for at least 10-min before the optical fiber was coupled for stimulation delivery.

An MGL-III-532 or MGL-III-589 laser (Opto Engine LLC, Ltd, Changchun, P. R. China) was used to deliver light pulses. The excitation spectrum of Chrimson has a λ_{max} at 590 nm. Due to the broad excitation spectrum, either 532 nm (green) or 589 nm (yellow) light were

used to excite this opsin.[10] The output of the optical fiber was calibrated to deliver 10 mW/mm^2 immediately before coupling on each testing day.

The stimulation pulse width (50 ms), frequency (10 Hz), and train duration (5 min) were selected to generate neurotransmitter release detectable by microdialysis using a 5-min dialysate sampling time. In preliminary experiments, we investigated stimulation pulse widths that varied from 5-2500 ms. We also investigated laser powers ranging from 5-20 mW/mm^2. Longer pulse widths were ultimately favored over higher laser power with shorter pulses to avoid tissue damage over longer stimulation times needed for microdialysis. There were no significant differences in stimulation output for frequencies over 10-30 Hz using 50% duty cycle and a 5-min train duration. A longer train duration was used previously by Correia *et al.* to investigate the role of serotonin transmission in locomotion.[42]

The first stimulation was delivered at ~ZT2 after 6-18 basal dialysate samples were collected and analyzed. Prior to reverse dialysis of drugs, three optical stimulations were delivered at 1-h intervals (**Fig. 4.1B**). After 90-120 min of intrastriatal drug perfusion, an additional three optical stimulations were delivered at 1-h intervals while drug perfusion continued. On day 1, four Chrimson-transfected mice were perfused with the D1-like antagonist SCH-23390 (100 μM) through the dialysis probe. On day 2, the same four Chrimson-transfected mice were perfused with 100 μM eticlopride (D2-like antagonist).

Eleven mice not receiving D1- or D2-like antagonists underwent brief (5 min) perfusion with 120 mM K^+ (KCl substituted isotonically for NaCl in aCSF) to stimulate neurochemical overflow[38,39,43] for peak identification. In **Fig. 4.S2,** data from a representative K^+-stimulated mouse are shown. Three Chrimson-transfected mice were

perfused with an SSRI (10 μM escitalopram) on day one to confirm serotonin peak identity (**Fig. 4.3A, B**). Four mice (three control and one Chrimson-transfected) were administered the COMT inhibitor tolcopone (10 mg/kg, intraperitoneal) to identify the 3-MT peak (**Fig. 4.2C**).

Dialysate analysis

High performance liquid chromatography was performed using an Amuza HTEC-500 integrated system (Amuza Corporation [formally known as Eicom], San Diego, CA). An Eicom Insight autosampler was used to inject standards and Eicom EAS-20s online autoinjectors were used to collect and inject dialysate samples online.[33] Chromatographic separation was achieved using an Eicom PP-ODS II column (4.6 mm ID x 30 mm length, 2 μm particle diameter) and a phosphate-buffered mobile phase (96 mM NaH_2PO_4 (Fluka #17844), 3.8 mM Na_2HPO_4 (Fluka #71633), pH 5.4, 2-2.8% MeOH (EMD #MX0475), 50 mg/L EDTA·Na_2 (Sigma #03682), and 500 mg/L sodium decanesulfonate (TCI #I0348) in water purified *via* a Milli-Q Synthesis A10 system (EMD Millipore Corporation, Billerica, MA). The column temperature was maintained at 21 °C. The volumetric flow rate was 450-500 μL/min. Electrochemical detection was performed using an Eicom WE-3G graphite working electrode with an applied potential of +450 mV *vs.* a Ag/AgCl reference electrode.

Dopamine (Sigma #H8502), 3-MT (Sigma #65390), and serotonin (Sigma #H9523) standards were prepared in ice-cold 1:1 mobile phase/aCSF (147 mM NaCl (Fluka #73575), 3.5 mM KCl (Fluka #05257), 1.0 mM $CaCl_2$ (Aldrich #499609), 1.0 mM NaH_2PO_4, 2.5 mM $NaHCO_3$ (Fluka #88208), 1.2 mM $MgCl_2$ (Aldrich #449172), pH 7.3 ± 0.03. (See supplemental information in Liu et al., 2020 for detailed information on formulating aCSF).[44] Standard curves encompassed physiological concentration ranges (0-10 nM; **Fig. 4.S5**). The limit of

detection was ≤300 amol (6 pM) for each analyte; the practical limit of quantification was ≤900 amol (18 pM). Dialysate samples were collected online at 5-min intervals using a dialysate flow rate of 1.8 μL/min and injected immediately onto the HPLC system for analysis.

In situ hybridization

We used RNAscope® technology (Advanced Cell Diagnostics Inc., Newark, CA) for *in situ* hybridization to colocalize mRNAs for D1 receptors in dorsal raphe neurons expressing SERT, VGLUT3, or both.[1,2,45,46] A DAT$^{IRES\,cre}$ mouse not transfected with Chrimson was sacrificed by cervical dislocation without isoflurane and the brain was removed, cryoprotected, and frozen. Coronal sections were cut at 16-μm on a cryostat at -15-20 °C and mounted on polylysine-coated slides.

In situ hybridization was conducted using the RNAscope® fresh-frozen V2 protocol. Briefly, sections were incubated in freshly prepared 4% paraformaldehyde (Sigma-Aldrich Cat#441244) in phosphate buffered saline for 15 min followed by sequential dehydration in 50% EtOH, 70% EtOH, and 100% EtOH for 5 min each. Sections were then incubated with the necessary reagents from the Multiplex Fluorescent Reagent Kit V2 (ACD #323110) in a HybEZ® oven. Probes were as follows: *Sert* (Mm-Slc6a4 Cat#315851) channel 1, *Vglut3* (Mm-Slc32a1 Cat#319191-C2) channel 2, and *Drd1* (Mm-Drd1a-C3 Cat# 406491-C3) channel 3. Opal dyes 520, 570, and 690 were paired with each probe, respectively (Cat#FP1487A, FP1488A, FP1497A). ProLong™ Diamond Antifade Mountant with DAPI (Molecular Probes P36966) was added to stain cell bodies.

Visualization was carried out using a Leica DMI8 or Zeiss LSM800 microscope and images were processed with LAS X and Zen software. Cell nuclei in each field of view were

identified *via* DAPI staining. The DAPI labeled nuclei associated with puncta for one or more mRNA probes were then counted. Data are reported as percent positive cells calculated by dividing the number of cells labeled with *Sert*, *Drd1*, and/or *Vglut3* by the total number of *Sert* labeled cells.

Histology

At the end of each experiment, the microdialysis probe was removed and the brain of each mouse was prepared for histology to verify probe and optical fiber placements, and Chrimson, mCherry, or eYFP expression. Subjects were exsanguinated with an overdose of 100 mg/kg pentobarbital (2 mL/kg administered at 50 mg/mL, ip) followed immediately by transcardial perfusion with 4% paraformaldehyde in PBS. Sections from the midbrain and dSTR were cut using a vibratome and mounted on microscope slides. Images were acquired using a Zeiss Axio Examiner microscope as follows: tdTomato and mCherry (550 nm excitation/605 nm emission), or eYFP (470 nm excitation/525 nm emission). Microdialysis probe and optical fiber tracks were visualized *via* light microscopy. Three of the 23 microdialysis subjects failed histology verification for probe or fiber placement. Data for these subjects were excluded from analyses.

Data analysis and statistics

The microdialysis time-course data were analyzed in terms of absolute neurochemical concentrations (nM) and as percents of mean pre-stimulation basal neurochemical levels (%basal). Overflow peaks following optical stimulation were identified and analyzed individually using the following criteria and procedures. (1) For each control mouse, the concentrations of six dialysate samples for each neurochemical immediately preceding the onset of the first optical stimulation were averaged (nM) and converted to mean 100% basal

levels. (2) For Chrimson-expressing mice on experimental days 1 and 2, basal levels of individual neurochemicals were determined separately by day. The concentrations of the six dialysate samples immediately preceding the onset of the first pre-drug or post-drug optical stimulation were averaged (nM) and converted to mean 100% basal levels. (3) The AUC for each stimulation peak, defined by the four dialysate samples after the onset of stimulation, was calculated by trapezoidal integration and is reported in nM or as a percent of mean pre-stimulation basal levels.

Statistical analyses were carried out using Prism, v.9.0.2 (GraphPad Inc., La Jolla, CA). Data are expressed as group means ± SEMs. Two-tailed *t*-tests (either unpaired or ratio paired, as appropriate) were used for two-group comparisons. Throughout, $P<0.05$ was considered statistically significant. Detailed statistics are summarized in **Table 4.S1**.

Results and discussion

Using microdialysis,[33,38,39] we quantified extracellular dopamine in a dopamine-rich projection region—the dSTR—during optical stimulation of midbrain dopamine cell bodies (**Fig. 4.1, Fig. 4.S1**). To induce dopamine release, we applied 50-ms square pulses at 10 Hz and 10 mW/mm^2 laser power. Stimulation pulse train durations were 5 minutes to match dialysate sampling times. These parameters were optimized to produce reproducible neurotransmitter release detectable *via* microdialysis. Activation of the excitatory opsin Chrimson[10] produced temporally specified increases in striatal extracellular dopamine levels (**Fig. 4.2A**). Control mice expressing mCherry or yellow fluorescent protein (YFP) in dopamine cell bodies showed no detectable changes in dopamine upon optical stimulation (**Fig. 4.2B**).

Basal (unstimulated) dialysate dopamine levels were not statistically different in Chrimson-expressing *vs.* control mice (**Fig. 4.2C**; see **Table 4.S1** for detailed statistics). Basal dopamine levels for control animals were normally distributed around the mean. In contrast, basal dopamine levels for Chrimson-expressing animals were not normally distributed. Individual dopamine concentrations fell mostly below the mean, apart from three animals, one of which was an outlier. Notably, this outlier is not the same animal that is an outlier for basal serotonin levels in Chrimson-transfected mice (**Fig. 4.4A** *vide infra*). As such, we chose to not to exclude outliers from analysis, although exclusion would have led to a statistically significant reduction in basal dopamine levels in Chrimson-transfected *vs.* control mice. Stimulated dopamine overflow, quantified as area under the curve (AUC), was greater in Chrimson-expressing *vs.* control mice (**Fig. 4.2D**; t_{18}=3.0, P<0.01). Dopamine levels were increased ~200 pM by optical stimulation.

In addition to dopamine, optical activation appeared to lead to increases in two other chromatographic peaks (**Fig. 4.S2**). We initially hypothesized that the larger peak (peak 2) was serotonin. However, since retention times commonly shift between standards and brain dialysate samples, we could not definitively identify peak 2 using serotonin-containing standards. We perfused a selective serotonin reuptake inhibitor (SSRI) through the dialysis membrane during intracerebral dialysis to investigate peak identity. Increases in peak areas in response to serotonin transporter inhibition identified a small, later eluting peak (peak 3) as serotonin (**Fig. 4.3A, B**; t_2=5.7, P<0.05).

Previous experience analyzing striatal tissue samples then led us to suspect that the remaining optically responsive peak was 3-methoxytyramine (3-MT). Dopamine is metabolized by catechol-*O*-methyltransferase (COMT) to produce 3-MT, which is hypothesized to function as a neuromodulator.[47,48] We administered the COMT inhibitor tolcapone systemically[49] and found that peak 2 was selectively decreased (**Fig. 4.3C**; t_3=9.6, P<0.01). We also perfused 3-MT through the dialysis membrane into dSTR, *i.e.*, *in vivo* standard addition, and observed a retention time match confirming the identity of peak 2 as 3-MT and ruling out the possibility that this peak was serotonin (**Fig. 4.3D**).

Having identified two optically (*i.e.*, biologically) responsive neurochemicals, in addition to dopamine, we quantified their basal dialysate levels. We found no differences in basal 3-MT or serotonin levels in Chrimson-expressing *vs.* control mice (**Fig. 4.4A**). Optogenetic stimulation of midbrain dopaminergic neurons evoked reproducible increases in 3-MT and serotonin in Chrimson-expressing but not control mice (**Fig. 4.4B,C**; t_{18}=3.1, P<0.01, t_{15}=4.4, P<0.001, respectively). Since basal neurochemical levels varied across individual mice (**Fig. 4.2C, 4A**), we also analyzed optically stimulated neurochemical levels

normalized to mean pre-stimulation basal levels (**Fig. 4.S3**). Concentration and %basal analyses similarly indicated that in addition to dopamine, 3-MT and serotonin overflow were increased in response to optogenetic stimulation of Chrimson-transfected dopamine neurons. Optical stimulation of control mice lacking opsin expression showed no nonspecific increases in neurochemicals associated with light-induced arousal.

We parsimoniously hypothesized that the increased overflow of serotonin associated with optical stimulation of dopamine neurons was mediated by activation of dopamine receptors on serotonin terminals in striatum. The mRNAs for DRD2 and DRD3 receptors (*i.e.*, D2-like) were previously identified in dorsal raphe.[50,51] Ren *et al.*[45] and Spaethling *et al*.[52] used single-cell transcriptomics to localize *Drd2* transcripts to serotonergic neurons. Using RNAseq, Dymecki and colleagues identified *Drd2* mRNA in dorsal raphe serotonin neurons specified by *Pet1* expression.[53]

A small number of DRN serotonin neurons has also been reported to contain *Drd1a* mRNA.[45,53] We carried out *in situ* hybridization to investigate colocalization of D1 receptor (*Drd1*) and serotonin transporter (*Sert*) mRNAs in the dorsal raphe nucleus (**Fig. 4.5A,B**). We included a probe for the vesicular glutamate transporter type 3 (VGLUT3) because a subpopulation of serotonergic neurons co-expresses VGLUT3[54] and projects to the striatum.[54,55] We found that ~25% of total *Sert*-positive cells in the dorsal raphe were positive for *Sert* mRNA alone (**Fig. 4.5C**). Approximately 10% of total *Sert*-positive cells showed colocalization of *Sert* and *Drd1* mRNA, while an additional 35% of *Sert*-positive cells showed *Drd1* and *Vglut3* mRNA colocalization. Positive and negative *in situ* hybridization controls are shown in Figure S4.

Since our data suggested that almost half of dorsal raphe serotonin neurons may express heterologous D1 receptors, we investigated whether blocking striatal D1-like receptors prevents optically stimulated serotonin overflow. We perfused SCH 23390, a D1-like receptor antagonist, into the dSTR. Basal dopamine (t_3=4.4, P<0.05) and serotonin (t_3=3.5, P<0.05) levels were increased by local D1-like receptor inhibition (**Fig. 4.6A,B**). Stimulated dopamine (t_3=6.2, P<0.01), 3-MT (t_3=4.8, P<0.05), and serotonin (t_3=4.5, P<0.05) levels were also increased by local perfusion of SCH 23390 (**Fig. 4.6B,C**). Elevations in striatal dopamine levels in response to SCH-23390 have been previously reported.[56] In addition to serotonin neurons, medium spiny neurons (MSNs) in striatum express D1 receptors. Blocking D1-receptors on MSNs disinhibits dopamine neurons causing an increase in dopamine levels.[57,58]

To focus on optically stimulated neurochemical levels, we normalized the SCH 23390 time-course data. Data prior to drug perfusion were normalized to pre-drug/pre-stimulation basal neurochemical levels determined in each mouse (**Fig. 4.7A**). Data collected during drug perfusion were normalized to post-drug/pre-simulation basal neurochemical levels. When normalized to the respective basal levels, elevation of stimulated 3-MT (t_3=3.7; P<0.05) remained (**Fig. 4.7A,B**). In contrast, potentiation of optically stimulated dopamine and serotonin levels were no longer evident during striatal SCH 23390 perfusion (**Fig. 4.7A,B**). Thus, increases in the stimulated AUC for serotonin calculated using dialysate concentrations (**Fig. 4.6C**) was largely the result of SCH 29930-induced increases in basal dialysate concentrations.

The D1-like receptor inhibitory increase in basal serotonin levels (**Fig. 4.6A**) can be explained by a circuit connecting dSTR to the DRN.[1] Approximately, 95% of projections from

the dSTR to the DRN are D1-expressing MSNs,[1] which tonically inhibit DRN (and presumably serotoninergic) neurons. Blocking D1-like receptors on MSNs dendritic spines[59] could reduce tonic inhibition of DRN cell populations leading to increased serotonin levels in the dSTR. Regardless, local inhibition of D1 heteroreceptors on serotonin terminals and/or MSNs did not *prevent* optically evoked striatal serotonin.

Mice that received the D1-like inhibitor on day 1 of microdialysis were perfused with eticlopride (ETC), a D2-like receptor antagonist, on day 2 (**Fig. 4.1A**). Inhibition of D2-like receptors, which are expressed as dopaminergic heteroreceptors and autoreceptors in striatum,[60] was not associated with changes in basal levels of dopamine, 3-MT, or serotonin (**Fig. 4.8A**). Though not statistically significant due to small sample sizes, eticlopride perfusion into the dSTR potentiated optically evoked dopamine and 3-MT analyzed either as basal (nM) concentrations (**Fig. 4.8B,C**) or %basal levels normalized to pre-stimulation basal (**Fig. 4.9A,B**). Previous studies have shown that extracellular dopamine is increased upon inhibition of presynaptic D_2 receptors.[61,62] Importantly, in the context of our current hypothesis, and similar to striatal D1-like receptor inhibition, D2-like inhibition did *not* block serotonin overflow associated with optically evoked dopamine release.

Functional interactions between the dopamine and serotonin systems have been investigated for more than 50 years.[63-65] In prefrontal cortex, dopamine receptor activation by the nonselective agonist apomorphine, local dopamine perfusion, or D2 autoreceptor inhibition by haloperidol each produced increases in serotonin levels in rats.[66] Systemic administration of apomorphine was also shown to increase extracellular serotonin in striatum and hippocampus.[67] Our findings indicate that optogenetic activation of midbrain

dopamine neurons expressing the excitatory opsin Chrimson produces temporally specified increases in striatal serotonin, as well as an active dopamine metabolite, 3-MT.

We tested hypotheses linking striatal dopamine and serotonin based on the idea that these neurotransmitters are released from different terminals in striatum. We found that serotonin overflow was not prevented by inhibition of striatal D1-like or D2-like receptors (**Figs. 4.6-9**). Our findings suggest that optically evoked dopamine does not produce serotonin release by stimulating dopamine receptors on striatal serotonin terminals (or direct/indirect pathway MSNs).

Our findings contrast with those of Jacobs and coworkers where apomorphine-induced or behaviorally evoked increases in striatal extracellular serotonin were inhibited by systemic and intrastriatal D2-like receptor inhibition.[67,68] Differences in species (rats *vs.* mice), drug (raclopride *vs.* eticlopride) and/or perfusion concentration (10 uM *vs.* 100 uM) might account for the discrepancies between studies. Jacobs and colleagues did not report on striatal dopamine levels in their studies, *i.e.*, apomorphine and the tail-pinch and light-dark-transition behaviors may have direct receptor/serotonin system effects that are different from those mediated by evoked dopamine.[69] Artigas and colleagues reported that reverse dialysis of D1-like or D2-like agonists into striatum in rats did not alter serotonin levels supporting the idea that dopamine-serotonin interactions are not mediated by striatal dopamine receptors.[40]

Another possibility is that serotonin is released from dopaminergic terminals *via* co-transmission or co-release. Co-transmission involves release of different neurotransmitters from different vesicle populations within the same neurons; co-release entails release of two or more neurotransmitters from the same vesicles.[70] Anatomical, genetic, and functional

evidence shows that neurons can have mixed neurochemical phenotypes (for review see[70-73] among others) and argues specifically for a serotonin/glutamate mixed phenotype.[54,55]

Regarding serotonin/dopamine interactions, under conditions where serotonin transporters are genetically or pharmacologically inactivated, serotonin appears to be taken up by dopamine transporters into dopamine neurons, indicated by double serotonin/tyrosine hydroxylase immunoreactivity in the substantia nigra pars compacta and ventral tegmental area.[74] Thus, SSRI treatment may result in serotonin being used as a 'false' transmitter by dopamine neurons. Studies on chronic SSRI administration using *in vivo* neurochemical monitoring are needed to test this hypothesis further. In any case, mice with wildtype serotonin transporter expression did not show serotonin colocalization in midbrain dopamine neurons suggesting that under typical circumstances, such as those investigated here, evidence is lacking for serotonin co-transmission or co-release by dopaminergic neurons.[74]

Beyond striatum, a dopaminergic pathway connects the substantia nigra to the dorsal raphe, which contains a majority of forebrain-projecting serotonin cell bodies (**Fig. 4.10**). Mesostriatal serotonergic afferents project from the dorsal raphe to the striatum.[2] In addition to striatum, optical activation of dopamine neurons could increase extracellular dopamine in the vicinity of midbrain dopamine cell bodies. Substantia nigra dopamine neurons exhibit activity-dependent somatodendritic dopamine release and D2-mediated autoinhibition.[3,75-77] Activation of nigral D2 autoreceptors might increase extracellular serotonin in the dorsal raphe *via* disinhibition.[78] Furthermore, optical stimulation of dopamine cell bodies could activate dopamine projections to the dorsal raphe (**Fig. 4.10**).

Both scenarios produce dopamine interactions with dorsal raphe serotonin neurons and ostensibly, could increase release of serotonin in striatum (and other brain regions).

Alternately, indirect mechanisms involving SNr-thalamus-cortex-dSTR and/or SNr-thalamus-cortex-DRN pathways cannot be ruled out.[79-82] Moreover, recent reports describe the presence of dopamine neurons in the rostral dorsal raphe nucleus.[83,84] Future experiments to parse out specific contributions from dopamine neurons in the SNr, SNc, VTA and DRN to dopamine-induced serotonin release will be informative. It is also possible that optical stimulation of dopamine neurons in Chrimson-transfected mice, in addition to releasing dopamine, is interoceptively detected by mice.[85] The perception, increased arousal, and/or reward associated with dopaminergic activity could lead to increases in extracellular serotonin by complex mechanisms not involving direct connections between the dopamine and serotonin systems.

Regardless of mechanism, the present findings indicate that optogenetic stimulation of midbrain dopamine neurons evokes striatal serotonin release. We recently reported similar findings elucidated by rapid-pulse voltammetry.[86] Dopamine-serotonin coupling is likely to be of importance to the facilitation of reward prediction, locomotor control, habit formation, and anhedonia.

Figures

Figure 4.1

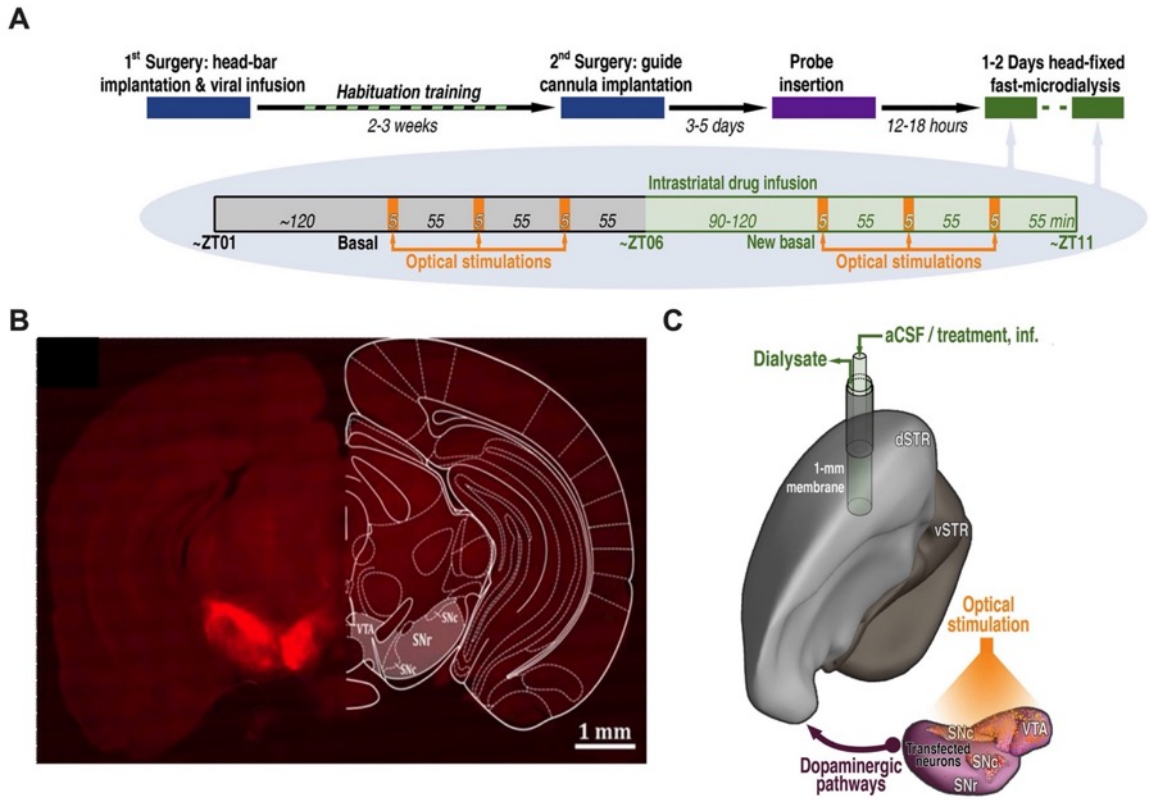

Figure 4.1: Optogenetic stimulation of dopamine cell bodies. A. Experimental paradigm and timelines. Chrimson-expressing mice underwent microdialysis over two consecutive days. Control mice (transfected with mCherry or eYFP) were dialyzed only on Day 1. **B.** Representative optical microscopy image of unilateral Chrimson-positive neurons in the substantia nigra and ventral tegmental area. The coronal brain atlas plate 58, adapted from *The Mouse Brain in Stereotaxic Coordinates,* Paxinos and Franklin, *2nd edition (2001) Academic Press*, is overlaid on the hemisphere contralateral to transfection. Ventral tegmental area (VTA), substantia nigra pars compacta (SNc), and substantia nigra pars reticulata (SNr) **C.** Model showing the location of the microdialysis probe in the dorsal striatum (dSTR) relative to Chrimson transfection and optical stimulation in the ipsilateral VTA, SNc, and SNr. Ventral striatum (vSTR), artificial cerebrospinal fluid (aCSF).

Figure 4.2

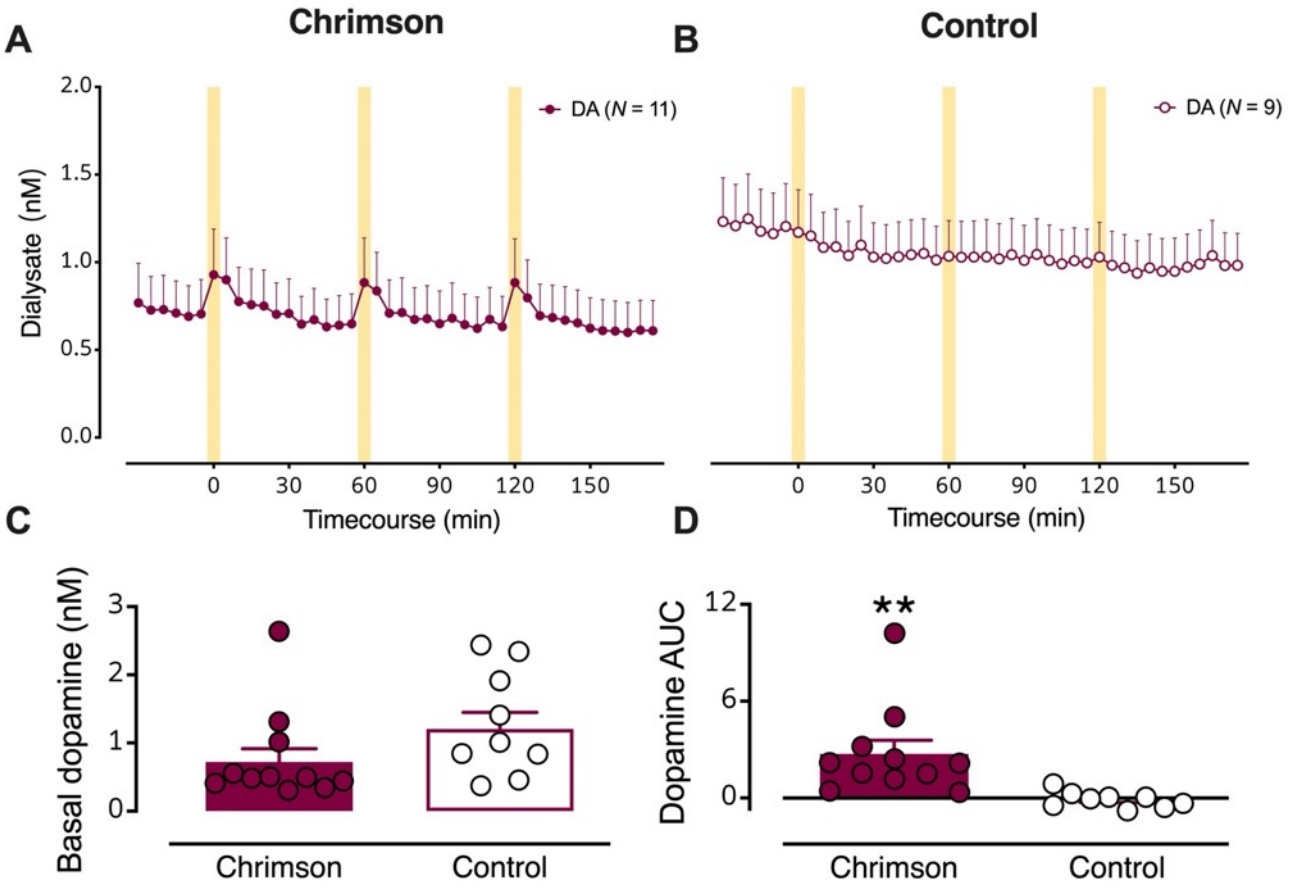

Figure 4.2: Optical stimulation of dopaminergic cell bodies produces dopamine release in striatal terminal regions. **A.** Dialysate dopamine levels were increased in response to optical stimulation in mice expressing Chrimson (*N*=11) **B.** but not in control mice (*N*=9). The yellow bars indicate optical stimulations (10 mw/mm^2, 50 ms pulse width @ 10 Hz for 5 min). **C.** Basal dopamine levels in mice transfected with Chrimson relative to control mice. **D.** Dopamine overflow, quantified by area under the curve, was increased in Chrimson expressing but not control mice. Data are means ± SEMs. $^{**}P<0.01$.

Figure 4.3

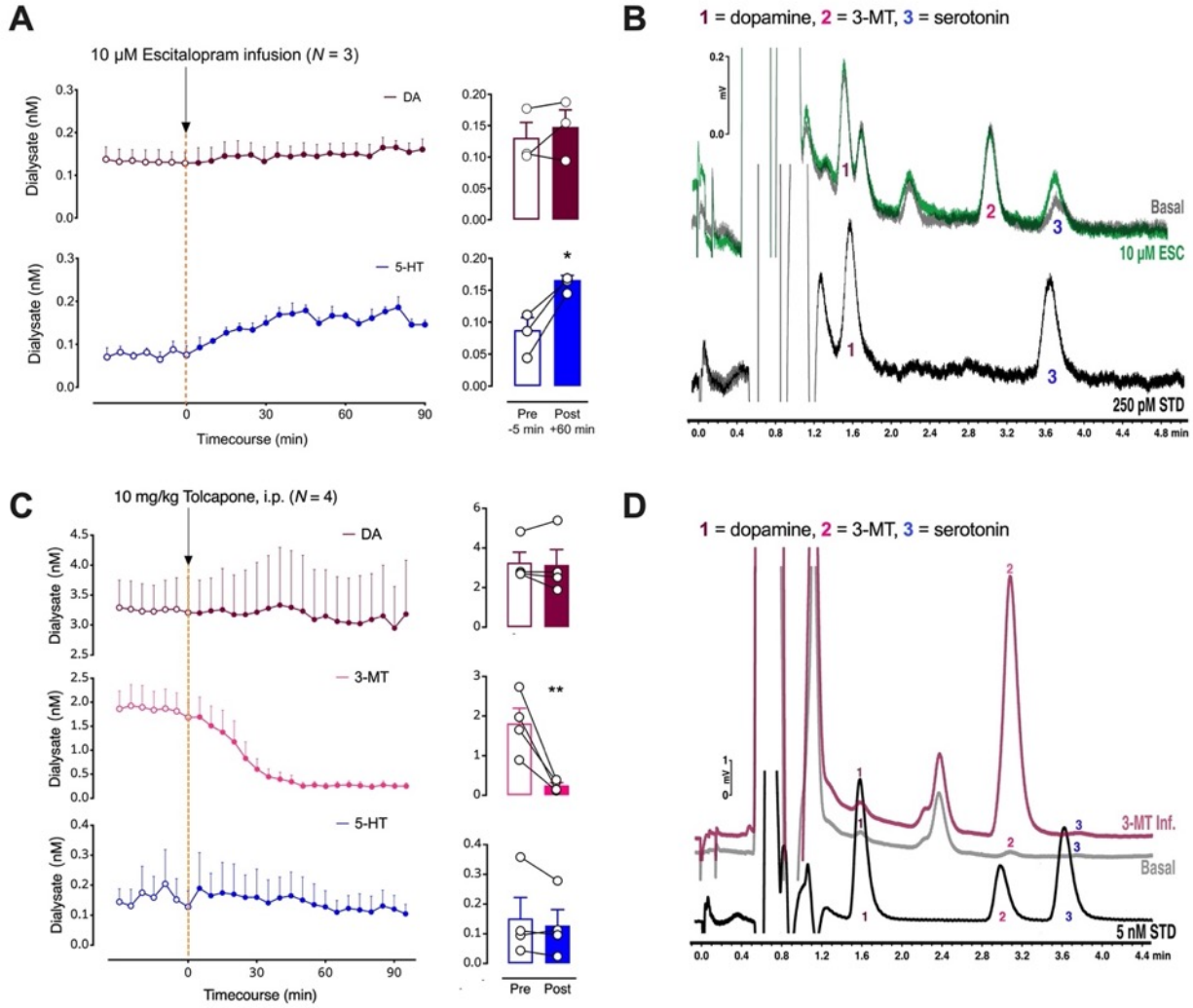
A
10 μM Escitalopram infusion (N = 3)
DA
5-HT
Dialysate (nM)
Timecourse (min)
Pre -5 min
Post +60 min
B
1 = dopamine, 2 = 3-MT, 3 = serotonin
Basal
10 μM ESC
250 pM STD
C
10 mg/kg Tolcapone, i.p. (N = 4)
DA
3-MT
5-HT
Dialysate (nM)
Timecourse (min)
Pre
Post
D
1 = dopamine, 2 = 3-MT, 3 = serotonin
3-MT Inf.
Basal
5 nM STD

Figure 4.3: A. The left panel shows the effects of intrastriatal perfusion of 10 μM escitalopram on dopamine (DA; top, red) and serotonin levels (5-HT; bottom, blue). Basal serotonin levels were significantly increased after escitalopram administration (right). **B.** Representative chromatograms showing dopamine (peak 1), 3-MT (peak 2), and serotonin (peak 3) from a control mouse under basal conditions (gray) and during perfusion of the selective serotonin reuptake inhibitor (SSRI) escitalopram (green). Peak 3 showed a large increase in response to local delivery of the SSRI suggesting that this peak was serotonin. A standard containing 500 pM dopamine (peak 1) and serotonin (peak 3) is overlaid in black. **C.** The left panel shows the effects of systemic administration of tolcapone, a catechol-*O*- methyltransferase (COMT) inhibitor on dopamine (DA; top, red), 3-methyltyramine (3-MT; middle, pink), and serotonin levels (5-HT; bottom, blue). The enzyme COMT converts dopamine to 3-MT. Only 3-MT (pink) was significantly reduced after tolcapone administration (right). **D.** Representative chromatograms showing dopamine (peak 1), 3-MT (peak 2), and serotonin (peak 3) after the intrastriatal perfusion of 50 nM 3-MT (red) *vs.* a basal dialysate sample from the same control mouse (gray). Reverse dialysis of 3-MT confirms peak 2 as 3-MT. A standard containing 5 nM dopamine (peak 1), 3-MT (peak 2), and serotonin (peak 3) is overlaid in black. Data in A and C are means ± SEMs. *$P<0.05$, **$P<0.01$. A peak sometimes appearing between peaks 1 and 2 was not responsive to optical stimulation or high K^+ perfusion, therefore, we did not attempt to identify this peak.

Figure 4.4

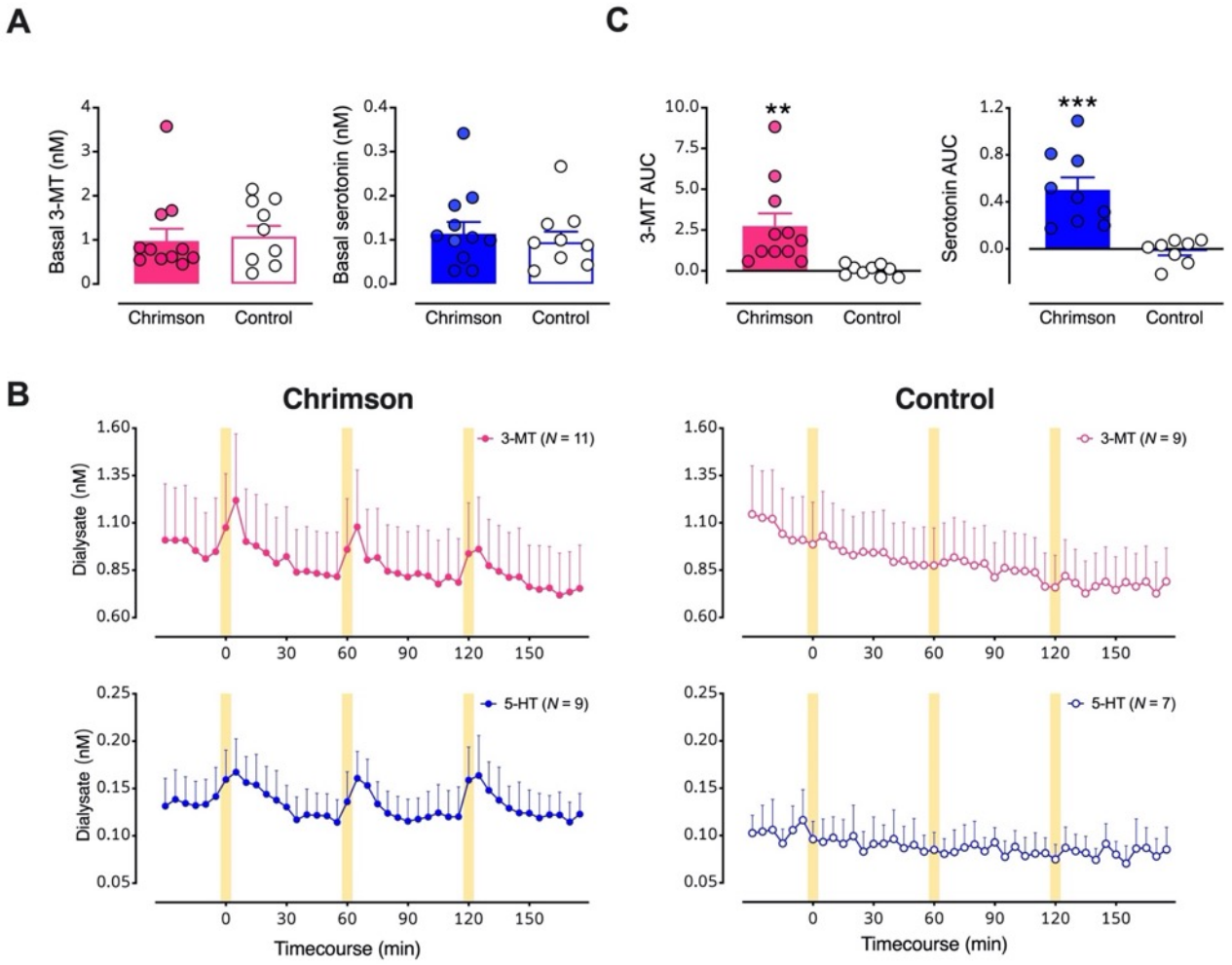

Figure 4.4: Optical stimulation of midbrain dopamine neurons evokes overflow of 3-methyltyramine (3-MT) and serotonin in dorsal striatum (dSTR). A. Basal dialysate levels of 3-MT (left, pink) and serotonin (right, blue) in mice with *vs.* without Chrimson transfection. **B.** Time course of stimulated 3-MT (pink) and serotonin (blue) in mice transfected with Chrimson (left) compared to mice transfected with a control protein (right). Yellow bars indicate 5-min optical stimulations. **C.** Comparisons of areas under the curve (AUC) for the overflow of 3-MT or serotonin produced by optical stimulation of dopamine neurons expressing Chrimson with respect to control mice. Data are means ± SEMs. $^{**}P<0.01$, $^{***}P<0.001$. In two mice per group, data for serotonin were below the detectable limit.

Figure 4.5

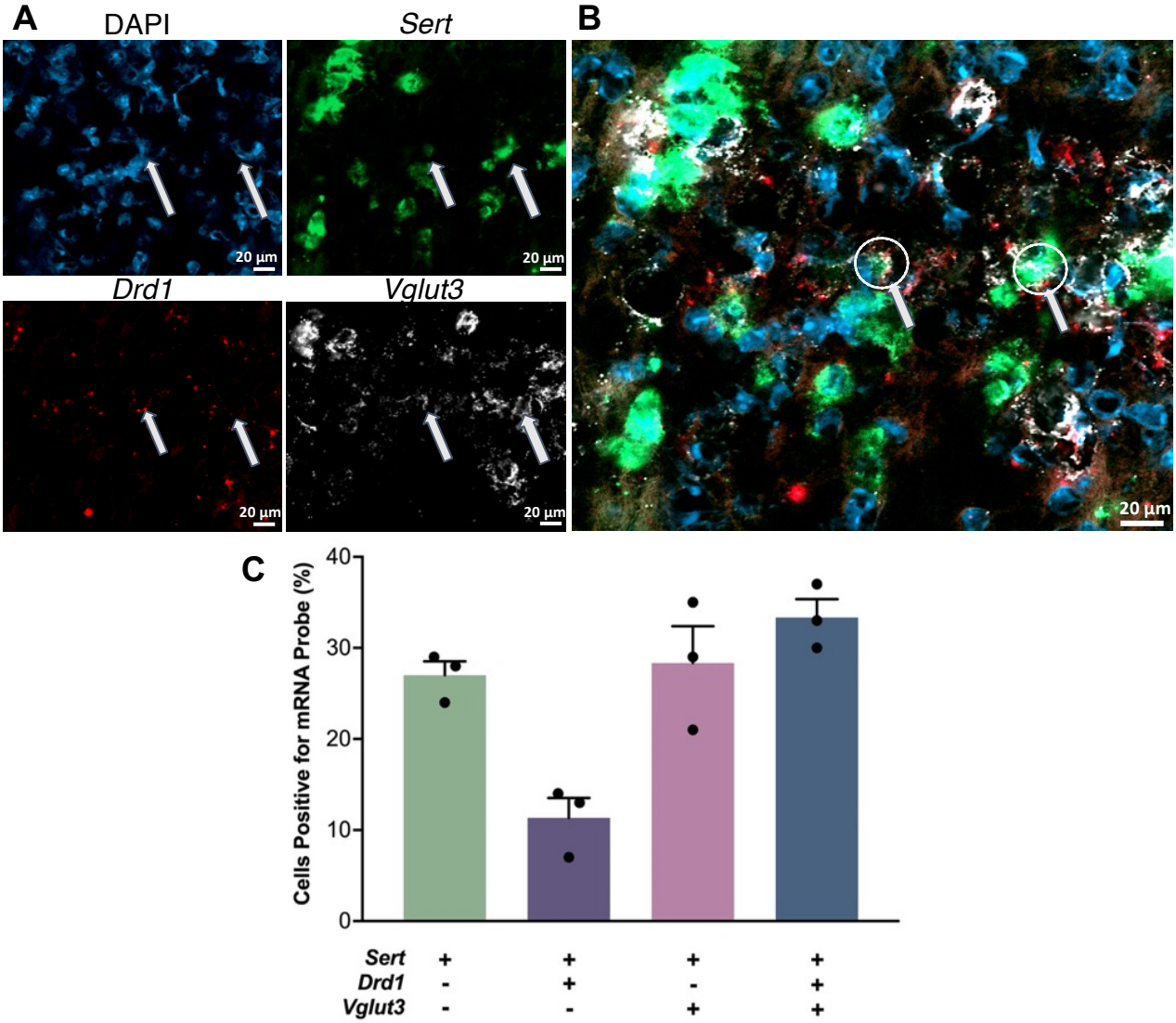

Figure 4.5: Co-localization of serotonin transporter (*Sert*), D1 dopamine receptor (*Drd1*), and vesicular glutamate transporter 3 (*Vglut3*) mRNA in the dorsal raphe nucleus. A. Cell nuclei were stained with DAPI (top left, blue). Antisense probes to localize *Sert* (top right, green), *Drd1* (bottom left, red), and *Vglut3* (bottom right, white) mRNA were visualized. Puncta for each mRNA were colocalized in some nuclei but did not necessarily overlap. **B.** Overlay of images in A. Arrows indicate examples of the three mRNAs colocalized in the same nuclei. **C.** Relative quantification of cells containing *Sert*, *Drd1*, and *Vglut3* mRNA with respect to the total number of *Sert* expressing cell bodies. (SEMs are for *n*=3 z-stack planes in a single mouse. A total of 248 cells were counted).

Figure 4.6

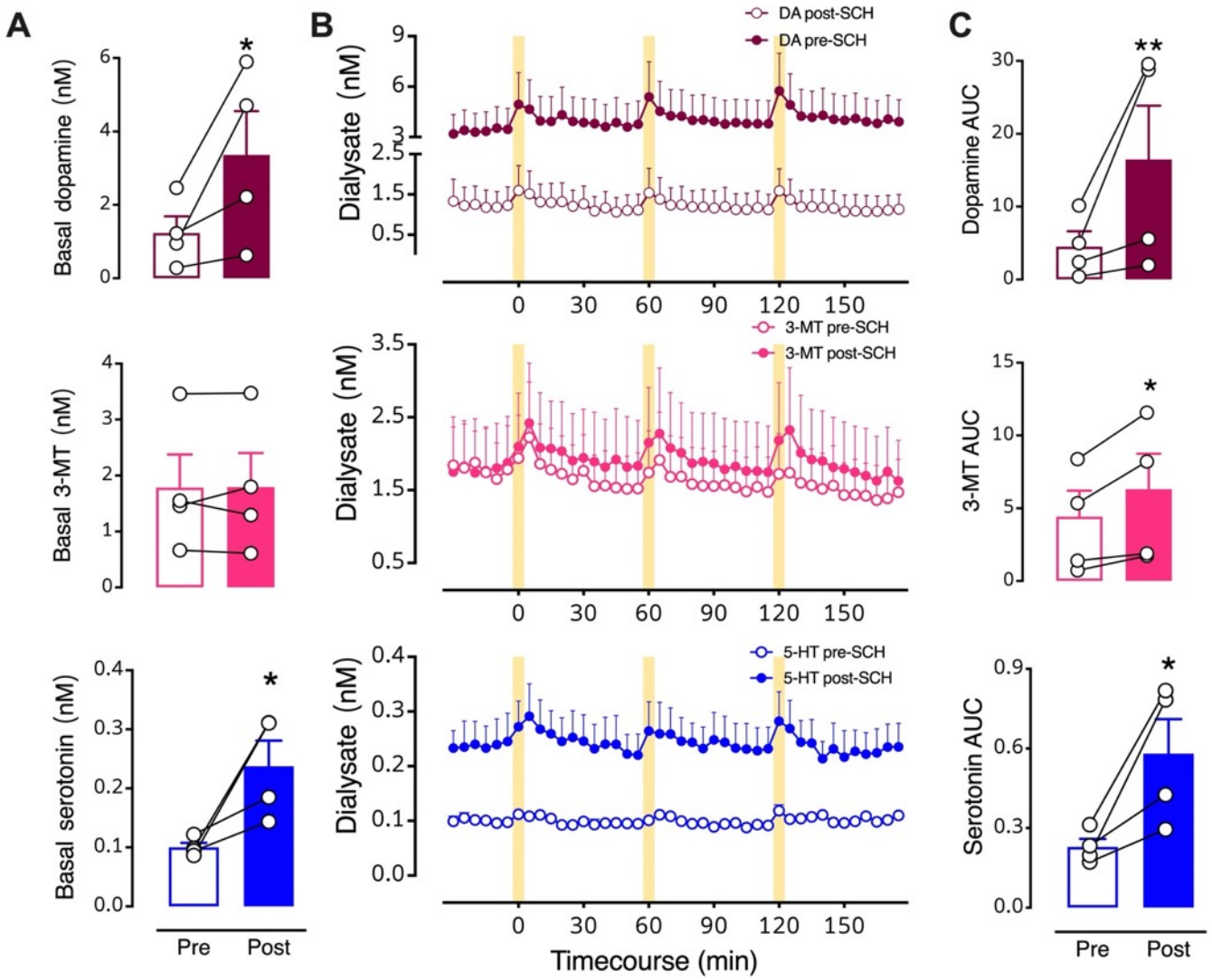

Figure 4.6: Intrastriatal perfusion of a D1-like receptor inhibitor. A. Basal levels for the three neurochemicals pre- *vs.* post-SCH 23390. **B.** Time courses before and during intrastriatal perfusion of 100 μM SCH 23390 showing optically stimulated increases in dopamine (red, top), 3-methyltyramine (3-MT; pink, middle), and serotonin (blue, bottom). **C.** Area under the curve (AUC) comparisons of overflow induced by optical stimulation prior to (Pre) and during (Post) SCH 23390 striatal perfusion. Following three pre-drug stimuli, SCH 23390 was perfused for 90-120 min in each mouse prior to the first post-drug stimulation (see Fig. III.1A for timeline). The data 30 min prior to the first post-drug stimulus were used to calculate post-drug basal levels. The drug was continuously perfused throughout the post-drug stimulation period. Data are means ± SEMs. Some error bars in B cannot be seen due to scale. *P<0.05, **P<0.01 pre- *vs.* post- initiation of drug perfusion. N=4 mice. Each basal data point in A represents the mean of six measurements taken just prior to the first pre- or post-drug stimulation (errors not shown). The AUC data points in C are means of each of the three stimuli (errors not shown).

Figure 4.7

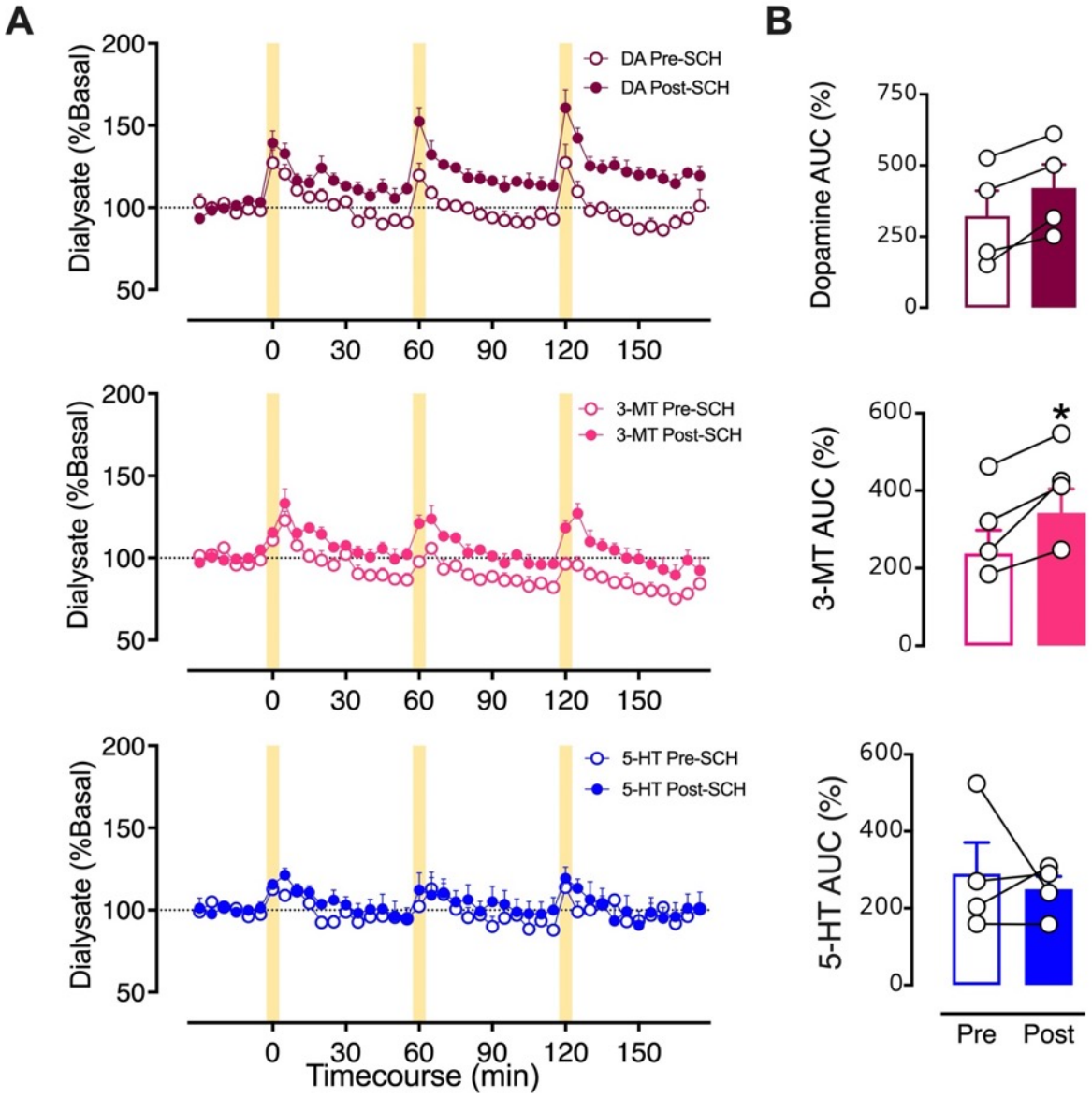

Figure 4.7: Effects of intrastriatal perfusion of a D1-like receptor inhibitor analyzed with respect to pre-stimulation basal levels. A. Time courses of optically stimulated neurochemical levels before and during intrastriatal perfusion of SCH 23390 (100 μM). **B.** Optically evoked overflow expressed as area under the curve for data normalized to pre-stimulation basal levels (AUC (%)). Data are means ± SEMs. *N*=4 mice. **P*<0.05. The AUC datapoints in C are means of the three stimuli for each mouse (errors not shown).

Figure 4.8

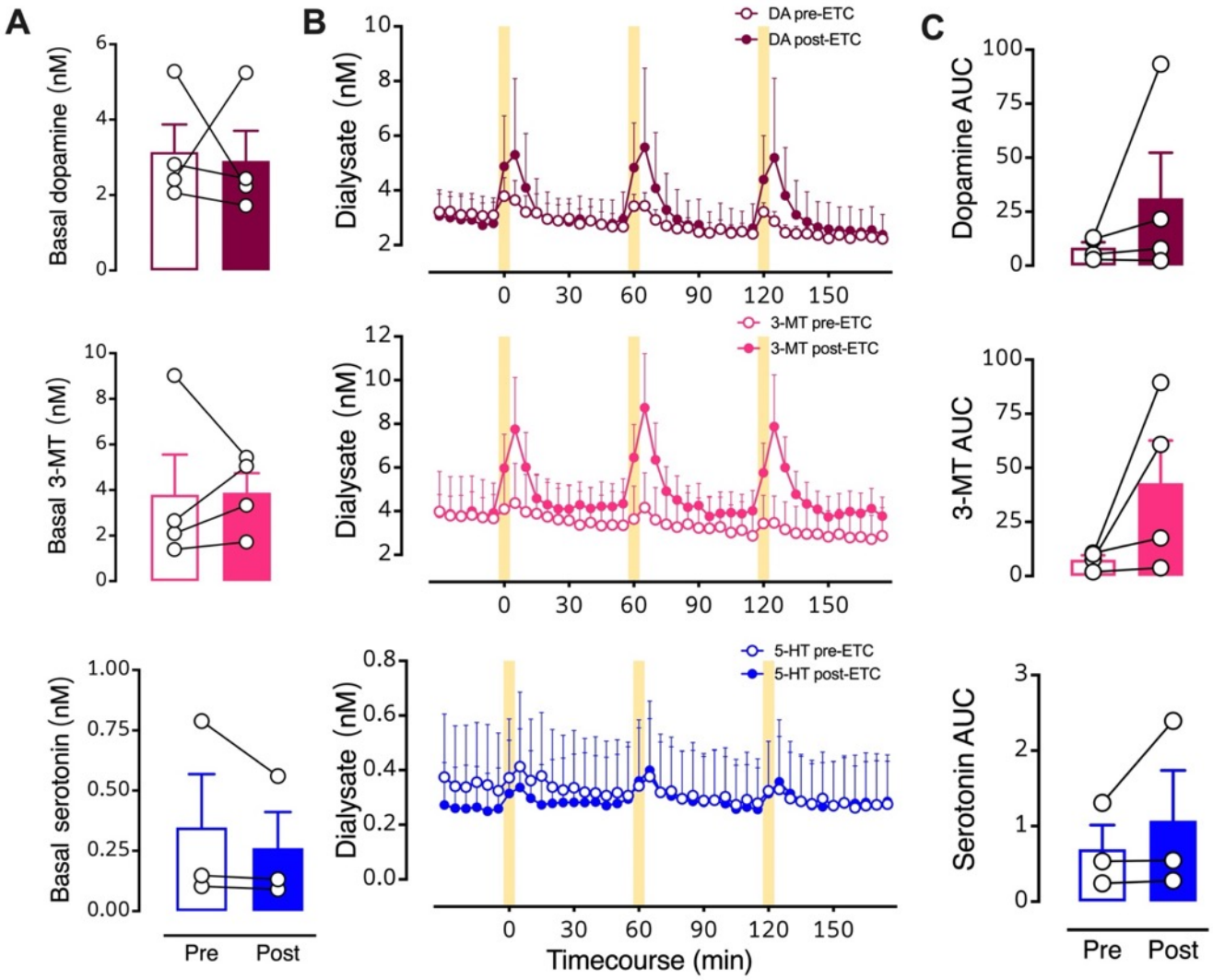

Figure 4.8: Intrastriatal perfusion of a D_2 antagonist does not prevent optically evoked serotonin. **A.** Pre- *vs.* post-eticlopride basal levels of all three neurochemicals. **B.** Time course before and during intrastriatal infusion of the D2-like receptor inhibitor eticlopride (100 μM). **C.** Areas under the curve (AUC) for optically stimulated neurochemical release prior to (Pre) and during (Post) eticlopride perfusion into striatum. Data are means ± SEMs for *N*=4 mice. Serotonin levels for one mouse were not detectable. Basal data points in A represent the means of six measurements just prior to the first stimulation (errors not shown). The AUC datapoints in C represent the means of three stimuli (errors not shown).

Figure 4.9

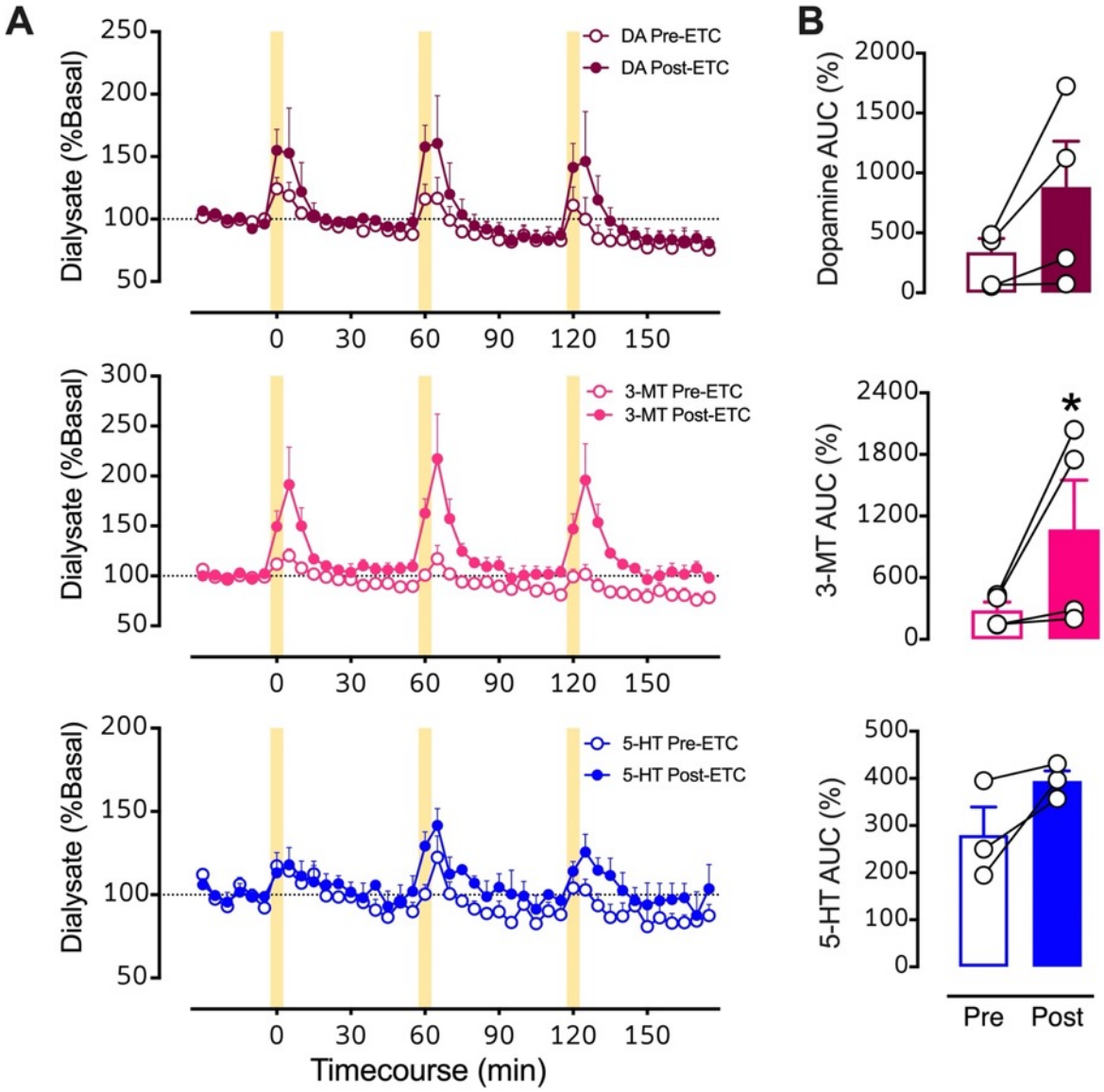

Figure 4.9: Effects of intrastriatal perfusion of a D_2 antagonist analyzed with respect to pre-stimulation basal levels. A. Time courses before and during intrastriatal perfusion of eticlopride (100 μM) showing basal and stimulated neurochemical levels expressed as percents of respective pre-stimulation basal levels. **B.** Optically evoked overflow expressed as area under the curve for data normalized to pre-stimulation basal levels (AUC (%)). Data are means ± SEMs for *N*=4 mice. Serotonin levels for one mouse were not detectable. **P*<0.05 *vs.* pre-drug. %Basal data points in A represent the means of six measurements just prior to the first stimulation (errors not shown). The AUC datapoints in C are the means of the three stimuli (errors not shown).

Figure 4.10

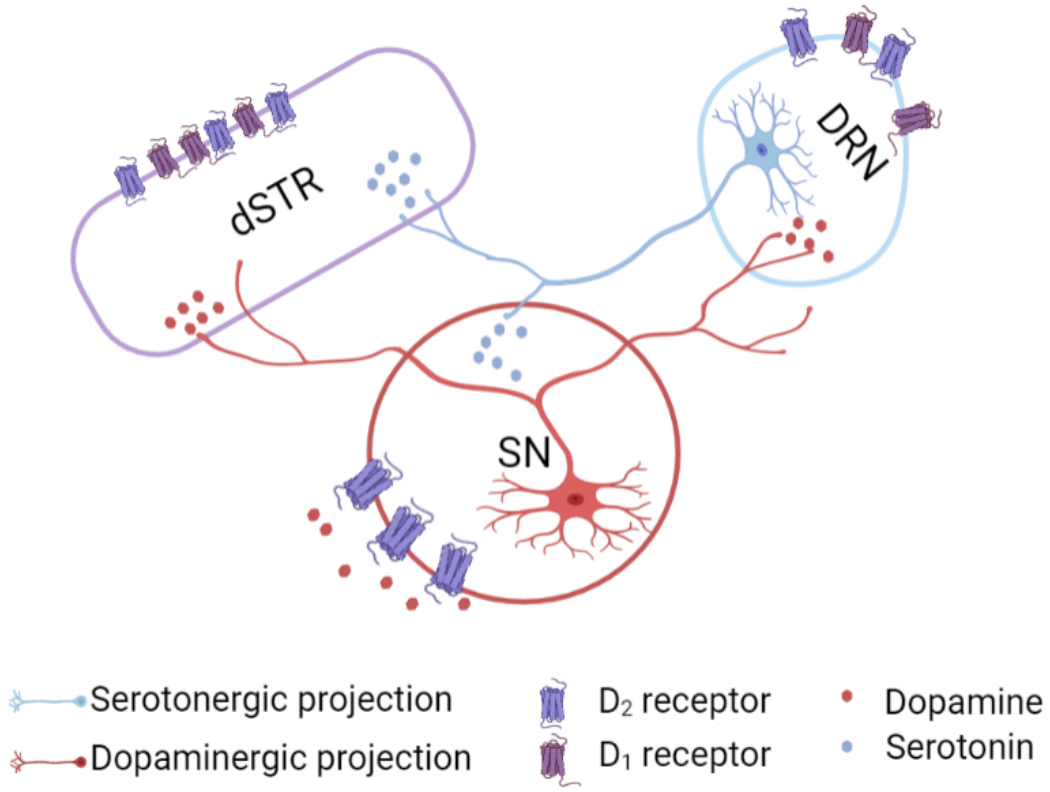

Figure 4.10: Proposed mechanisms of dopamine-mediated serotonin release. The substantia nigra (SN) sends dense dopaminergic projections to the striatum (nigrostriatal pathway) and to the dorsal raphe nucleus (DRN).[1] The DRN sends serotonergic projections to dopaminergic cell bodies in the SN and to the striatum.[2] We found that optical activation of midbrain dopamine neurons produces striatal serotonin release that was not blocked by striatal D1- or D2-like receptor inhibition. Another possible mechanism for dopamine-mediated serotonin release is that an optogenetically induced increase in dopamine in the SN, which promotes D2 somatodendritic autoreceptor activation[3] and subsequent disinhibition of serotonin cell bodies in the DRN, produces serotonin release in the striatum. Alternately, optically induced dopamine release in DRN could act *via* local D1 or D2-like receptors to increase the probability of firing of DRN serotonin neurons projecting to dSTR.

Figure 4.S1

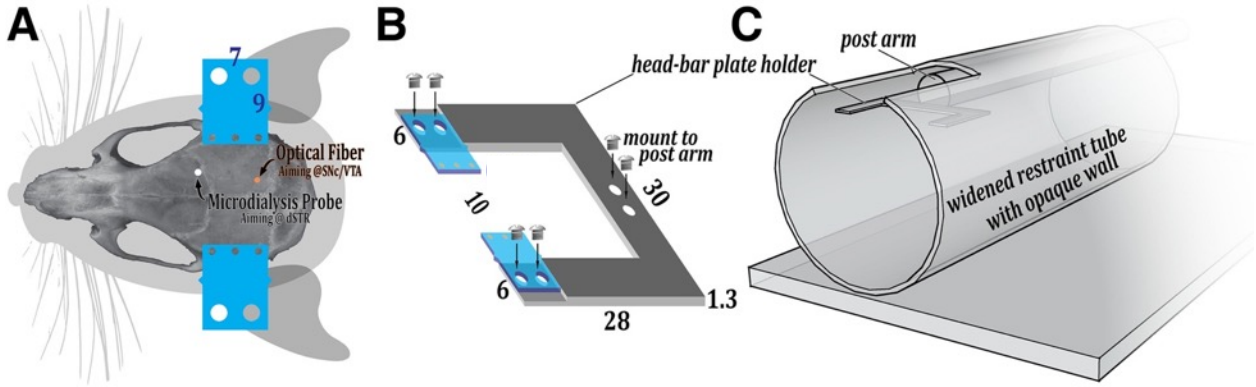

Figure 4.S1: Head-fixed recording set-up. A. Schematic showing the locations of the head-bar implants (in blue and to scale) and the stimulation (stim) and recording (dSTR) site craniotomies relative to a mouse skull. **B.** Schematic of the head-bar plate holder (in gray and to scale). The head-bar plate holder was 30 mm long, 28 mm wide, and 1.3 mm thick. The mini-plates, which attach the holder to the head bars, were 9 mm long, 7 mm wide, and 0.65 mm thick, with a 10 mm gap between them. **C.** Schematic of the custom head-fixed tube used for fast microdialysis recordings with optical stimulation. The restraint tube (2" diameter), constructed of opaque (black) plexiglass, provided loose restraint to reduce spontaneous and stimulated physical movement, which can evoke movement-induced dopamine release artifacts in dorsal striatum.

Figure 4.S2

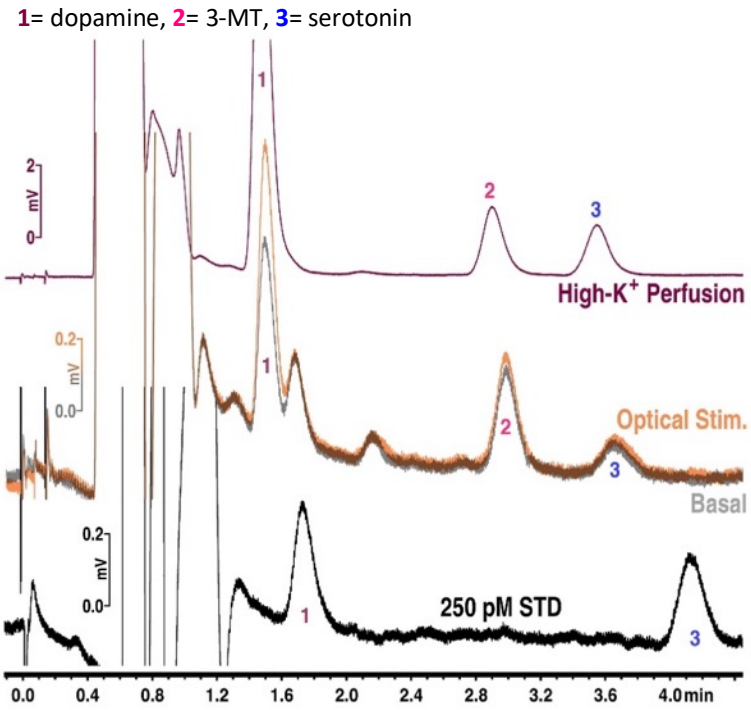

Figure 4.S2: Optical stimulation of midbrain dopamine neurons increases in striatal serotonin and 3-methoxytyramine. Representative chromatograms from a Chrimson-transfected mouse under basal conditions (gray), and in response to optical stimulation (orange) or high-K^+ perfusion (red). Both optical stimulation and high-K^+ perfusion induced increases in neurochemicals (peaks 2 and 3), in addition to dopamine (peak 1). Chromatogram of a standard containing 250 pM dopamine (peak 1) and serotonin (peak 3) is shown in black. Peaks 2 and 3 in the dialysate samples could not be definitively identified based on comparison with retention times in the standard chromatogram.

Figure 4.S3

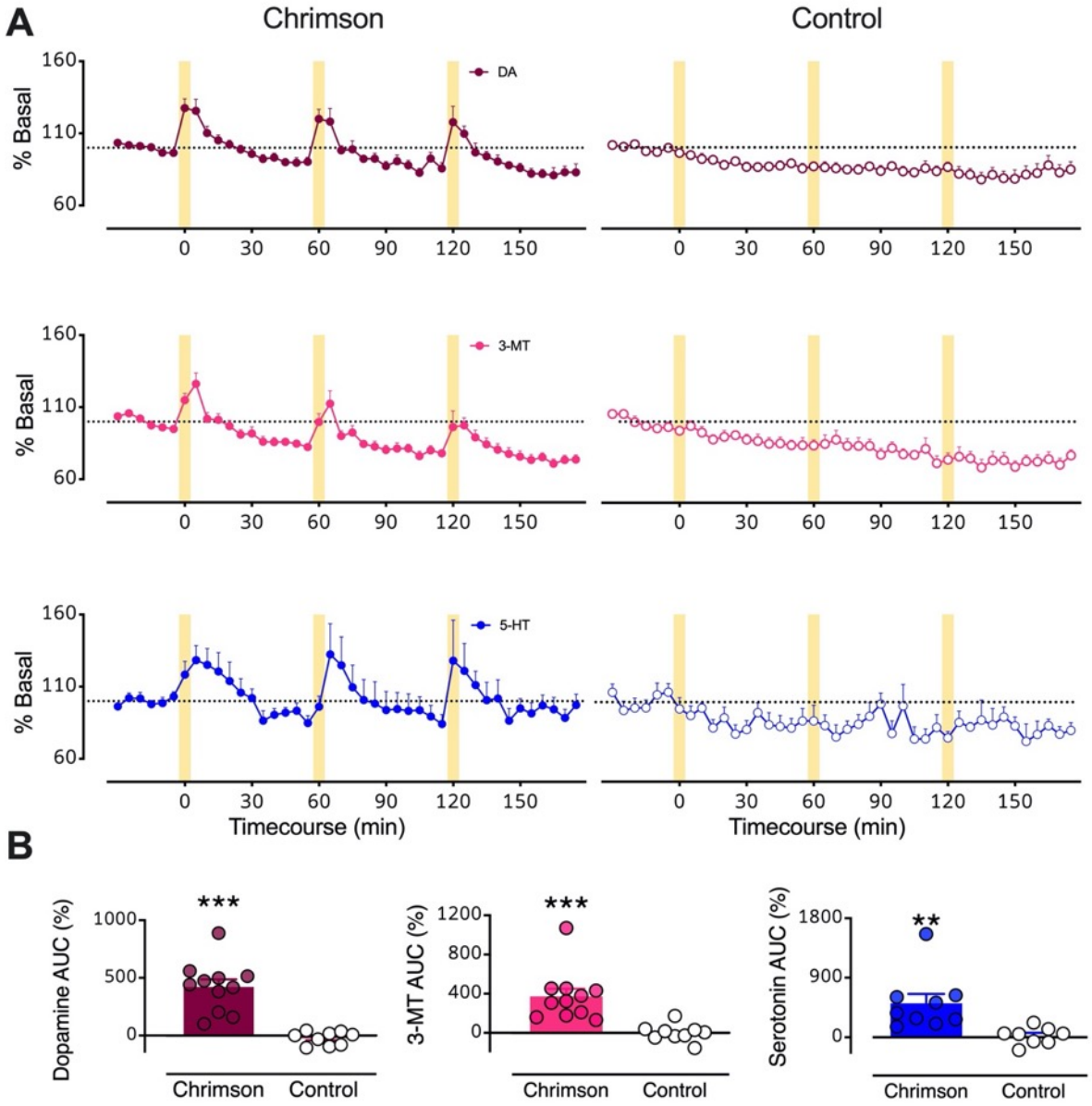

Figure 4.S3: Normalized responses to optical stimulation. A. Time courses of %basal dialysate levels for DA (top, red), 3-MT (middle, pink), and serotonin (5-HT; bottom, blue) in mice expressing Chrimson (left) *vs.* mice transfected with a control protein (right). Optically induced overflow of dopamine, 3-MT, and serotonin were only detected in the Chrimson animals. **B.** The magnitudes of overflow are represented as areas under the curve percent (AUC (%)). Dialysate serotonin concentrations were below the detectable threshold in 2/11 Chrimson mice and 2/9 control mice. The yellow bars indicate optical stimulations (5 min). $^{**}P<0.01$ and $^{***}P<0.001$.

Figure 4.S4

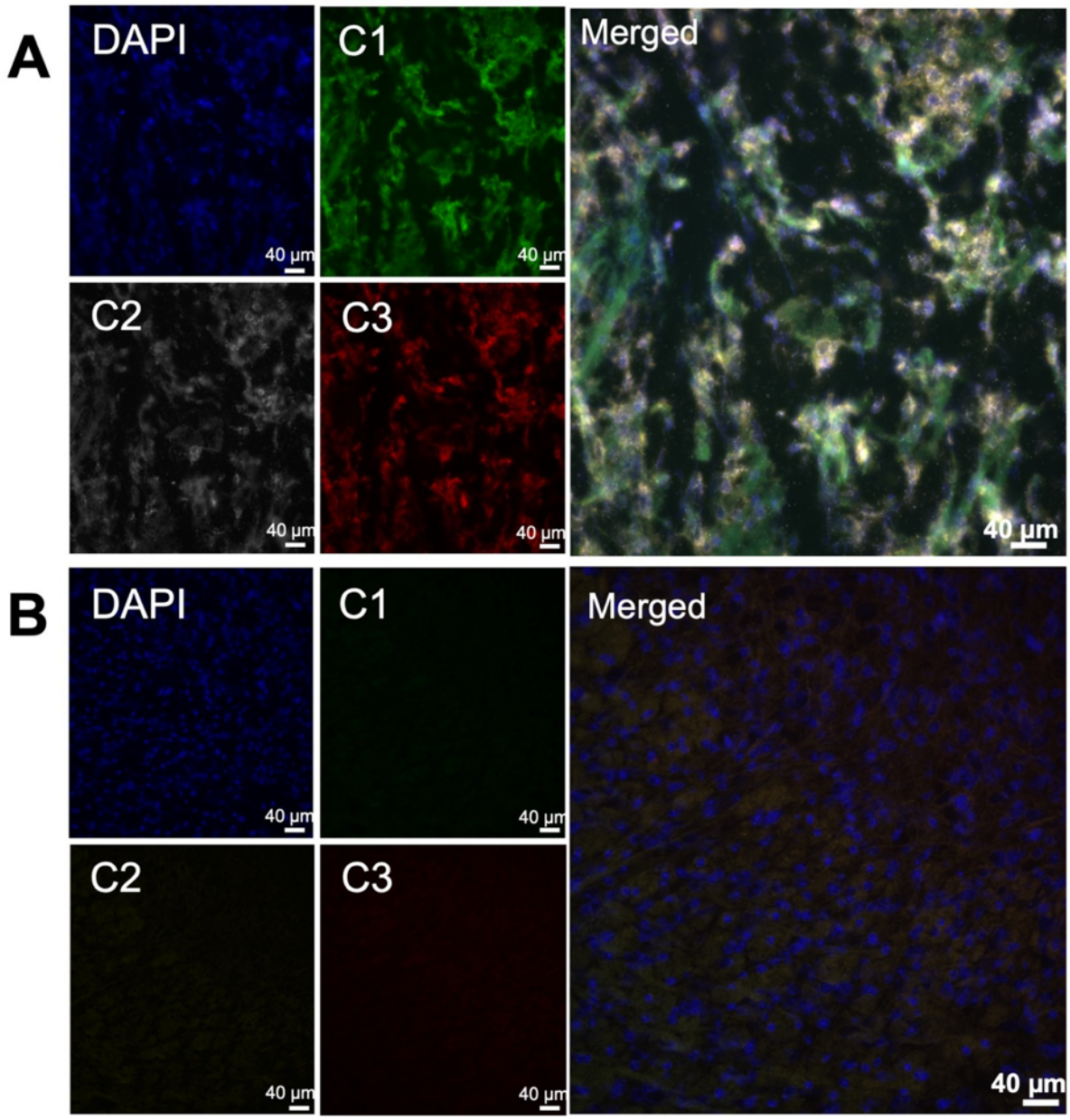

Figure 4.S4: RNAscope *in situ* hybridization controls in dorsal raphe. A. The RNAscope® Multiplex Fluorescent Assay as a 3-plex positive control. The RNA polymerase II subunit RPB1 (Polr2a, C1 channel), cyclophilin B (PPIB, C2 channel), and ubiquitin C (UBC, C3 channel) are mRNAs found in all mouse cells. Cell nuclei stained by DAPI are shown in blue. The overlay is shown on the right **B.** The RNAscope® Multiplex Fluorescent Assay as a 3-plex negative control. A probe for DapB, an mRNA that codes for a reductase enzyme from *Bacillus subtilis*, was used in all three channels with each of the opal dyes to evaluate background staining.

Figure 4.S5

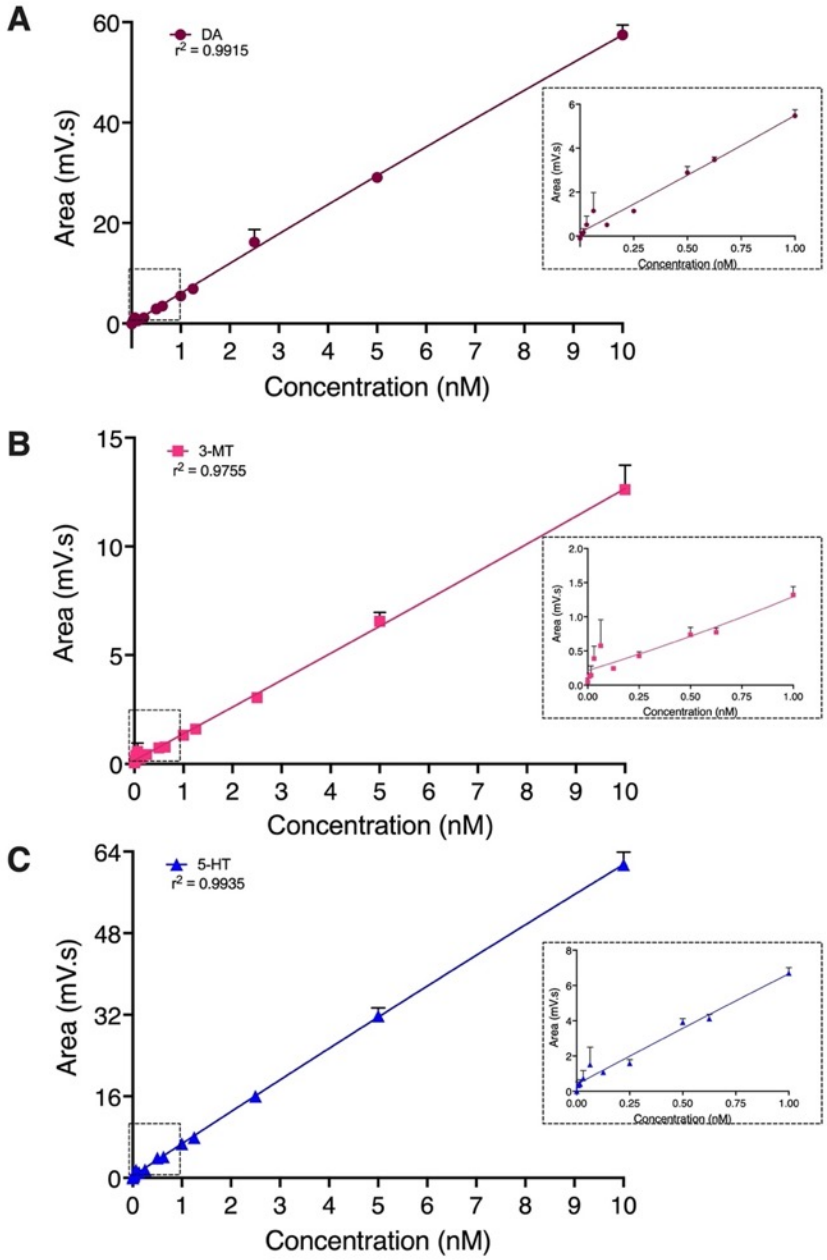

Figure 4.S5: Standard curves for dopamine, 3-methyltyramine 3-MT), and serotonin. Fourteen standards (0 nM, 0.008 nM, 0.016 nM, 0.032 nM, 0.063 nM, 0.125 nM, 0.250 nM, 0.500 nM, 0.625 nM, 1 nM, 1.25 nM, 2.5 nM, 5 nM, and 10 nM) were injected into the HPLC (20 µL volumes) to create standard curves. Insets are zoomed in on the lower concentrations ranging from 0-1 nM. Quadratic curve-fits were applied to **A.** dopamine, **B.** 3-MT, and **C.** serotonin standards. Each point represents *N*=3 replicates measured on different days. Error bars (standard errors of the means) are too small to be visualized in some cases.

Table 4.S1

Table S1: Statistical summary

FIGURE	COMPARISON	TEST	RESULTS	SIGNIFICANT?
2C	Basal DA: control *vs.* Chrimson	Unpaired two-tailed t-test	t (18)=1.6; *P*>0.1	No
2D	**AUC DA: control *vs.* Chrimson**	**Unpaired two-tailed t-test**	**t (18)=3.0; *P*<0.01**	**
3A	DA: 5 mins pre- *vs.* 60 mins post-ESC	Paired two-tailed t-test	t (2)=0.92; *P*>0.4	No
3A	**5HT: 5 mins pre- *vs.* 60 mins post-ESC**	**Paired two-tailed t-test**	**t (2)=5.7; *P*<0.05**	*
3C	DA: 5 mins pre vs. 60 mins post TOL	Ratio paired two-tailed t-test	t (3) = 0.83; *P*>0.46	No
3C	**3MT: 5 mins pre vs. 60 mins post TOL**	**Ratio paired two-tailed t-test**	**t (3) = 9.6; *P*<0.01**	**
3C	5HT: 5 mins pre vs. 60 mins post TOL	Ratio paired two-tailed t-test	t (3) = 1.3; *P*>0.29	No
4A	Basal 3MT: control *vs.* Chrimson	Unpaired two-tailed t-test	t (18)=0.27; *P*>0.7	No
4A	Basal 5HT: control *vs.* Chrimson	Unpaired two-tailed t-test	t (18)=0.52; *P*>0.6	No
4C	**AUC 3MT: control vs. Chrimson**	**Unpaired two-tailed t-test**	**t (18)=3.1; *P*<0.01**	**
4C	**AUC 5HT: control vs. Chrimson**	**Unpaired two-tailed t-test**	**t (15)=4.4; *P*<0.001**	***
6A	**Basal DA: pre- *vs.* post-SCH**	**Ratio paired two-tailed t-test**	**t (3)=4.4; *P*<0.05**	*
6A	Basal 3MT: pre- *vs.* post-SCH	Ratio paired two-tailed t-test	t (3) = 0.17; *P*>0.87	No
6A	**Basal 5HT: pre- *vs.* post-SCH**	**Ratio paired two-tailed t-test**	**t (3) = 3.5; *P*<0.05**	*
6C	**AUC DA: pre- *vs.* post-SCH**	**Ratio paired two-tailed t-test**	**t (3) = 6.2; *P*<0.05**	**
6C	**AUC 3MT: pre- *vs.* post-SCH**	**Ratio paired two-tailed t-test**	**t (3) = 4.8; *P*<0.05**	*
6C	**AUC 5HT: pre- v*s.* post-SCH**	**Ratio paired two-tailed t-test**	**t (3) = 4.5; *P*<0.05**	*
7B	AUC (%) DA: pre vs. post SCH	Ratio paired two-tailed t-test	t (3) = 2.4; *P*<0.1	Trend
7B	**AUC (%) 3MT: pre vs. post SCH**	**Ratio paired two-tailed t-test**	**t (3) = 3.7; *P*<0.05**	*
7B	AUC (%) 5HT: pre vs. post SCH	Ratio paired two-tailed t-test	t (3) = 0.41; *P*>0.71	No
8A	Basal DA: pre vs. post ETC	Ratio paired two-tailed t-test	t (3) = 0.31; *P*>0.78	No
8A	Basal 3MT: pre vs. post ETC	Ratio paired two-tailed t-test	t (3) = 0.81; *P*>0.47	No
8A	Basal 5HT: pre vs. post ETC	Ratio paired two-tailed t-test	t (2) = 2.7; *P*>0.11	No
8C	AUC DA: pre vs. post ETC	Ratio paired two-tailed t-test	t (3) = 1.5; *P*<0.23	No

8C	AUC 3MT: pre vs. post ETC	Ratio paired two-tailed t-test	t (3) = 3.1; *P*<0.06	Trend
8C	AUC 5HT: pre vs. post ETC	Ratio paired two-tailed t-test	t (2) = 1.4; *P*>0.28	No
9B	AUC (%) DA: pre vs. post ETC	Ratio paired two-tailed t-test	t (3) = 2.6; *P*<0.08	Trend
9B	**AUC (%) 3MT: pre vs. post ETC**	**Ratio paired two-tailed t-test**	**t (3) = 4.4; *P*<0.05**	*****
9B	AUC (%) 5HT: pre vs. post ETC	Ratio paired two-tailed t-test	t (2) = 1.8; *P*>0.21	No
S3B	**AUC (%) DA: control vs. chrimson**	**Unpaired two-tailed t-test**	**t (18) = 5.9; *P*<0.001**	*******
S3B	**AUC (%) 3MT: control vs. chrimson**	**Unpaired two-tailed t-test**	**t (18) = 4.1; *P*<0.001**	*******
S3B	**AUC (%) 5HT: control vs. chrimson**	**Unpaired two-tailed t-test**	**t (15) = 3.1; *P*<0.01**	******

References

1. Pollak Dorocic, I.; Fürth, D.; Xuan, Y.; Johansson, Y.; Pozzi, L.; Silberberg, G.; Carlén, M.; Meletis, K., A whole-brain atlas of inputs to serotonergic neurons of the dorsal and median raphe nuclei. *Neuron* **2014,** *83* (3), 663-678.

2. Muzerelle, A.; Scotto-Lomassese, S.; Bernard, J. F.; Soiza-Reilly, M.; Gaspar, P., Conditional anterograde tracing reveals distinct targeting of individual serotonin cell groups (b5-b9) to the forebrain and brainstem. *Brain Structure and Function* **2016,** *221* (1), 535-61.

3. Hikima, T.; Lee, C. R.; Witkovsky, P.; Chesler, J.; Ichtchenko, K.; Rice, M. E., Activity-dependent somatodendritic dopamine release in the substantia nigra autoinhibits the releasing neuron. *Cell Reports* **2021,** *35* (1), 108951.

4. Bernstein, J. G.; Boyden, E. S., Optogenetic tools for analyzing the neural circuits of behavior. *Trends in Cognitive Science* **2011,** *15* (12), 592-600.

5. Boyden, E. S., Optogenetics: Using light to control the brain. *Cerebrum* **2011,** *2011*, 16.

6. Kim, C. K.; Adhikari, A.; Deisseroth, K., Integration of optogenetics with complementary methodologies in systems neuroscience. *Nat Rev Neurosci* **2017,** *18* (4), 222-235.

7. Entcheva, E.; Kay, M. W., Cardiac optogenetics: A decade of enlightenment. *Nature Reviews Cardiology* **2020**.

8. Han, X., In vivo application of optogenetics for neural circuit analysis. *ACS Chemical Neuroscience* **2012,** *3* (8), 577-84.

9. Deisseroth, K., Optogenetics. *Nature Methods* **2011,** *8* (1), 26-29.

10. Klapoetke, N. C.; Murata, Y.; Kim, S. S.; Pulver, S. R.; Birdsey-Benson, A.; Cho, Y. K.; Morimoto, T. K.; Chuong, A. S.; Carpenter, E. J.; Tian, Z.; Wang, J.; Xie, Y.; Yan, Z.; Zhang, Y.;

Chow, B. Y.; Surek, B.; Melkonian, M.; Jayaraman, V.; Constantine-Paton, M.; Wong, G. K.; Boyden, E. S., Independent optical excitation of distinct neural populations. *Nature Methods* **2014,** *11* (3), 338-46.

11. Madisen, L.; Mao, T.; Koch, H.; Zhuo, J. M.; Berenyi, A.; Fujisawa, S.; Hsu, Y. W.; Garcia, A. J., 3rd; Gu, X.; Zanella, S.; Kidney, J.; Gu, H.; Mao, Y.; Hooks, B. M.; Boyden, E. S.; Buzsaki, G.; Ramirez, J. M.; Jones, A. R.; Svoboda, K.; Han, X.; Turner, E. E.; Zeng, H., A toolbox of cre-dependent optogenetic transgenic mice for light-induced activation and silencing. *Nature Neuroscience* **2012,** *15* (5), 793-802.

12. Johansen, J. P.; Hamanaka, H.; Monfils, M. H.; Behnia, R.; Deisseroth, K.; Blair, H. T.; LeDoux, J. E., Optical activation of lateral amygdala pyramidal cells instructs associative fear learning. *Proceedings of the National Academy of Sciences* **2010,** *107* (28), 12692-12697.

13. Ohmura, Y.; Tanaka, K. F.; Tsunematsu, T.; Yamanaka, A.; Yoshioka, M., Optogenetic activation of serotonergic neurons enhances anxiety-like behaviour in mice. *The International Journal of Neuropsychopharmacology* **2014,** *17* (11), 1777-1783.

14. Chaudhury, D.; Walsh, J. J.; Friedman, A. K.; Juarez, B.; Ku, S. M.; Koo, J. W.; Ferguson, D.; Tsai, H.-C.; Pomeranz, L.; Christoffel, D. J.; Nectow, A. R.; Ekstrand, M.; Domingos, A.; Mazei-Robison, M. S.; Mouzon, E.; Lobo, M. K.; Neve, R. L.; Friedman, J. M.; Russo, S. J.; Deisseroth, K.; Nestler, E. J.; Han, M.-H., Rapid regulation of depression-related behaviours by control of midbrain dopamine neurons. *Nature* **2013,** *493* (7433), 532-536.

15. Lee, K.; Claar, L. D.; Hachisuka, A.; Bakhurin, K. I.; Nguyen, J.; Trott, J. M.; Gill, J. L.; Masmanidis, S. C., Temporally restricted dopaminergic control of reward-conditioned movements. *Nature Neuroscience* **2020,** *23* (2), 209-216.

16. Moran, R. J.; Kishida, K. T.; Lohrenz, T.; Saez, I.; Laxton, A. W.; Witcher, M. R.; Tatter, S. B.; Ellis, T. L.; Phillips, P. E.; Dayan, P.; Montague, P. R., The protective action encoding of serotonin transients in the human brain. *Neuropsychopharmacology* **2018,** *43* (6), 1425-1435.

17. Fischer, A. G.; Ullsperger, M., An update on the role of serotonin and its interplay with dopamine for reward. *Frontiers in Human Neuroscience* **2017,** *11*, 484.

18. Browne, C. J.; Abela, A. R.; Chu, D.; Li, Z.; Ji, X.; Lambe, E. K.; Fletcher, P. J., Dorsal raphe serotonin neurons inhibit operant responding for reward via inputs to the ventral tegmental area but not the nucleus accumbens: Evidence from studies combining optogenetic stimulation and serotonin reuptake inhibition. *Neuropsychopharmacology* **2019,** *44* (4), 793-804.

19. Altieri, S.; Singh, Y.; Sibille, E., Serotonergic pathways in depression. In *Neurobiology of depression*, CRC Press: 2011; Vol. 20115633, pp 143-170.

20. Niederkofler, V.; Asher, T. E.; Dymecki, S. M., Functional interplay between dopaminergic and serotonergic neuronal systems during development and adulthood. *ACS Chemical Neuroscience* **2015,** *6* (7), 1055-1070.

21. Dremencov, E.; Gispan-Herman, I.; Rosenstein, M.; Mendelman, A.; Overstreet, D. H.; Zohar, J.; Yadid, G., The serotonin–dopamine interaction is critical for fast-onset action of antidepressant treatment: In vivo studies in an animal model of depression. *Progress in Neuro-Psychopharmacology and Biological Psychiatry* **2004,** *28* (1), 141-147.

22. de Abreu, M. S.; Maximino, C.; Cardoso, S. C.; Marques, C. I.; Pimentel, A. F. N.; Mece, E.; Winberg, S.; Barcellos, L. J. G.; Soares, M. C., Dopamine and serotonin mediate the impact of stress on cleaner fish cooperative behavior. *Hormones and Behavior* **2020,** *125*, 104813.

23. Hashemi, P.; Dankoski, E. C.; Lama, R.; Wood, K. M.; Takmakov, P.; Wightman, R. M., Brain dopamine and serotonin differ in regulation and its consequences. *Proceedings of the National Academy of Sciences* **2012,** *109* (29), 11510-11515.

24. Daw, N. D.; Kakade, S.; Dayan, P., Opponent interactions between serotonin and dopamine. *Neural Networks* **2002,** *15* (4-6), 603-616.

25. Di Giovanni, G.; Esposito, E.; Di Matteo, V., Role of serotonin in central dopamine dysfunction: 5ht modulation of da function. *CNS Neuroscience & Therapeutics* **2010,** *16* (3), 179-194.

26. Bengel, D.; Murphy, D. L.; Andrews, A. M.; Wichems, C. H.; Feltner, D.; Heils, A.; Mossner, R.; Westphal, H.; Lesch, K. P., Altered brain serotonin homeostasis and locomotor insensitivity to 3, 4-methylenedioxymethamphetamine ("ecstasy") in serotonin transporter-deficient mice. *Mol Pharmacol* **1998,** *53* (4), 649-55.

27. Dunlap, L. E.; Andrews, A. M.; Olson, D. E., Dark classics in chemical neuroscience: 3,4-methylenedioxymethamphetamine. *ACS Chemical Neuroscience* **2018,** *9* (10), 2408-2427.

28. Drake, L. R.; Scott, P. J. H., Dark classics in chemical neuroscience: Cocaine. *ACS Chemical Neuroscience* **2018,** *9* (10), 2358-2372.

29. Abbruscato, T. J.; Trippier, P. C., Dark classics in chemical neuroscience: Methamphetamine. *ACS Chemical Neuroscience* **2018,** *9* (10), 2373-2378.

30. Avery, M. C.; Krichmar, J. L., Neuromodulatory systems and their interactions: A review of models, theories, and experiments. *Front. Neural Circuits* **2017,** *11*.

31. Zangen, A.; Nakash, R.; Overstreet, D.; Yadid, G., Association between depressive behavior and absence of serotonin-dopamine interaction in the nucleus accumbens. *Psychopharmacology* **2001,** *155* (4), 434-439.

32. *Microdialysis techniques in neuroscience*. Humana Press: Totowa, NJ, 2013; Vol. 75.

33. Sampson, M. M.; Yang, H.; Andrews, A. M., Advanced microdialysis approaches resolve differences in serotonin homeostasis and signaling. In *Compendium of in vivo monitoring in real-time molecular neuroscience*, WORLD SCIENTIFIC: 2017; pp 119-140.

34. Altieri, S. C.; Yang, H.; O'Brien, H. J.; Redwine, H. M.; Senturk, D.; Hensler, J. G.; Andrews, A. M., Perinatal vs genetic programming of serotonin states associated with anxiety. *Neuropsychopharmacology* **2015,** *40* (6), 1456-70.

35. Ngo, K. T.; Varner, E. L.; Michael, A. C.; Weber, S. G., Monitoring dopamine responses to potassium ion and nomifensine by in vivo microdialysis with online liquid chromatography at one-minute resolution. *ACS Chemical Neuroscience* **2017,** *8* (2), 329-338.

36. Zhang, J.; Jaquins-Gerstl, A.; Nesbitt, K. M.; Rutan, S. C.; Michael, A. C.; Weber, S. G., In vivo monitoring of serotonin in the striatum of freely moving rats with one minute temporal resolution by online microdialysis-capillary high-performance liquid chromatography at elevated temperature and pressure. *Anal Chem* **2013,** *85* (20), 9889-97.

37. Liu, Y.; Zhang, J.; Xu, X.; Zhao, M. K.; Andrews, A. M.; Weber, S. G., Capillary ultrahigh performance liquid chromatography with elevated temperature for sub-one minute separations of basal serotonin in submicroliter brain microdialysate samples. *Anal Chem* **2010,** *82* (23), 9611-6.

38. Yang, H.; Sampson, M. M.; Senturk, D.; Andrews, A. M., Sex- and sert-mediated differences in stimulated serotonin revealed by fast microdialysis. *ACS Chemical Neuroscience* **2015,** *6* (8), 1487-1501.

39. Yang, H.; Thompson, A. B.; McIntosh, B. J.; Altieri, S. C.; Andrews, A. M., Physiologically relevant changes in serotonin resolved by fast microdialysis. *ACS Chemical Neuroscience* **2013,** *4* (5), 790-8.

40. Ferre, S.; Cortes, R.; Artigas, F., Dopaminergic regulation of the serotonergic raphe-striatal pathway: Microdialysis studies in freely moving rats. *The Journal of Neuroscience* **1994,** *14* (8), 4839-4846.

41. Shin, G.; Gomez, A. M.; Al-Hasani, R.; Jeong, Y. R.; Kim, J.; Xie, Z.; Banks, A.; Lee, S. M.; Han, S. Y.; Yoo, C. J.; Lee, J. L.; Lee, S. H.; Kurniawan, J.; Tureb, J.; Guo, Z.; Yoon, J.; Park, S. I.; Bang, S. Y.; Nam, Y.; Walicki, M. C.; Samineni, V. K.; Mickle, A. D.; Lee, K.; Heo, S. Y.; McCall, J. G.; Pan, T.; Wang, L.; Feng, X.; Kim, T. I.; Kim, J. K.; Li, Y.; Huang, Y.; Gereau, R. W. t.; Ha, J. S.; Bruchas, M. R.; Rogers, J. A., Flexible near-field wireless optoelectronics as subdermal implants for broad applications in optogenetics. *Neuron* **2017,** *93* (3), 509-521 e3.

42. Correia, P. A.; Lottem, E.; Banerjee, D.; Machado, A. S.; Carey, M. R.; Mainen, Z. F., Transient inhibition and long-term facilitation of locomotion by phasic optogenetic activation of serotonin neurons. *Elife* **2017,** *6*.

43. Mathews, T. A.; Fedele, D. E.; Coppelli, F. M.; Avila, A. M.; Murphy, D. L.; Andrews, A. M., Gene dose-dependent alterations in extraneuronal serotonin but not dopamine in mice with reduced serotonin transporter expression. *The Journal of Neuroscience Methods* **2004,** *140* (1-2), 169-81.

44. Liu, Q.; Zhao, C.; Chen, M.; Liu, Y.; Zhao, Z.; Wu, F.; Li, Z.; Weiss, P. S.; Andrews, A. M.; Zhou, C., Flexible multiplexed in2o3 nanoribbon aptamer-field-effect transistors for biosensing. *iScience* **2020,** *23* (9), 101469.

45. Ren, J.; Isakova, A.; Friedmann, D.; Zeng, J.; Grutzner, S. M.; Pun, A.; Zhao, G. Q.; Kolluru, S. S.; Wang, R.; Lin, R.; Li, P.; Li, A.; Raymond, J. L.; Luo, Q.; Luo, M.; Quake, S. R.; Luo, L., Single-cell transcriptomes and whole-brain projections of serotonin neurons in the mouse dorsal and median raphe nuclei. *Elife* **2019,** *8*.

46. Huang, K. W.; Ochandarena, N. E.; Philson, A. C.; Hyun, M.; Birnbaum, J. E.; Cicconet, M.; Sabatini, B. L., Molecular and anatomical organization of the dorsal raphe nucleus. *eLife* **2019,** *8*.

47. Saller, C. F.; Salama, A. I., 3-methoxytyramine accumulation: Effects of typical neuroleptics and various atypical compounds. *Naunyn-Schmiedeberg's Archives of Pharmacology* **1986,** *334* (2), 125-132.

48. Sotnikova, T. D.; Beaulieu, J.-M.; Espinoza, S.; Masri, B.; Zhang, X.; Salahpour, A.; Barak, L. S.; Caron, M. G.; Gainetdinov, R. R., The dopamine metabolite 3-methoxytyramine is a neuromodulator. *PLoS ONE* **2010,** *5* (10), e13452.

49. Kaakkola, S.; Wurtman, R. J., Effects of comt inhibitors on striatal dopamine metabolism: A microdialysis study. *Brain Research* **1992,** *587* (2), 241-249.

50. Mansour, A.; Meador-Woodruff, J. H.; Bunzow, J. R.; Civelli, O.; Akil, H.; Watson, S. J., Localization of dopamine d2 receptor mrna and d1 and d2 receptor binding in the rat brain and pituitary: An in situ hybridization-receptor autoradiographic analysis. *J Neurosci* **1990,** *10* (8), 2587-600.

51. Suzuki, M.; Hurd, Y. L.; Sokoloff, P.; Schwartz, J. C.; Sedvall, G., D3 dopamine receptor mrna is widely expressed in the human brain. *Brain Research* **1998,** *779* (1-2), 58-74.

52. Spaethling, J. M.; Piel, D.; Dueck, H.; Buckley, P. T.; Morris, J. F.; Fisher, S. A.; Lee, J.; Sul, J. Y.; Kim, J.; Bartfai, T.; Beck, S. G.; Eberwine, J. H., Serotonergic neuron regulation informed by in vivo single-cell transcriptomics. *FASEB J* **2014,** *28* (2), 771-80.

53. Niederkofler, V.; Asher, T. E.; Okaty, B. W.; Rood, B. D.; Narayan, A.; Hwa, L. S.; Beck, S. G.; Miczek, K. A.; Dymecki, S. M., Identification of serotonergic neuronal modules that affect aggressive behavior. *Cell Rep* **2016,** *17* (8), 1934-1949.

54. Belmer, A.; Beecher, K.; Jacques, A.; Patkar, O. L.; Sicherre, F.; Bartlett, S. E., Axonal non-segregation of the vesicular glutamate transporter vglut3 within serotonergic projections in the mouse forebrain. *Frontiers in Cellular Neuroscience* **2019,** *13*, 193.

55. Wang, H.-L.; Zhang, S.; Qi, J.; Wang, H.; Cachope, R.; Mejias-Aponte, C. A.; Gomez, J. A.; Mateo-Semidey, G. E.; Beaudoin, G. M. J.; Paladini, C. A.; Cheer, J. F.; Morales, M., Dorsal raphe dual serotonin-glutamate neurons drive reward by establishing excitatory synapses on vta mesoaccumbens dopamine neurons. *Cell Reports* **2019,** *26* (5), 1128-1142.e7.

56. Bourne, J. A., Sch 23390: The first selective dopamine d1-like receptor antagonist. *CNS Drug Reviews* **2006,** *7* (4), 399-414.

57. Cameron, D. L.; Williams, J. T., Dopamine d1 receptors facilitate transmitter release. *Nature* **1993,** *366* (6453), 344-347.

58. Burke, D. A.; Rotstein, H. G.; Alvarez, V. A., Striatal local circuitry: A new framework for lateral inhibition. *Neuron* **2017,** *96* (2), 267-284.

59. Nishi, A.; Kuroiwa, M.; Shuto, T., Mechanisms for the modulation of dopamine d(1) receptor signaling in striatal neurons. *Frontiers in Neuroanatomy* **2011,** *5*, 43.

60. Ford, C. P., The role of d2-autoreceptors in regulating dopamine neuron activity and transmission. *Neuroscience* **2014,** *282*, 13-22.

61. Jenkins, B. G.; Sanchez-Pernaute, R.; Brownell, A. L.; Chen, Y. C.; Isacson, O., Mapping dopamine function in primates using pharmacologic magnetic resonance imaging. *The Journal of Neuroscience* **2004,** *24* (43), 9553-60.

62. Martelle, J. L.; Nader, M. A., A review of the discovery, pharmacological characterization, and behavioral effects of the dopamine d2-like receptor antagonist eticlopride. *CNS Neuroscience & Therapeutics* **2008,** *14* (3), 248-262.

63. Samanin, R.; Garattini, S., The serotonergic system in the brain and its possible functional connections with other aminergic systems. *Life Sciences* **1975,** *17* (8), 1201-9.

64. Kostowski, W., Interactions between serotonergic and catecholaminergic systems in the brain. *Pol J Pharmacol Pharm* **1975,** *27* (Suppl), 15-24.

65. Waldmeier, P. C.; Delini-Stula, A. A., Serotonin--dopamine interactions in the nigrostriatal system. *Eur J Pharmacol* **1979,** *55* (4), 363-73.

66. Petty, F.; Kramer, G.; Moeller, M., Does learned helplessness induction by haloperidol involve serotonin mediation? *Pharmacol Biochem Behav* **1994,** *48* (3), 671-6.

67. Mendlin, A.; Martin, F. J.; Jacobs, B. L., Involvement of dopamine d2 receptors in apomorphine-induced facilitation of forebrain serotonin output. *Eur J Pharmacol* **1998,** *351* (3), 291-8.

68. Mendlin, A.; Martin, F. J.; Jacobs, B. L., Dopaminergic input is required for increases in serotonin output produced by behavioral activation: An in vivo microdialysis study in rat forebrain. *Neuroscience* **1999,** *93* (3), 897-905.

69. Martin-Ruiz, R.; Ugedo, L.; Honrubia, M. A.; Mengod, G.; Artigas, F., Control of serotonergic neurons in rat brain by dopaminergic receptors outside the dorsal raphe nucleus. *Journal of Neurochemistry* **2001,** *77* (3), 762-75.

70. Vaaga, C. E.; Borisovska, M.; Westbrook, G. L., Dual-transmitter neurons: Functional implications of co-release and co-transmission. *Curr Opin Neurobiol* **2014,** *29*, 25-32.

71. Nusbaum, M. P.; Blitz, D. M.; Marder, E., Functional consequences of neuropeptide and small-molecule co-transmission. *Nature Reviews Neuroscience* **2017,** *18* (7), 389-403.

72. Granger, A. J.; Wallace, M. L.; Sabatini, B. L., Multi-transmitter neurons in the mammalian central nervous system. *Curr Opin Neurobiol* **2017,** *45*, 85-91.

73. Hnasko, T. S.; Edwards, R. H., Neurotransmitter corelease: Mechanism and physiological role. *Annu Rev Physiol* **2012,** *74*, 225-43.

74. Zhou, F. C.; Lesch, K. P.; Murphy, D. L., Serotonin uptake into dopamine neurons via dopamine transporters: A compensatory alternative. *Brain Research* **2002,** *942* (1-2), 109-19.

75. Kalivas, P. W.; Duffy, P., A comparison of axonal and somatodendritic dopamine release using in vivo dialysis. *J Neurochem* **1991,** *56* (3), 961-7.

76. Cheramy, A.; Leviel, V.; Glowinski, J., Dendritic release of dopamine in the substantia nigra. *Nature* **1981,** *289* (5798), 537-42.

77. Geffen, L. B.; Jessell, T. M.; Cuello, A. C.; Iversen, L. L., Release of dopamine from dendrites in rat substantia nigra. *Nature* **1976,** *260* (5548), 258-60.

78. Lee, E. H.; Geyer, M. A., Dopamine autoreceptor mediation of the effects of apomorphine on serotonin neurons. *Pharmacology Biochemistry and Behavior* **1984,** *21* (2), 301-11.

79. Silkis, I., Mutual influence of serotonin and dopamine on the functioning of the dorsal striatum and motor activity (hypothetical mechanism). *Neurochemical Journal* **2014,** *8*, 149-161.

80. Pollak Dorocic, I.; Fürth, D.; Xuan, Y.; Johansson, Y.; Pozzi, L.; Silberberg, G.; Carlén, M.; Meletis, K., A whole-brain atlas of inputs to serotonergic neurons of the dorsal and median raphe nuclei. *Neuron* **2014,** *83* (3), 663-78.

81. Gerfen, C. R.; Bolam, J. P., Chapter 1 - the neuroanatomical organization of the basal ganglia. In *Handbook of behavioral neuroscience*, Steiner, H.; Tseng, K. Y., Eds. Elsevier: 2016; Vol. 24, pp 3-32.

82. Mathur, B. N.; Lovinger, D. M., Serotonergic action on dorsal striatal function. *Parkinsonism Relat Disord* **2012,** *18 Suppl 1*, S129-31.

83. Cho, J. R.; Chen, X.; Kahan, A.; Robinson, J. E.; Wagenaar, D. A.; Gradinaru, V., Dorsal raphe dopamine neurons signal motivational salience dependent on internal state, expectation, and behavioral context. *The Journal of Neuroscience* **2021,** *41* (12), 2645-2655.

84. Lin, R.; Liang, J.; Luo, M., The raphe dopamine system: Roles in salience encoding, memory expression, and addiction. *Trends Neurosci* **2021,** *44* (5), 366-377.

85. Luis-Islas, J.; Luna, M.; Floran, B.; Gutierrez, R., Optoception: Perception of optogenetic brain stimulation. *bioRxiv* **2021**, 2021.04.22.440969.

86. Movassaghi, C. S.; Perrotta, K. A.; Yang, H.; Iyer, R.; Cheng, X.; Dagher, M.; Fillol, M. A.; Andrews, A. M., Simultaneous serotonin and dopamine monitoring across timescales by rapid pulse voltammetry with partial least squares regression. *Anal Bioanal Chem* **2021,** *413* (27), 6747-6767.

CHAPTER 5

Global Conclusions and Future Directions

Sex differences in prenatal stress and SSRI exposure

In Chapter 2, I show evidence that male offspring are more susceptible to the long-term effects of prenatal stress. However, the behavioral tests and analyses were completed during non-stressful conditions. The adult offspring receive no more stressful stimuli from birth to adult analyses. This informs us that prenatal stress is affecting male baseline behavior but not female. I hypothesize that prenatal stress, while not altering baseline behavior, may cause female offspring to be more susceptible to stressful events. Sex differences in risk of developing anxiety and depression, specifically pertaining to stress have been found.[1,2] For example, Herbison *et al.* saw in a human pregnancy cohort study prenatal stress had a higher contribution to male depression and anxiety symptoms than females.[2] Whereas, postnatal and early life stress contributed more to female depression and anxiety symptoms. One way to investigate these sex differences would be to stress the offspring as adults prior to behavioral or neurochemical testing. In Chapter 2, I also only neurochemically analyzed male mice due to their behavioral differences found. It is imperative to further test females as well to get a full picture of what is occurring neurochemically in both male and female adult offspring.

Second, it would be interesting to further dive into why males are more susceptible to prenatal stress than females. I suggest in the future to conduct histological experiments to determine if there are any transporter, receptor, or neuronal innervation differences between sexes. Specifically, the serotonin transporter (SERT) could be a key factor in these differences since I did see differences in SSRI induced serotonin overflow in males born to stressed mothers (Chapter 2). There has also been interesting in targeting some of the serotonin receptors as novel therapeutics for anxiety and depression, *i.e.* serotonin 2A.[3]

Investigating if there are serotonin 2A expression differences in stressed offspring compared to controls could further uncover the role of this receptor in depression and anxiety. I do not believe serotonin 1A is involved since experiments using 8OH-DPAT, a serotonin 1A agonist, did not show any significant differences between groups.

Finally, due to the interactions between stress, the serotonin system, and the HPA axis[4-10], which I outlined in Chapter 1, I suggest looking more into stress hormones in the offspring. I hypothesize that stressed males will have elevated corticosterone levels under basal and stressful conditions, whereas stress females will only have increased corticosterone levels under stressful conditions.

KOR modulation of serotonin in dysphoria

My secondary project focused on how kappa opioid receptors (KOR) modulate serotonin in dysphoria. In animals, dysphoria is detected *via* aversive/avoidance responses in behavior assessments. The KOR agonists are known to cause dysphoric effects in humans[11], and aversive effects in animals.[12-15] However, as discussed in chapter 3, the role of serotonin in KOR induced aversion is still up for debate due to contradictory data. While this data is preliminary for a much larger project, I found a possible explanation for the discrepancies in studies within the literature. I hypothesize these discrepancies are due to 1) route/location of KOR agonist administration, 2) location of analysis, and 3) neuronal subtypes being activated, *i.e.,* GABA or serotonin.

With my own data, I found systemic administration of a KOR agonist produced no changes in serotonin. However, local administration of the agonist into either the ventral striatum (vST) or the ventral hippocampus (vHPC) caused dose dependent increase in serotonin within the same region. Future studies should investigate perfusing the agonist

into the dorsal raphe nucleus (DRN), where the serotonin cell bodies are found, and taking samples from the vST or vHPC. I hypothesize this route and location of administration will result in a decrease in serotonin in the vST and vHPC. Furthermore, I hypothesize activation of KOR in the DRN is on serotonin neurons, while activation in the projection regions of vST or vHPC are activating KOR on GABAergic interneurons. Future studies involving pharmacological manipulations should then be carried out to investigate the indirect role of GABAergic neurons with regard to KOR-induced increases in serotonin.

Finally, my work set up and optimized conditioned place aversion (CPA) paradigm in the lab for future studies to occur. In addition, I have optimized our HPLC methods to enable 5-min (or less) online dialysate sampling time for concurrent dopamine and serotonin sampling. This short sampling time will allow sufficient samples to be collected during the 30-min CPA behavioral test, as opposed to conventional microdialysis sampling, which is on the order of 10-20 min per sample. Analyzing brain dialysate samples during CPA would allow for direct correlation between neurotransmitter levels and behavior. Since I have already shown serotonin increases with local perfusion, I hypothesize that disinhibiting serotonin neurons via KORs expressed on GABAergic neurons will increase extracellular serotonin and produce place aversion. Studies can specifically target serotonin neuron populations and subpopulations (using intersectional genetics) using optogenetics and chemogenetics to determine the necessity of increased vST extracellular serotonin in the aversive phenotype.

Interplay of KOR, serotonin, and stress in anxiety and depression

The serotonin and kappa opioid systems have been implicated in the mechanisms of stress and stress-related psychiatric disorders. While there are many studies pointing to the possible roles of these systems in stress-related disorders, the etiology of stress-related mood disorders is still largely unknown. My work begins to explore how these systems work together in a prenatally stress mouse model. I found adult male mice born to stressed mothers showed increased serotonin concentrations in the vHPC in response to citalopram administration. Furthermore, the presence of kappa opioid receptor activation caused a potentiation of these increases with citalopram. These effects were rescued in the male mice whose mothers had been treated with citalopram *in utero.* This suggests the mice born to stressed mothers could have alterations in kappa opioid receptors and SERT. I hypothesize that prenatal stress increases KOR receptor expression and sensitivity. There is evidence that stress and KOR activation cause increased SERT surface membrane expression.[16] Future studies should examine KOR and SERT expression in stressed compared to control mice using RNAscope and immunocytochemistry. I hypothesize stressed mice to have increased KOR and SERT expression compared to controls.

Though my two projects were completely slightly separately, in the future studies should conjoin these two projects to further understand these system interactions. One potential experiment is to give stressed dams a KOR antagonist to determine if KOR antagonism also protects offspring from stress-induced behavioral and neurochemical alterations. Second, future studies should examine how stress, whether prenatal or adult, effects susceptibility to KOR-induced place aversion and alterations in neurotransmission during testing days. I hypothesize stress to potentiate the place aversion phenotype.

Furthermore, investigate whether SSRI administration rescues the aversive phenotype in stress and control mice. These experiments could help further knowledge on how these two systems are interacting in the presence of stress.

Conclusion

In conclusion, my work furthers the knowledge in the field of stress, serotonin, and kappa opioid receptors. The prenatal stress work suggests the possibility of benefits for mothers with mood and anxiety disorders to continue taking medications through pregnancy. Continuing SSRI use could lead to resilience of offspring developing mood and anxiety disorders. Furthermore, continued work involving stress, serotonin, and kappa opioid receptors in relation to mood and anxiety disorders could offer new insights on novel therapeutic targets through the better understanding of the mechanisms of these disorders.

References

1. Henry, L. M.; Steele, E. H.; Watson, K. H.; Bettis, A. H.; Gruhn, M.; Dunbar, J.; Reising, M.; Compas, B. E., Stress Exposure and Maternal Depression as Risk Factors for Symptoms of Anxiety and Depression in Adolescents. *Child Psychiatry Hum Dev* **2020,** *51* (4), 572-584.

2. Herbison, C. E.; Allen, K.; Robinson, M.; Newnham, J.; Pennell, C., The impact of life stress on adult depression and anxiety is dependent on gender and timing of exposure. *Dev Psychopathol* **2017,** *29* (4), 1443-1454.

3. Dong, C.; Ly, C.; Dunlap, L. E.; Vargas, M. V.; Sun, J.; Hwang, I. W.; Azinfar, A.; Oh, W. C.; Wetsel, W. C.; Olson, D. E.; Tian, L., Psychedelic-inspired drug discovery using an engineered biosensor. *Cell* **2021,** *184* (10), 2779-2792 e18.

4. Firk, C.; Markus, C. R., Review: Serotonin by stress interaction: a susceptibility factor for the development of depression? *J Psychopharmacol* **2007,** *21* (5), 538-44.

5. Fuller, R. W., Serotonin receptors involved in regulation of pituitary-adrenocortical function in rats. *Behav Brain Res* **1996,** *73* (1-2), 215-9.

6. Adell, A.; Garcia-Marquez, C.; Armario, A.; Gelpi, E., Chronic stress increases serotonin and noradrenaline in rat brain and sensitizes their responses to a further acute stress. *J Neurochem* **1988,** *50* (6), 1678-81.

7. Davis, S.; Heal, D. J.; Stanford, S. C., Long-lasting effects of an acute stress on the neurochemistry and function of 5-hydroxytryptaminergic neurones in the mouse brain. *Psychopharmacology (Berl)* **1995,** *118* (3), 267-72.

8. De Kloet, E. R.; Kovacs, G. L.; Szabo, G.; Telegdy, G.; Bohus, B.; Versteeg, D. H., Decreased serotonin turnover in the dorsal hippocampus of rat brain shortly after adrenalectomy: selective normalization after corticosterone substitution. *Brain Res* **1982,** *239* (2), 659-63.

9. De Kloet, E. R.; Versteeg, D. H.; Kovacs, G. L., Aldosterone blocks the response to corticosterone in the raphe-hippocampal serotonin system. *Brain Res* **1983,** *264* (2), 323-7.

10. Lefebvre, H.; Contesse, V.; Delarue, C.; Feuilloley, M.; Hery, F.; Grise, P.; Raynaud, G.; Verhofstad, A. A.; Wolf, L. M.; Vaudry, H., Serotonin-induced stimulation of cortisol secretion from human adrenocortical tissue is mediated through activation of a serotonin4 receptor subtype. *Neuroscience* **1992,** *47* (4), 999-1007.

11. Pfeiffer, A.; Brantl, V.; Herz, A.; Emrich, H. M., Psychotomimesis mediated by kappa opiate receptors. *Science* **1986,** *233* (4765), 774-6.

12. Chefer, V. I.; Backman, C. M.; Gigante, E. D.; Shippenberg, T. S., Kappa opioid receptors on dopaminergic neurons are necessary for kappa-mediated place aversion. *Neuropsychopharmacology* **2013,** *38* (13), 2623-31.

13. Cunningham, C. L.; Gremel, C. M.; Groblewski, P. A., Drug-induced conditioned place preference and aversion in mice. *Nature Protocols* **2006,** *1* (4), 1662-70.

14. Ehrich, J. M.; Messinger, D. I.; Knakal, C. R.; Kuhar, J. R.; Schattauer, S. S.; Bruchas, M. R.; Zweifel, L. S.; Kieffer, B. L.; Phillips, P. E.; Chavkin, C., Kappa Opioid Receptor-Induced Aversion Requires p38 MAPK Activation in VTA Dopamine Neurons. *The Journal of Neuroscience* **2015,** *35* (37), 12917-31.

15. Prus, A. J.; James, J. R.; Rosecrans, J. A., Chapter 4 Conditioned Place Preference. 18.

16. Schindler, A. G.; Messinger, D. I.; Smith, J. S.; Shankar, H.; Gustin, R. M.; Schattauer, S. S.; Lemos, J. C.; Chavkin, N. W.; Hagan, C. E.; Neumaier, J. F.; Chavkin, C., Stress produces aversion and potentiates cocaine reward by releasing endogenous dynorphins in the ventral striatum to locally stimulate serotonin reuptake. *The Journal of Neuroscience* **2012,** *32* (49), 17582-96.